acta
geologica
polonica

Vol. 40, No. 3–4 Warszawa 1990

MACIEJ BĄBEL & ALICJA KASPRZYK

Gypsum ooids from the Middle Miocene (Badenian) evaporites of southern Poland

ABSTRACT: The gypsum ooids found in the Miocene evaporites of Poland were investigated in optic and scanning microscopy. Cortical fabric was recognized and interpreted in terms of environmental conditions. The cortices are built of porous and massive layers. The former are interpreted as originated in supersaturated in respect of gypsum and agitated brine, the latter — in supersaturated but relatively less agitated brine. The lateral disappearing of the porous layers, replaced by the massive gypsum, can result from the primary growth of radial massive polycrystals or from the local recrystallization. Rounded, mainly massive gypsum grains without clear concentric structure, exhibiting partly chaotic and partly quasi-radial arrangement of crystals, are interpreted as ooids or accretionary grains originated in relatively less agitated brine than the porous gypsum ooids. Cortical crystals are predominatly oriented radially with their 010 crystallographic planes tangential to the ooid surface. This orientation is explained as a result of: (*i*) competitive growth of the lens-shaped cortical crystals, (*ii*) initial accretion of crystals (nucleation or deposition according to the snow-ball mechanism) with the 010 tangential to the substrate. The latter possibility could be realized because supposed, produced by abrasion, microcrystalline fragments of gypsum, flattened along the 010 perfect cleavage plane, might become deposited or adsorbed on the ooid, with the largest 010 surface parallel to the substrate, in such a way creating the oriented nuclei of new cortical crystals.

INTRODUCTION

Uncalcareous ooids produced by evaporitic precipitation are poorly recognized both in recent and ancient sediments. Anhydrite ooids were noted by VOORTHUYSEN (1951) from the Upper Jurassic of the Netherlands. Halite ooids are known from recent deposits of the Dead Sea coast (WEILER, SASS & ZAK 1974) and the Hutt Lagoon in Australia (ARAKEL 1988), as well as from the Upper Silurian evaporites of the Michigan Basin (SCHREIBER, TUCKER & TILL 1986, p. 210). KARCZ & ZAK (1987) described round clusters of halite crystals, up to 3 mm in size, growing in turbulent brine of the canals connecting saline pools. Recent mirabilite ooids, spherulites and pisolites (15 mm in size) were found in the salt lakes of Canada (LAST 1984, 1989). The mirabilite ooids were also observed in salinas of Spain (Dr. PUEYO MUR, *personal inf.* 1985). Gypsum ooids have been mentioned from the Late Miocene (Messinian)

evaporites of the Central-Southern Apennines (CIARANFI & *al.* 1978, 1980; SCHREIBER 1978) and Cyprus (SCHREIBER 1978, p. 66). Moreover, CAROZZI (1963) and RADWAŃSKI & BIRKENMAJER (1977) interpreted half-moon calcareous ooids as primarily having cortices partly composed of calcium sulfate which was subsequently dissolved.

This paper offers a study of gypsum ooids occurring in the Middle Miocene (Badenian) evaporites of Fore-Carpathian Depression in southern Poland, and first reported by the present authors several years ago (KASPRZYK & BĄBEL 1986).

GEOLOGIC SETTING

The Middle Miocene (Badenian) evaporites occur in the upper part of the marine sedimentary succession in the Fore-Carpathian basin of the Central Paratethys (RADWAŃSKI 1968, 1969; KWIATKOWSKI 1972; GARLICKI 1979; PAWŁOWSKI, PAWŁOWSKA & KUBICA 1985). The evaporites are represented by gypsum deposits along the northern margin of the Fore-Carpathian Depression (Text-fig. 1). The best outcrops of the gypsum deposits are situated south of the Holy Cross Mts, along the Nida river (KWIATKOWSKI 1972). In the section of the Nida gypsum, up to 54 m thick, WALA (1961, 1962, 1963, 1979) distinguished 18 lithostratigraphic units, lettered *a* through *r*. Nearly all these units have their lithologic equivalents in the gypsum succession of the Staszów region, 50 km NE of the Nida river (KASPRZYK 1988, 1989, 1990). In the Wiśniowa-*1* borehole, situated nearby Staszów, the gypsum ooids were found as the only place of oolitic sediments (Text-fig. 1; KASPRZYK & BĄBEL 1986).

The evaporitic sequence pierced by the Wiśniowa borehole starts with giant gypsum intergrowths (unit *a* in Fig. 1; *see* BĄBEL 1987, 1990). It is overlain by banded selenites of the grass-like appearance, intercalated with stromatolitic gypsum (units *b-e; see* KWIATKOWSKI 1970, 1972; KUBICA 1983; PAWŁOWSKI, PAWŁOWSKA & KUBICA 1985; KASPRZYK 1989, 1990). Higher, a lithologic variety composed of the rod-like chaotically arranged selenites, named the skeletal gypsum, occurs (unit *f; see* KWIATKOWSKI 1972). This gypsum gradually passes upward into layers with longer (exceeding 18 cm), curved crystals typical of the so-called sabre-like gypsum deposits (PAWŁOWSKI, PAWŁOWSKA & KUBICA 1985, p. 36; BĄBEL 1986). They form units *g* and *i*, separated by fine-grained laminated gypsum (unit *h*). The overlying deposits represent alabaster-like gypsum (KWIATKOWSKI 1970, 1972) and gypsum laminites with sparse selenites (unit *j*). The upper part of the sequence is composed of: clayey-carbonate-gypsum laminites and clay (units *k* and *l*), alabaster-like gypsum (unit *l*), gypsum laminites with selenitic clusters and interbeds (unit *m*) and breccias with gypsum and carbonate fragments in marly-gypsum matrix (unit *n*). The sequence is overlain by a 1 m thick layer of porous limestone.

THE OOLITIC LAYER

The oolitic layer, 28 cm thick, was found in the upper part of the borehole Wiśniowa, within the gypsum laminites with selenitic clusters (unit *m* in Text-fig. 1). The oolitic sediment has distinctly detrital character and fills the

pocket-like depressions between selenitic crystals (Pl. 1, Fig. 1; *see also* KASPRZYK & BĄBEL 1986, Fig. 1), thus impressively indicating that the crystals primarily grew on the bottom of the basin (*see* HARDIE & EUGSTER 1971). Both sedimentary structures and features of the ooids indicate that the oolitic sediment is found not in the place of its origin (probably coastal shoals subjected to intensive evaporation and activity of waves; *see* WEILER, SASS

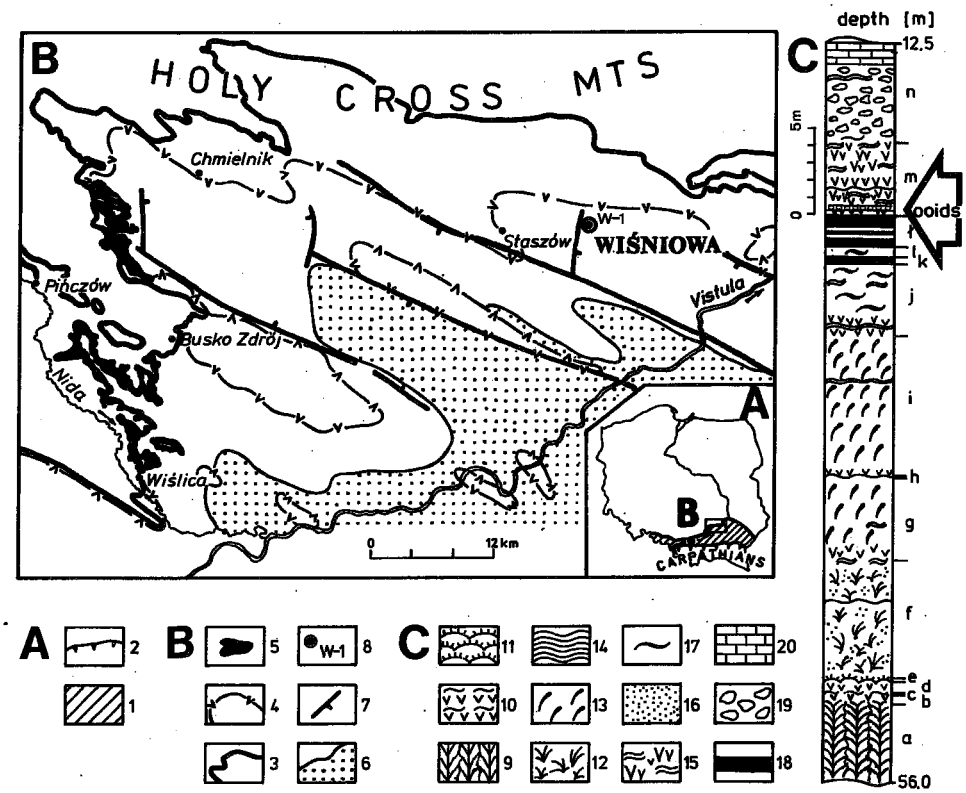

Fig. 1

Location of the Wiśniowa borehole against the Middle Miocene (Badenian) deposits in Poland

A — Extent of the Middle Miocene (Badenian) deposits in the Fore-Carpathian Depression in southern Poland; locality *Swoszowice* is indicated by a black dot

1 — Middle Miocene (Badenian) deposits, **2** — Carpathian overthrust

B — Extent of the Middle Miocene (Badenian) deposits in the northern part of the Fore-Carpathian Depression (*after* KUBICA 1983; simplified)

3 — Extent of the Middle Miocene (Badenian) deposits, **4** — extent of the Middle Badenian sulfate deposits, **5** — gypsum deposits on the surface, **6** — anhydrites and partly dehydrated gypsum deposits under the surface, **7** — main faults, **8** — location of the Wiśniowa borehole

C — Column of the Middle Miocene (Badenian) gypsum deposits in the Wiśniowa borehole and location of the gypsum oolitic layer (*arrowed*)

9 — Large crystal intergrowths of the *glassy gypsum;* **10** — banded selenites of the grass-like appearance; **11** — stromatolitic gypsum; **12** — chaotically arranged crystals of the *skeletal gypsum* deposits; **13** — the *sabre-like gypsum* deposits with long, curved selenites; **14** — laminated gypsum; **15** — laminated gypsum with selenitic clusters; **16** — fine-crystalline, sugar-like gypsum; **17** — massive, alabaster-like gypsum; **18** — clayey-carbonate-gypsum laminites and clay; **19** — gypsum and carbonate breccias with marly-gypsum matrix; **20** — porous limestone

& ZAK 1974; LAST 1989) but it was redeposited into relatively deeper part of the basin (KASPRZYK & BĄBEL 1986), although placed still in the photic zone, as proved by the algal filaments included in the gypsum crystals (Pl. 1, Figs 1, 4).

The oolitic layer is built of rounded gypsum grains of average sizes of about 0.6—1 mm scattered in a fine-grained gypsum matrix impurited by carbonates, clay and organic matter (Pl. 1, Fig. 3). Scarcely, intraclasts of microcrystalline gypsum, several mm in size (Pl. 1, Fig. 1), and euhedral, mostly lenticular gypsum crystals and their fragments are visible (Pl. 7, Fig. 1; Pl. 8, Figs 2—3; Pl. 13, Fig. 1). In the upper part of the layer the matrix is very poor and the sediment has a character of grainstone (Pl. 1, Figs 1—2). Most of the grains show at least partly developed concentric structure, *i. e.* a nucleus and a cortex, and thus can be described as ooids (FABRICIUS 1977, p. 38). The largest ooids found were 2 mm in size (KASPRZYK & BĄBEL 1986, Fig. 6).

Some rounded grains do not exhibit clearly concentric and radial structure and represent rounded single crystals, the 100 swallow-tail twins (probably bottom-nucleated and abraded in time of redeposition) and aggregates of crystals. The latter (Pl. 1, Figs 2—3; Pl. 2, Figs 1, 5; Pl. 4, Figs 1—3, 7—8; Pl. 5, Fig. 2) have the most unclear derivation. They can be treated as abraded fragments of the older sediments (*i. e.* gypsum intraclasts), completely recrystallized earlier ooids (*i. e.* diagenetic forms) or accretionary grains primarily growing in the brine of the evaporitic basin, similarly as halite and mirabilite grains described by KARCZ & ZAK (1987) and LAST (1984, 1989). The origin of these gypsum grains will be discussed at the end of the paper.

In the following chapters the present authors focus the attention on the grains having the character of ooids.

STRUCTURE OF OOIDS OBSERVED IN POLISHED SECTIONS

A concentric structure, frequently very weakly or partly developed, is visible almost in every grain. A radial structure is observed scarcely as radial arrangement of crystal boundaries (Pl. 2, Figs 1, 3; Pl. 3, Figs 1, 6, 9—10; Pl. 4, Fig. 4). Every ooid has a relatively large nucleus built both of the single gypsum crystal and of the aggregate of many crystals. Large crystals are transparent in opposite to the microcrystalline aggregates which are white and non-transparent (Pl. 2, Figs 1—12; Pl. 3, Figs 1—12; Pl. 4, Figs 1—8). The cortices are composed of less or more concentric layers of white, opaque and relatively more dark translucent gypsum. White color probably results from internal reflection and diffusion of light from surfaces of numerous micropores, and may be also from inclusions of foreign mineral. The white cortical layers usually show constant thickness unlike the layers of transparent gypsum between them. The white layers are often discontinuous. They coalesce, cut each other (in abraded and dissolved ooids), gradually disappear passing into areas composed of transparent gypsum, or they simply pinch out (*see* Text-fig. 2 *and* Pl. 2, Figs 1—12; Pl. 3, Figs 1—12; Pl. 4, Figs 1—6). The disappearing of the white layers is sometimes very abrupt (*see* Text-fig. 2 *and* Pl. 2, Figs 4, 10; Pl. 3, Figs 1, 6, 9—10; Pl. 4, Fig. 3). The external part of the cortices is usually built of a thick rim of transparent gypsum, often with tooth-like outer surface (Pl. 2, Fig. 3; Pl. 3, Figs 2, 11; Pl. 4, Figs 3—4, 5—6, 8). Similar white and dark cortical layers (*see* CIARANFI & *al.* 1978, Fig. 3; 1980, Fig. 8) and external "overgrowth rims" (SCHREIBER 1978, p. 66) occur in the gypsum ooids from the Apennines.

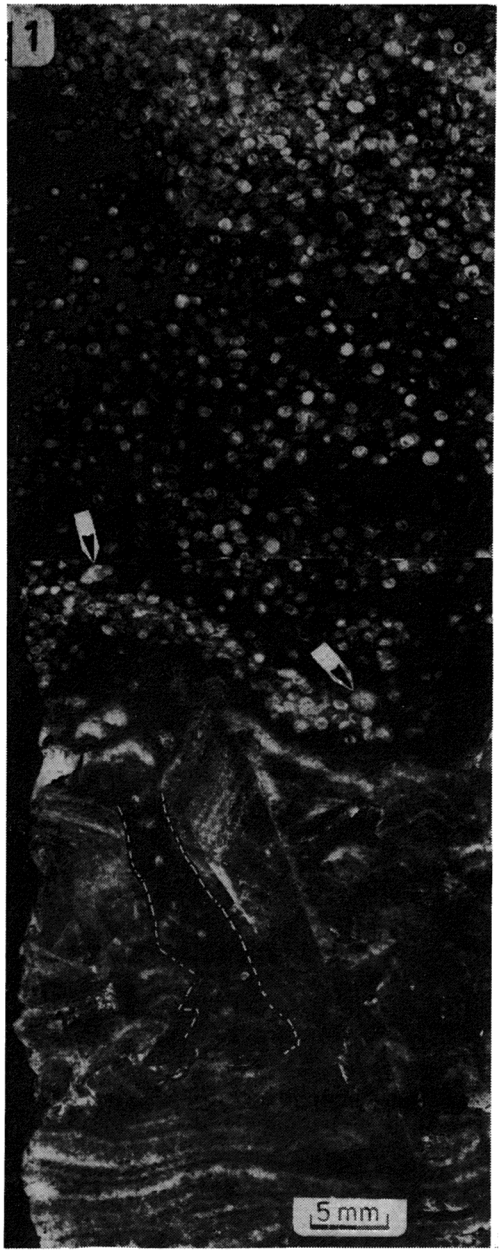

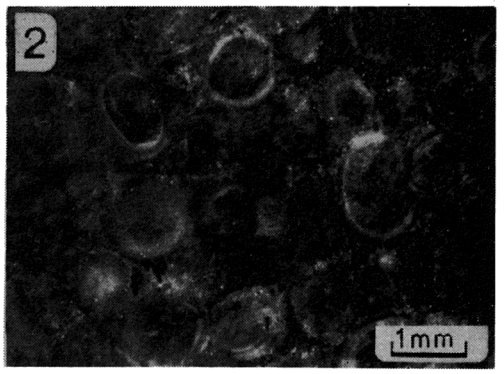

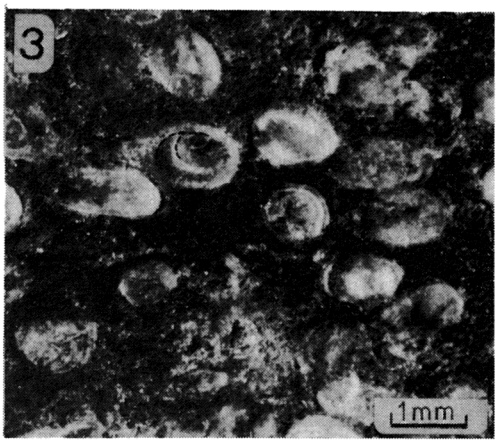

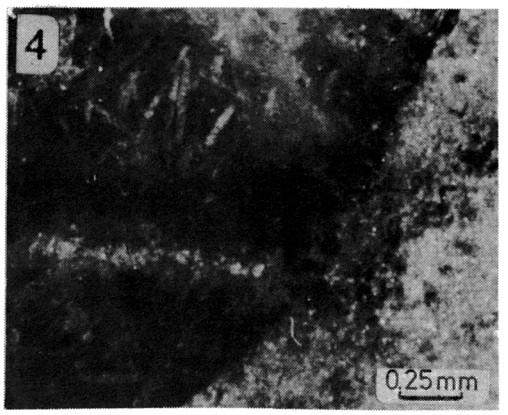

1 — Gypsum oolitic layer overlying laminated gypsum with selenites; oolitic grains and intraclasts (*arrowed*) are placed in dark gypsum matrix impurited by calcite, clay and organic matter; hollow filled with detrital gypsum and ooids is outlined; algal filaments (*white*) are included along growth zones of 120 crystal face; polished section

2 — Gypsum grainstone with pitted contacts and some grains devoid of concentric structure; polished slab

3 — Gypsum ooids within clay-gypseous matrix; note regenerated ooid and grains without concentric structure; polished slab

4 — Selenitic crystal, including algal filaments oriented subvertically, within fine-grained laminated gypsum (*right*). Substrate of oolitic layer; polished slab

Photos by L. ŁUSZCZEWSKA (Figs 2—4) and B. DROZD (Fig. 1)

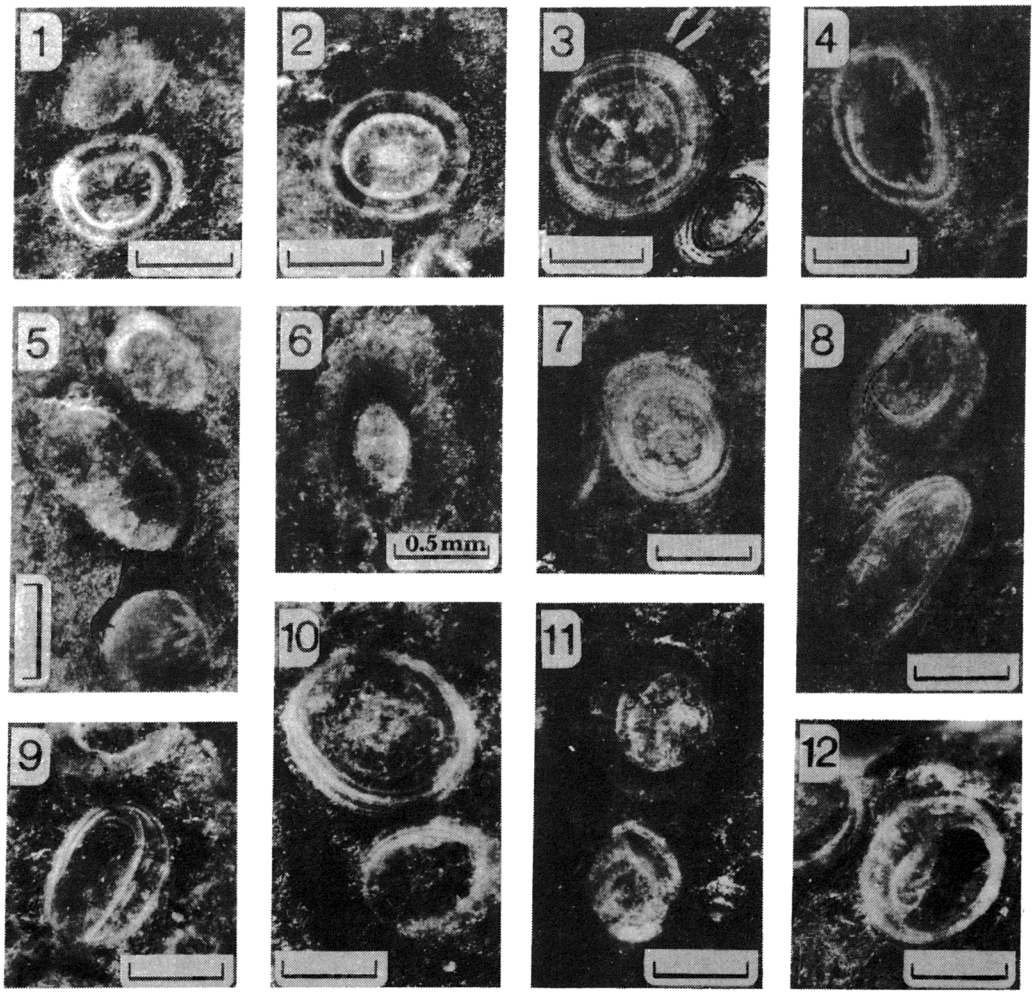

1-3 — Gypsum ooids with well developed radial-concentric structure; partly abraded or dissolved ooid with external rim (Fig. 3, *arrowed*) is pitted into regenerated ooid; note grain with unclear concentric structure (Fig. 1, *top*)

4 — Abraded or dissolved gypsum ooid with discontinuous white cortical layer and nucleus built of large gypsum crystal

5-6 — Gypsum ooids with unclear concentric structure; in Fig. 5 abraded or dissolved ooids, with external rims; one ooid with nucleus built of large gypsum crystal (*bottom*)

7-12 — Eccentric (Figs 7, 9—10, 12), abraded or dissolved (Figs 8—10), and regenerated gypsum ooids (Figs 8—9, 11); white discontinuous cortical layers coalesce (Fig. 10), cut each other (Figs 8—9, 11), and gradually disappear (Figs 7—8, 12); note grain with unclear concentric structure (Fig. 11, *bottom*)

Polished slabs; dark areas within ooids represent more transparent gypsum; scale bars = 0.5 mm; photos by B. MALINOWSKA and A. SZYMAŃSKI

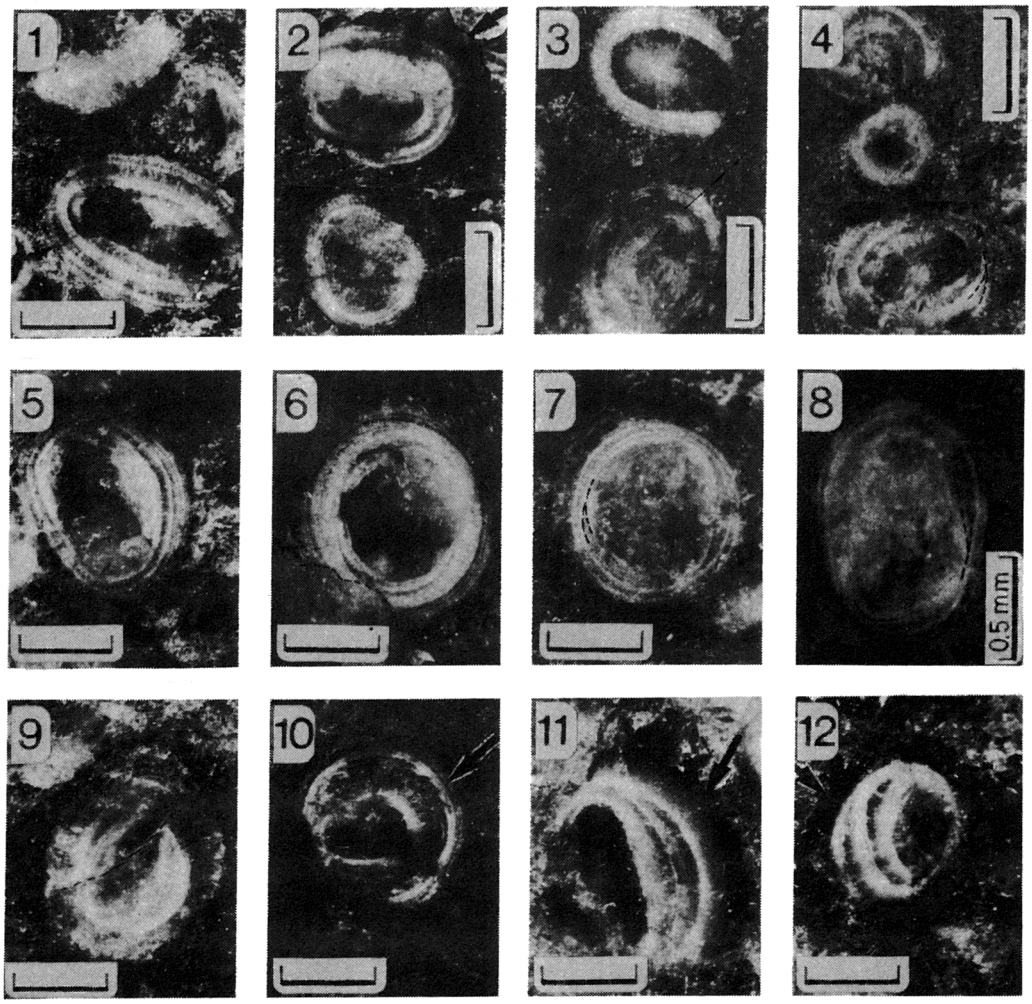

1-12 — Abraded or dissolved (Figs 1—10, 12), broken (Figs 1, 3—4 *top*, 10—11), cracked (Fig. 9), and regenerated gypsum ooids (Figs 4, 7, 8, 12); white cortical layers are discontinuous; nuclei are composed of large (Figs 1, 5—6, 10—11) or fine crystals (Figs 7—8); crystals protruding from nucleus (Fig. 6, *left;* Fig. 9, *top right;* Fig. 10, *bottom right side*) with apices blunted (abraded?) are covered by successive cortical layers; similar crystals form an imbricated pattern in Fig. 10 (*arrowed*); small grain with unclear concentric structure in Fig. 4 (*centre*) probably represents tangential section of an ooid; in Figs 2, 11 and 12 large external rims with tooth-like or wavy outer surface (*arrowed*) coat one side of ooid, in Fig. 11 flat side; note pitted contact in Fig. 6

Polished slabs; dark areas within ooids represent more transparent gypsum; scale bars = 0.5 mm; photos by B. MALINOWSKA, A. SZYMAŃSKI (Figs 1—7, 9—12) and B. DROZD (Fig. 8)

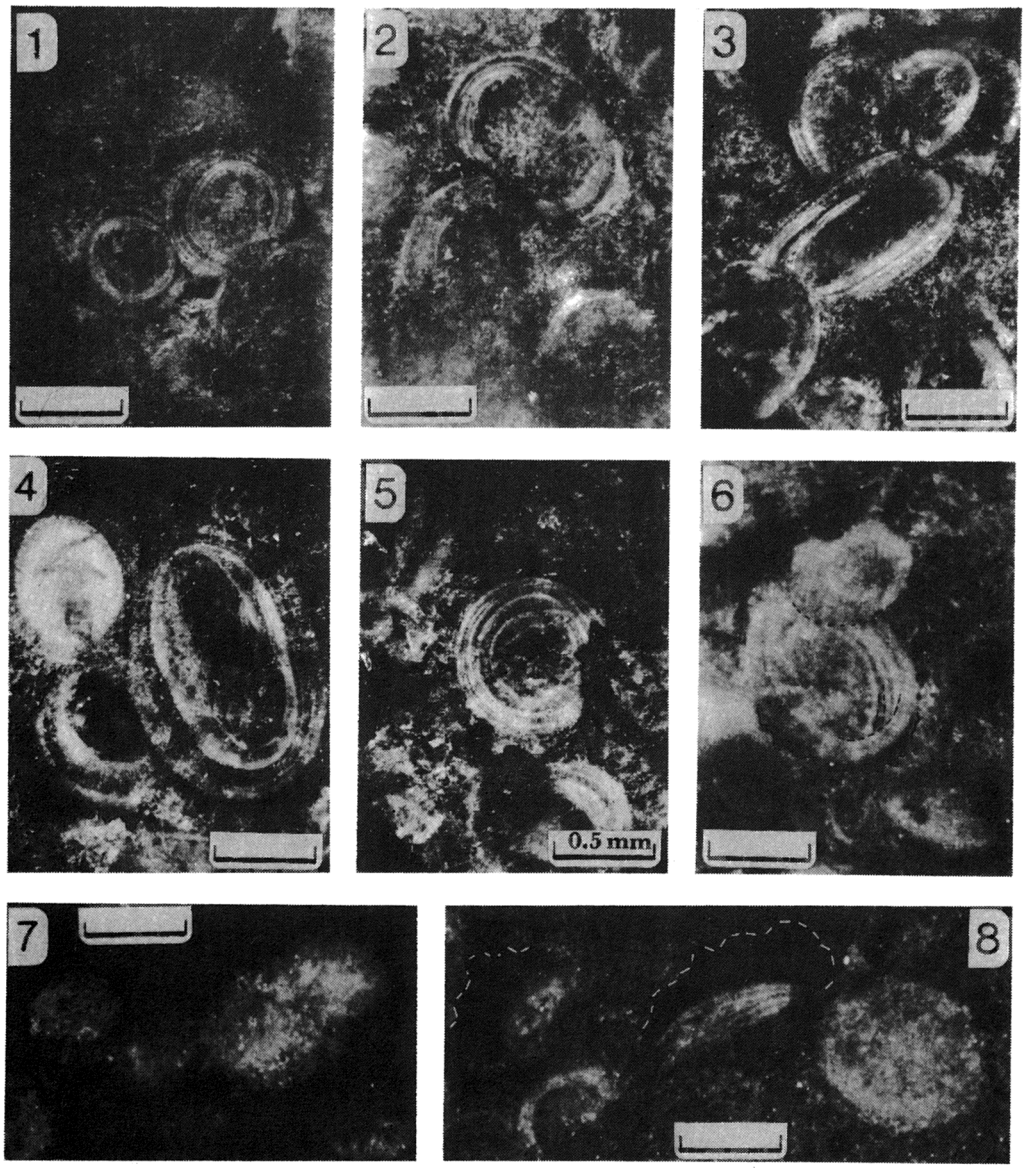

1-6 — Pitted gypsum ooids with smooth, dish-like (Figs 1—4, 6) and dentate (Fig. 5) contacts (two upper ooids *in* Fig. 3 and small ooid *in* Fig. 4 can be broken, *compare* Fig. 8); white cortical layers laterally disappear (in Fig. 2, *top* — replaced by massive crystals protruding from nucleus); note: regenerated ooid (Fig. 6), quasi-radial arrangement of crystals within nucleus (Fig. 4, *top left*), dark external rims (Figs 2—6), and grains with unclear concentric structure

7-8 — Microcrystalline gypsum grains devoid of concentric-radial structure and broken gypsum ooids with large external rims (Fig. 8)

Polished slabs; dark areas within grains represent more transparent gypsum; scale bars = 0.5 mm; photos by A. SZYMAŃSKI and B. MALINOWSKA (Figs 1—5), L. ŁUSZCZEWSKA (Figs 6, 8) and B. DROZD (Fig. 7)

On the polished sections it is the best to recognize specific types of ooids, such as: eccentric (which dominate), concentric, cracked, broken, abraded or dissolved, regenerated, distorted (?), and pitted (*see* Text-fig. 2; Pl. 1, Fig. 3; Pl. 2, Figs 1—12; Pl. 3, Fig. 1—12; Pl. 4, Figs 1—6, 8; *and* KASPRZYK & BĄBEL 1986, Fig. 5), as well as gypsum grapestones (*see* Pl. 5, Figs 1—2; *and* KASPRZYK & BĄBEL 1986, Fig. 6).

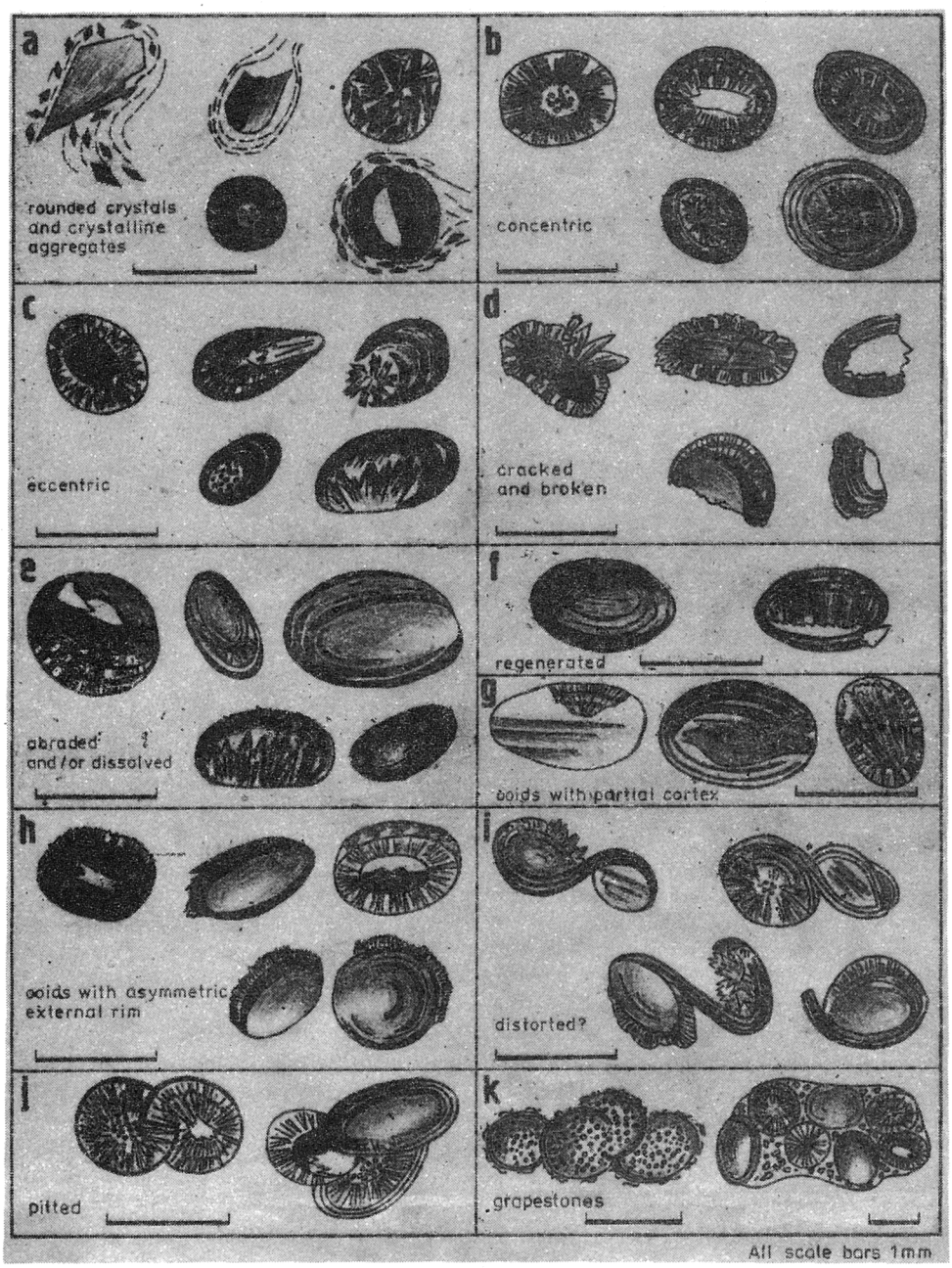

Fig. 2. Types and structure of gypsum ooids and grains of the oolitic layer, recognized in polished sections

OBSERVATIONS OF OOIDS IN THIN SECTIONS

A concentric structure is hardly, and only in some grains visible under a polarizing microscope. First of all a radial structure, *i. e.* radial arrangement of gypsum crystals, is noticeable in many grains. Every grain is built of gypsum and many of them contain numerous included carbonate, mainly calcite crystals. Negative results of alizarine red-*S* staining of several crystals suggest also the occurrence of dolomite.

NUCLEUS

Distinguishing of a nucleus and cortex under polarizing microscope in many cases is problematic. The nucleus is distinguishable from the cortex according to the following features:

i) uniform light extinction of crystals;
ii) sharp crystal boundaries;
iii) crystal boundaries showing arrangements not dependant on the shape of the grain, *i. e.* unordered or chaotic, where straight boundaries do not tend to be radial;
iv) content of numerous carbonate crystals (Pl. 11, Fig. 4; Pl. 12, Fig. 3).

A boundary between the nucleus and cortex is usually not sharp. In many grains a nucleus and cortex are undistinguishable at all and the grains do not exhibit radial structure (Pl. 7, Fig. 1; Pl. 9, Fig. 1; Pl. 10, Figs 1—2; Pl. 13, Fig. 1). A typical feature observed in some external parts of such grains is quasi-radial arrangement of crystals and associated sweeping light extinction. There are many transitional forms between the rounded grains with completely unordered structure and the ooids with perfect radial and concentric structure. Some grains with unordered structure represent the ooids cut not equatorially; they are smaller than the other ones (Pl. 3, Fig. 4; Pl. 9, Fig. 1).

RADIAL STRUCTURE OF THE CORTEX

In the cross polarized light radial cortical crystals exhibit sweeping or irregular light extinction (Pl. 6, Fig. 2; Pl. 7, Figs 1—2; Pl. 8, Fig. 1b; Pl. 9, Figs 1—2; Pl. 10, Figs 1b—2b; Pl. 11, Fig. 1; Pl. 14, Figs 1—2; Pl. 15, Figs 1—2).

Boundaries of the separate crystals are obscured and only in some places recognizable as sharp lines. The sweeping extinction is not continuous. Within crystals small elongated fields relatively uniformly extincting light are noticeable (Pl. 9, Fig. 2; Pl. 14, Fig. 2; Pl. 15, Figs 1—2). Such fields are defined as *subcrystals* (KENDALL & BROUGHTON 1978, p. 521; note that there is also another meaning of that term). It is to emphasize that such subcrystals do not necessary correspond with one crystal unit because what is seen as a subcrystal in the polarized light can result from amalgamation of many crystals smaller than the thickness of a thin section. The cortical subcrystals are usually parallelly grouped in a fan-like aggregates, often penetrating each other (Pl. 7, Fig. 2; Pl. 9, Fig. 2; Pl. 14, Fig. 2). Axes of elongation of the subcrystals tend to be arranged radially, normal to the ooid surface. In extreme cases the axes are inclined to the ooid surface more than 20°.

CONCENTRIC STRUCTURE OF THE CORTEX

A concentric structure is marked, more or less apparently, only in some cortices by carbonate crystals or by "Becke lines".

The most pronounced concentric structure is formed by dense radial Becke lines forming bands 0.02—0.05 mm thick having distinctly high relief (Pl. 8, Fig. 1a; Pl. 9, Fig. 2; Pl. 11, Figs 3—4; Pl. 12, Fig. 2; Pl. 14, Fig. 2; Pl. 15, Fig. 2; Pl. 16, Fig. 1). In plane polarized light the bands are relatively darker than other parts of the ooids. Some bands, especially in the thick thin sections, show slightly brownish color changing its intensity together with rotating of a microscopic stage.

The dense Becke lines within the bands reflect the radial arrangement of crystal boundaries or intercrystalline pores. Such pores were recognized under a scanning microscope. The apparent high relief of the bands can result from refraction and reflection of light on dense crystal boundaries and intercrystalline pores or on rough, water-etched surface of band (*see* WINCHELL 1949, p. 83).

There were also observed very narrow bands, limited by parallel concentric Becke lines which move outwards themselves together with lowering of the microscopic stage (Pl. 11, Figs 1—2). The radial structures within these bands are scarcely visible. The movement of the Becke lines indicate that they have refractive indices lower than the surrounding medium. This difference probably results from the microporous structure of the bands. The refractive indices can be lowered due to existence of air in the pores, similarly as it is noted in microporous aragonitic ooids (ILLING 1954, LOREAU & PURSER 1973, RICHTER 1983).

The most perfect concentric, and radial structure occur in the ooids with the bands formed by Becke lines (*compare* Pl. 8, Fig. 1; Pl. 9, Fig. 2; Pl. 11, Figs 3—4; *and* Pl. 7, Figs 1—2; Pl. 9, Fig. 1; Pl. 10, Figs 1—2; Pl. 12, Figs 3—4; Pl. 13, Fig. 1). The more thickness and number of bands, the more perfect concentric and radial structure, and the more apparent black extinction cross (Pl. 8, Fig. 1). Similarly as white layers in polished sections, the bands exhibit relatively constant thickness unlike the layers between them.

The external rim (Pl. 5, Fig. 3; Pl. 8, Figs 1—2; Pl. 10, Fig. 2; Pl. 11, Figs 3—4; Pl. 12, Figs 1, 4; Pl. 14, Fig. 2; Pl. 16, Fig. 1) is composed of the relatively large crystals which show uniform light extinction and straight traces of cleavage planes, recognized as the 010 ones (light extinction is parallel to them, *see* Pl. 14, Fig. 2; Pl. 15, Fig. 1; *and* KERR 1959). The crystals are in optic continuity with the internal parts of the ooids. Many rims have tooth-like external crystal terminations or a wavy outer surface (Pl. 8, Figs 1—2). The wavy surface can be interpreted as resulted from abrasion or dissolution in time of redeposition or earlier. The rims were never found on broken surfaces of the ooids, so the growth of rims evidently took place before redeposition of the ooids. Many rims contain calcite inclusions. In some rims dark patches of opaque substance, interpreted as organic matter, are observed, forming a wavy line parallel with the ooid surface (Pl. 12, Fig. 1). The inclusions are grouped into patches within the concave parts of the waves just as if they were trapped inside convexities between rounded crystal apices. The rims are developed in asymmetric way on the one flattened side of the grain (*see* Text-fig. 2 *and* Pl. 5, Fig. 3; Pl. 8, Figs 1—2; Pl. 10, Fig. 2; Pl. 12, Fig. 3).

The parts of the cortex between the bands having positive relief are similar to the external rims. The larger crystals observed there show the traces of the 010 cleavage planes oriented parallel to the ooid surface, in places sharp boundaries and more uniform light extinction (Pl. 14, Fig. 2; Pl. 15, Fig. 1).

Large carbonate crystals are situated within these parts of cortices and never within the bands formed by Becke lines (Pl. 11, Figs 2, 4; Pl. 14, Fig. 2; Pl. 15, Fig. 2). Carbonate crystals range in sizes from micritic to larger forms, up to 0.28 mm in size, but those included into cortices usually do not exceed 0.05 mm. Tiny carbonate crystals, or micrite, form discontinuous envelopes within cortices, often at a base of the external rim (Pl. 5, Fig. 3; Pl. 6, Fig. 1; Pl. 8, Fig. 1; Pl. 11, Fig. 4; Pl. 12, Figs 1—2, 4; Pl. 13, Fig. 1; Pl. 14, Fig. 2; Pl. 15, Fig. 1; Pl. 16, Fig. 1). The crystals are euhedral and anhedral. The habit of the euhedral crystals is rhomboidal and prismatic (Pl. 12, Figs 2—3). The carbonate crystals, randomly scattered within cortices, also form less of more recognizable envelopes (Pl. 6, Fig. 1; Pl. 8, Fig. 3; Pl. 12, Fig. 4; Pl. 15, Fig. 2).

ORIENTATION OF CORTICAL CRYSTALS

In the well developed cortices, especially those exhibiting concentric Becke lines, in the cross polarized light crystals extinct light in four opposite sectors forming a figure resembling a black cross (Pl. 6, Fig. 2; Pl. 7, Fig. 1; Pl. 8, Fig. 1b; Pl. 15, Fig. 1). Such a cross indicates that cortical crystals are regularly oriented, at least in a statistical manner. In ooids having a nucleus built of one gypsum crystal cortical crystals are in optic continuity with a nucleus strictly on two opposite sides of it (Pl. 8, Fig. 1b; Pl. 9, Fig. 2).

The orientation of cortical crystals is difficult to determine in the polarized light directly because in monoclinic gypsum not all optic axes are parallel with the morphological ones and individual crystals are too small to be noticed optically.

The observations reveal that in some cortices traces of the 010 cleavage planes are oriented more or less parallel to the ooid surface (Pl. 14, Fig. 2; Pl. 15, Fig. 1). Elongation of cortical subcrystals (defined as fields of uniform extinction) in most cases coincides with the lower vibration direction, *i. e.* with the direction of optically slower (Text-fig. 3). Roughly estimating, more than 2/3 cortical subcrystals show such characteristic.

From the above features the authors interpreted that cortical crystals are oriented, at least statistically, with their 010 plane tangential to the ooid surface or, in other words, with their crystallographic axis *b* radial. When the axis *b* is oriented radially, there are two possible extreme

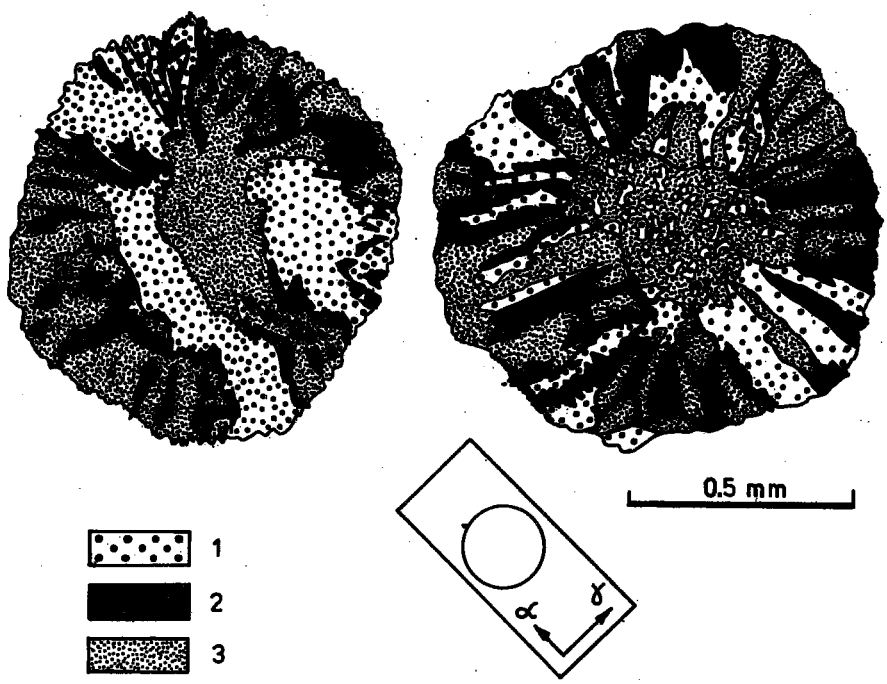

Fig. 3. Vibration directions in two examplary gypsum ooids (drawings from thin sections); polarized light, crossed nicols; vibration direction of polarizer — NS, analyzer — WE; gypsum plate as shown

Interference colors: **1** — blue; **2** — sensitive violet; **3** — red, up to yellow

positions of the gypsum indicatrix in the cortex, both having the same refractive indices for *b* direction ($n_\beta = 1.522$, the *b* direction is parallel to the optic axis *X*, *see* Text-fig. 4). One indicatrix has maximal refractive index n_γ in direction perpendicular to *b* equal 1.529 when this direction coincides with optic axis *Z*, the second one n_α equal 1.520 when this direction coincides with optic axis *X*. Certainly in the cortices statistically compromise values will be observed; the indicatrix with referactive index perpendicular to *b* equal 1.5245, *i. e.* the mean between 1.520 and 1.529 (*compare* SHEARMAN, TWYMAN & ZAND KARIMI 1970, p. 564), which is in conformity with the observable data.

It is possible to foresee that in a spherical gypsum ooid having cortical crystals ideally statistically distributed around a nucleus, all the crystals with the axis *b* exactly radial, in any equatorial cross-section there will be occurred about 32% of cortical crystals with higher vibration direction radial and 68% of crystals with lower vibration direction radial (Text-fig. 4). These values result from the fact that in such cross-sections every cortical crystal is observed exactly in direction of the plane of the optic axes, and thus the view reflects the positive optical character of gypsum with angle of the optic axes equal 58°. If the cortical crystals are ideally distributed, with every position defined by rotation around axis *b* equally probable, the 32% of crystals (58°/180° = 0.32) will have the higher vibration direction radial and the other 68%, *i. e.* about 2/3 of all crystals — the lower vibration direction radial. The observed data are again in conformity with these ideal values.

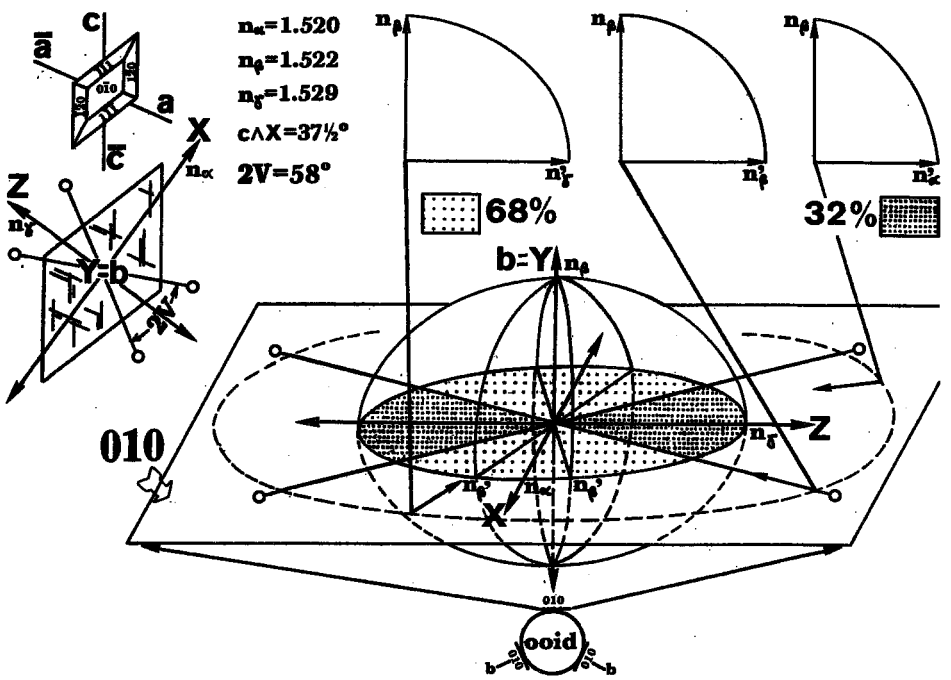

Fig. 4. Scheme explaining distribution of cortical crystals with lower (68%) and higher direction vibration radial (32%) in the ideal gypsum ooid composed of crystals, all of which have the crystallographic axic *b* oriented radially, as seen in the equatorial section; detailed explanation in the text

Upper left: Relation of crystallographic (*a, b, c*) to optic (*X, Y, Z*) axes of gypsum

Orientation of axes *a, b, c* (the *b* axis is perpendicular to plane of drawing) and indexation of crystal faces *according to* PALACHE, BERMAN & FRONDEL (1951); orientation of axes *X, Y, Z* in the cleaved fragment of gypsum and optic characteristics of gypsum *according to* KERR (1959)

SEM OBSERVATIONS OF OOIDS

Both cross-sections and cortical surfaces of the ooids were observed under a scanning microscope. The cross-sections were etched by water, the cortical surfaces only slightly washed.

The cortical surfaces show porous and massive fabric (Pl. 17, Fig. 1; Pl. 18, Figs 1—2; Pl. 19, Figs 1—2; Pl. 20; Pl. 21, Figs 1—2; Pl. 22, Figs 1—2; Pl. 23, Figs 1—2; Pl. 24, Figs 1—2). The porous cortices are built of many differently oriented crystals. The crystals are always elongated in shape and range in size from fractions of micron (Pl. 19, Fig. 1) to several microns (Pl. 19, Fig. 2). The shape of crystals varies from rhomboidal or lens-like to more tabular and stubby nearly always with larger faces convex. That shape resembles gypsum crystals having some variants of the lenticular habit, observed in the direction of their flatness. Some crystals show rounded or irregular shape without typical flat faces (Pl. 23, Fig. 2; Pl. 24, Figs 1—2). Groups of crystals elongated more or less parallelly to each other are observed in some porous cortical surfaces. They form wavy or swirl patterns and penetrate each other (Pl. 20; Pl. 22, Figs 1—2; Pl. 23, Fig. 1; Pl. 24, Figs 1—2). Some groups are composed of crystals which are parallel in the crystallographic sense. Such crystals are often integrated into massive units or polycrystals (= crystals built of slightly misoriented blocks), which often show re-entrant angles on their opposite side parts, similarly as in the aggregate of parallel lenticular crystals (Pl. 22, Figs 1—2; Pl. 24, Figs 1—2). The 010 cleavage planes are often recognizable arranged more or less parallelly to the ooid surface. Cortical layers exfoliate and cortical crystals split off just along these planes (Pl. 4, Fig. 8; Pl. 17, Figs 1—2; Pl. 18, Figs 1—2; Pl. 21, Fig. 1; Pl. 25, Fig. 1). In some places the tangential position of a crystallographic axis *c* is recognizable due to apparent crystal morphology, cleavage, etch pits or intercrystalline pores showing the shape of negative gypsum crystals (*see* Pl. 17, Fig. 1; Pl. 19, Fig. 2; Pl. 22, Figs 1—2; Pl. 24, Figs 1—2; *and* BĄBEL 1990). Most of the cortical crystals are deeply rooted in the interior of the ooid and they exhibit only their external terminations. Only singular crystals seem not to be rooted (Pl. 22, Fig. 1; Pl. 23, Fig. 2).

The cortical surfaces show also unporous massive fabric. The gradational transitions from porous to massive fabric frequently occur within one cortical layer (Pl. 17, Fig. 1; Pl. 21, Figs 1—2). The transitional areas are built of crystals which are more tightly welded into polycrystalline massive units. The size of crystals within the massive surfaces is larger than those of the porous ones. In places the crystals overlap probably due to their competition in tangential lateral growth (Pl. 3, Fig. 10; Pl. 21, Fig. 2; Pl. 24, Fig. 2).

In the etched cross-sections the radial structure of the ooids is well visible. The cortical crystals, in places exhibiting lenticular shape, are elongated more or less normally to the ooid surface and traces of their 010 planes, etched by water, are oriented tangentially (Pl. 17, Figs 1—2; Pl. 18, Fig. 2; Pl. 25, Fig. 2; Pl. 26; Pl. 27, Figs 1—2; Pl. 28, Figs 1—2; Pl. 29, Figs 1—2; Pl. 30, Figs 1—2). Similar etch striations running along the 010 planes were illustrated by SIESSER & ROGERS (1976, Figs 4—5) and WARREN (1982, Fig. 7c). The lateral gradations from porous to massive fabric are also observed (Pl. 28, Fig. 1). The carbonate crystals are exhibited by etching of the more soluble surrounding gypsum (Pl. 26).

Within some cortices the splitting of crystals into lens-shaped parallel forms perpendicular to traces of the 010 planes is visible (Pl. 27, Fig. 2; Pl. 28, Figs 1—2; Pl. 29, Figs 1—2). The *compromise boundaries* between cortical crystals indicating their *competitive growth* (BATHURST 1971, pp. 421—423) occur especially within external rims (Pl. 27, Fig. 1). Along the centrifugal direction there is also noticeable another structure; a coalescence and mergence of individual cortical crystals into larger polycrystals (*see* KENDALL & BROUGHTON 1978), within which the boundaries of crystal blocks were not etched (Pl. 25, Fig. 2; Pl. 28, Figs 1—2; Pl. 29, Fig. 1).

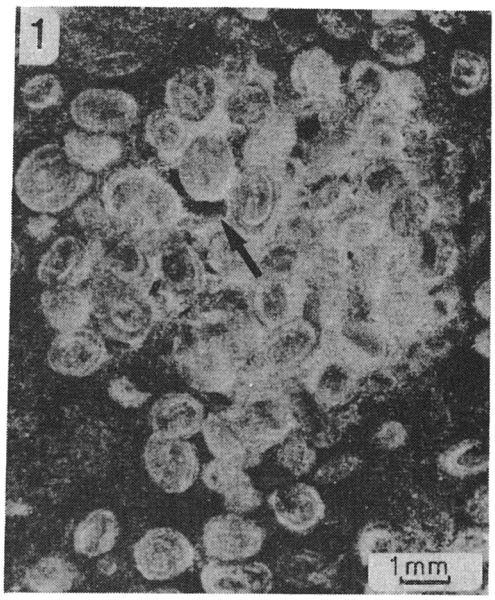

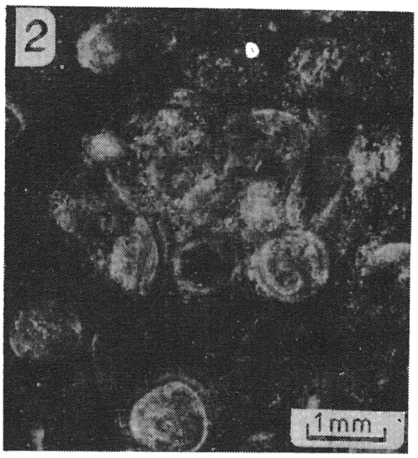

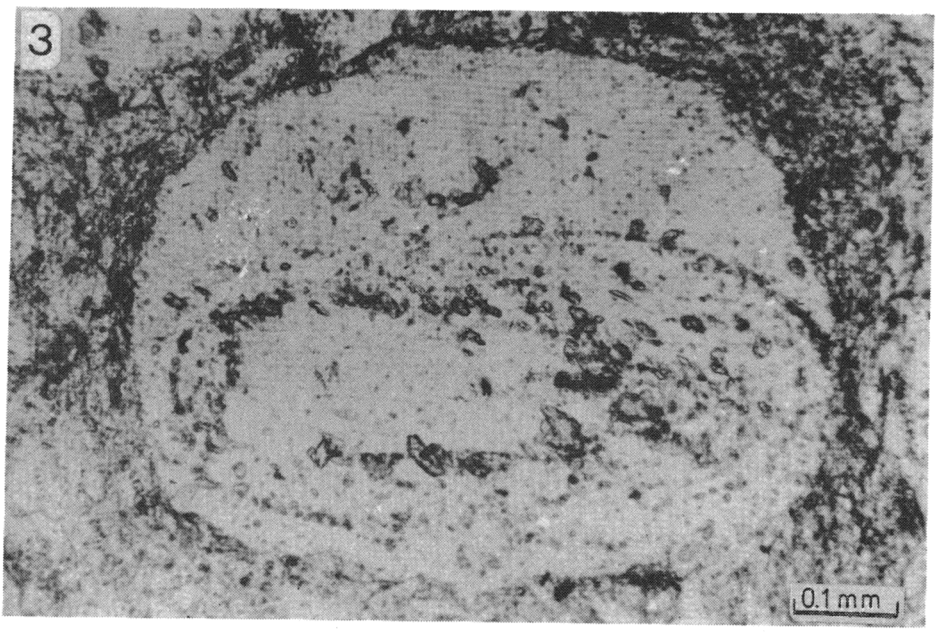

1-2 — Gypsum grapestones within dark carbonate-clay-gypseous matrix; note pitted contacts and empty pores (Fig. 1, *dark, arrowed*) within grapestone, and grains devoid of concentric structure; polished surfaces; photos by S. ULATOWSKI (Fig. 1) and L. ŁUSZCZEWSKA (Fig. 2)
3 — Eccentric, partly abraded or dissolved gypsum ooid showing external rim (or cortex), coating one flat side of nucleus, and discontinuous envelopes of calcite crystals (*dark*); polarized light, parallel nicols

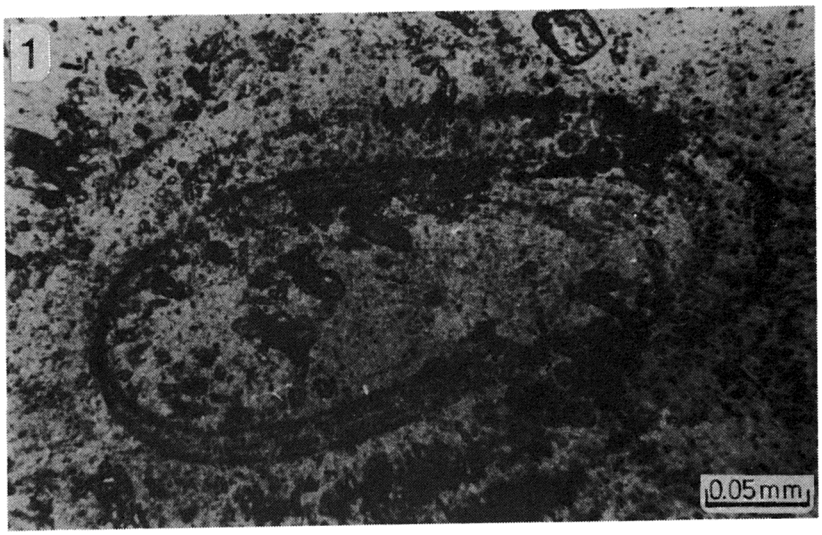

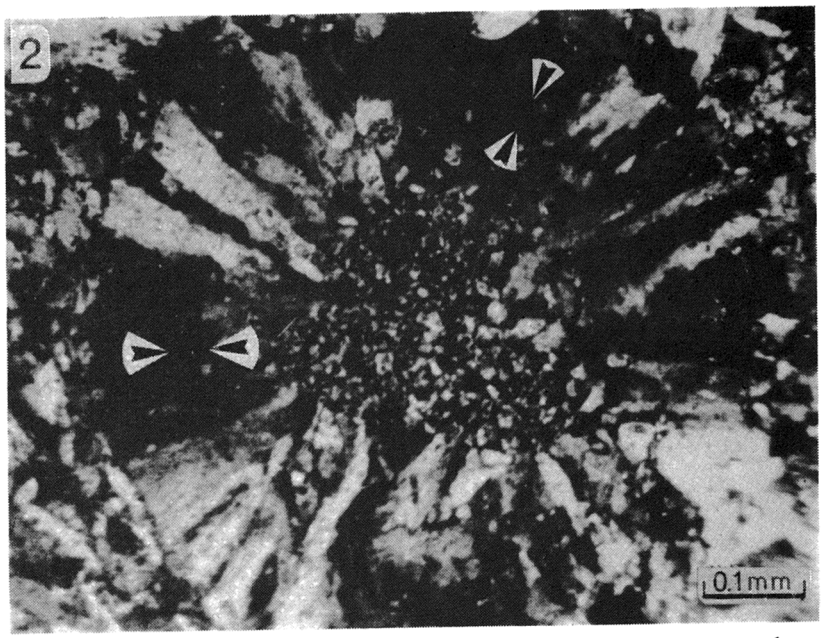

1 — Eccentric gypsum ooid with calcite crystals (*dark*) forming discontinuous and coalescing envelopes; polarized light, parallel nicols

2 — Gypsum ooid with microcrystalline gyp. um-calcite nucleus and radial cortical crystals showing sweeping light extinction, and sharp and obliterated boundaries; note partly visible black extinction cross and concentric band (*arrowed*) formed by dense radial subcrystals corresponding to band of radial Becke lines seen under parallel nicols; polarized light, crossed nicols

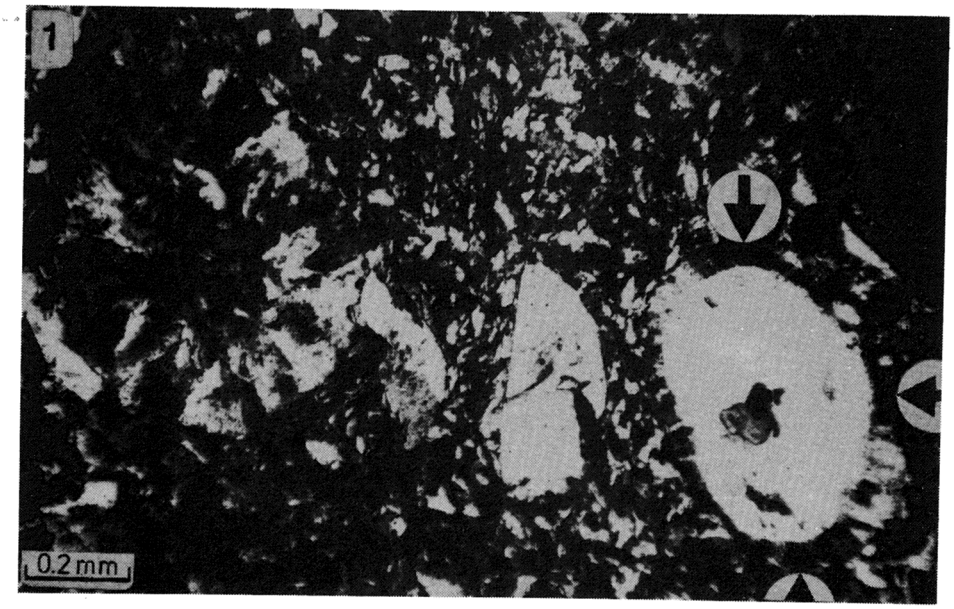

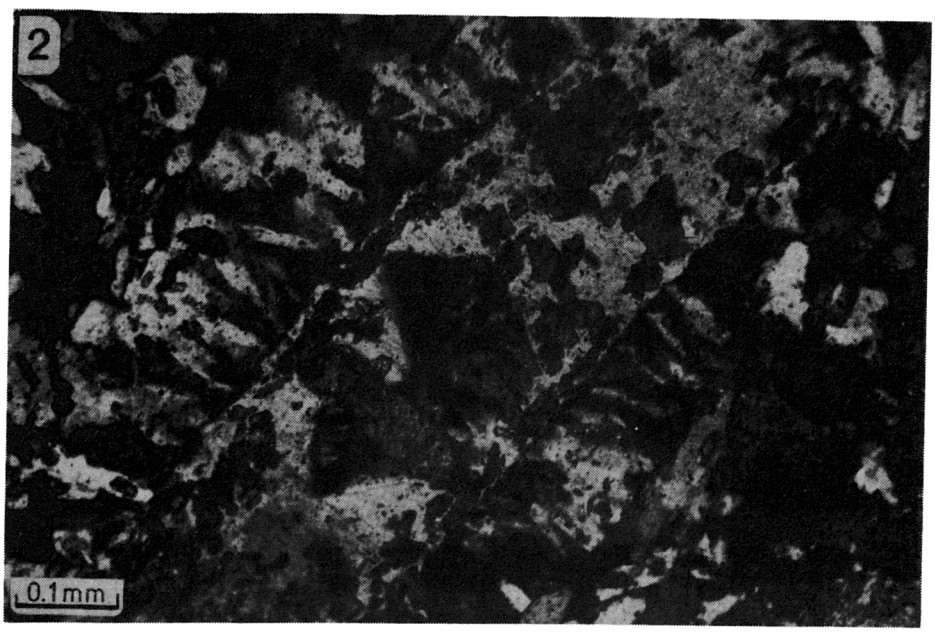

1 — Gypsum ooids (*right*), one broken along 010 and with very thin cortex (*centre*), and grain exhibiting neither apparent radial nor concentric structure (*left*); nuclei, built of round crystals, contain calcite inclusions; cortex of right ooid shows radial structure and, partly, black extinction cross (*arrowed*); polarized light, crossed nicols

2 — Gypsum ooid with flat gypsum crystal as a nucleus; calcite crystals (*dark*) are, partly, arranged parallelly with nucleus boundaries (within flat crystal probably along its growth zones); cortical crystals, rooted along flat nucleus boundaries, form rows of fan-like aggregates showing sweeping light extinction and obliterated boundaries; polarized light, partly crossed nicols

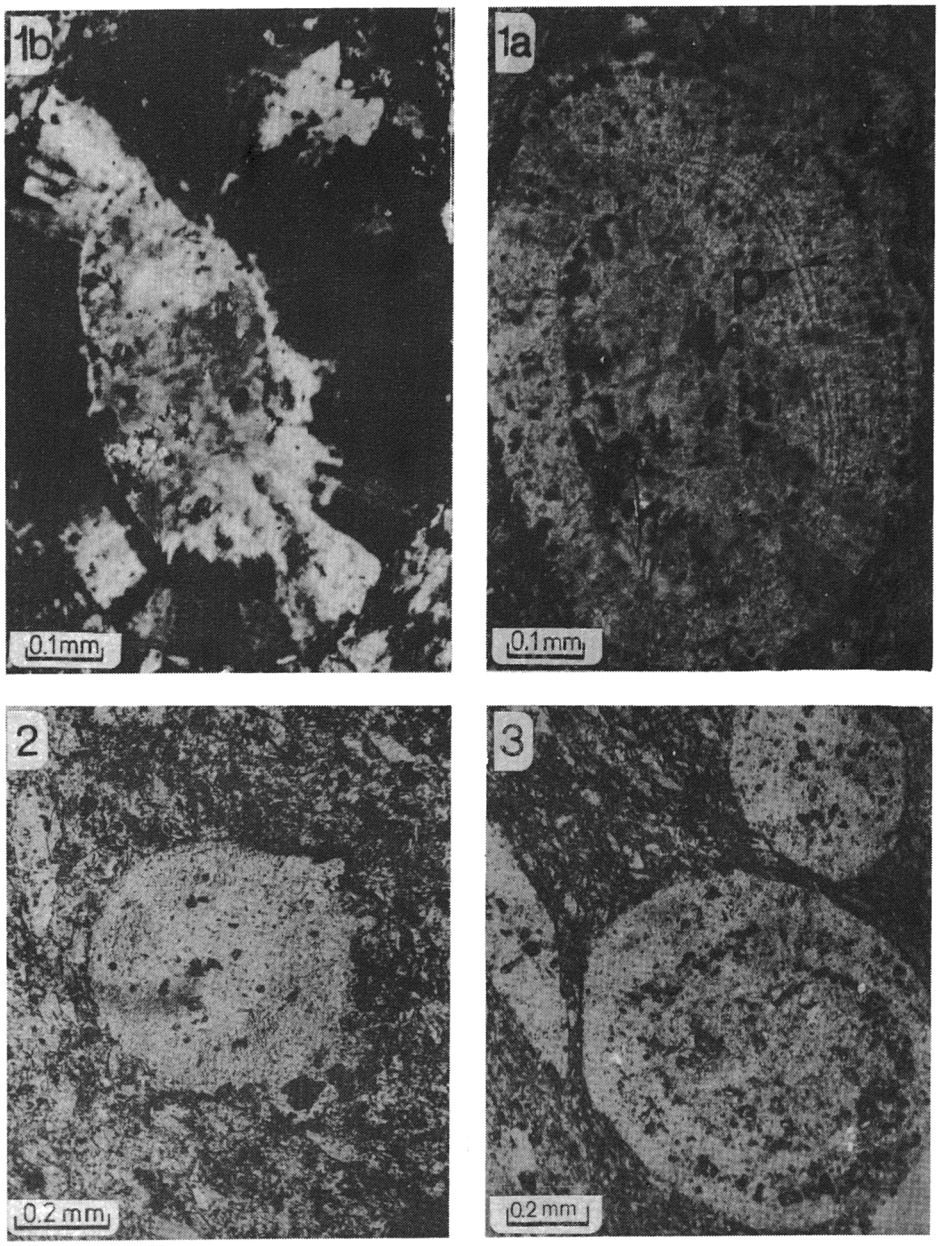

1a-1b — Gypsum ooid showing radial-concentric structure and syntaxial external rim along one side. Note: concentric discontinuous laminae (Fig. 1a: *p, gray*) formed by dense radial Becke lines; tooth-saw outer surface of rim (*top*); sweeping light extinction and black extinction cross in cortex (Fig. 1b); unclear boundary nucleus/cortex and cortical crystals syntaxial to nucleus in opposite sides of it (Fig. 1b, *top left – bottom right*); dark calcite crystals within nucleus and forming envelope at the base of external rim (Fig. 1a)
2 — Gypsum ooid showing external rim with tooth-like crystal apices; note calcite crystals (*dark*)
3 — Gypsum ooid, small grain, and lenticular crystal within carbonate-clay-gypseous matrix; note dark calcite crystals, within the ooid arranged concentrically

Polarized light, parallel (Figs 1a, 2—3) and crossed nicols (Fig. 1b)

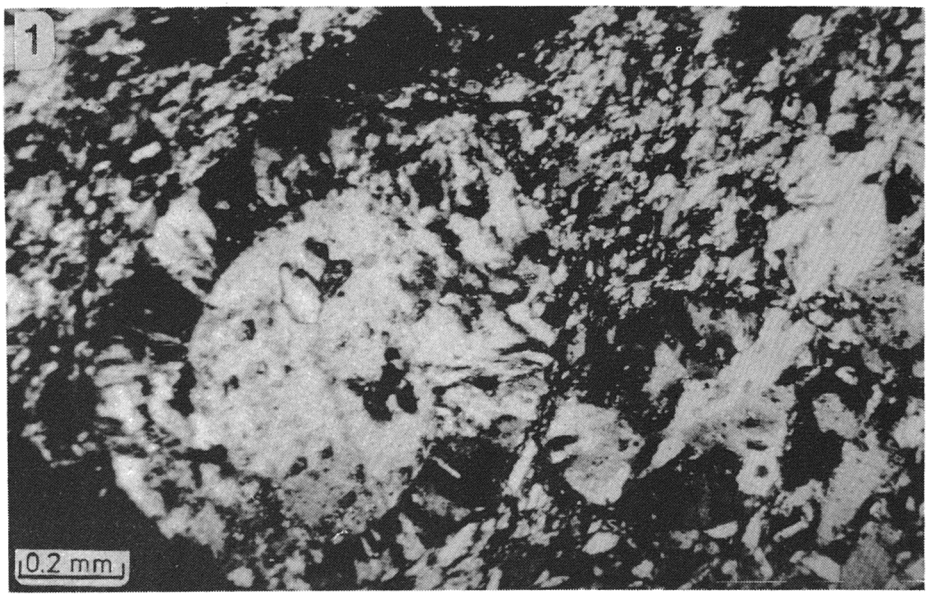

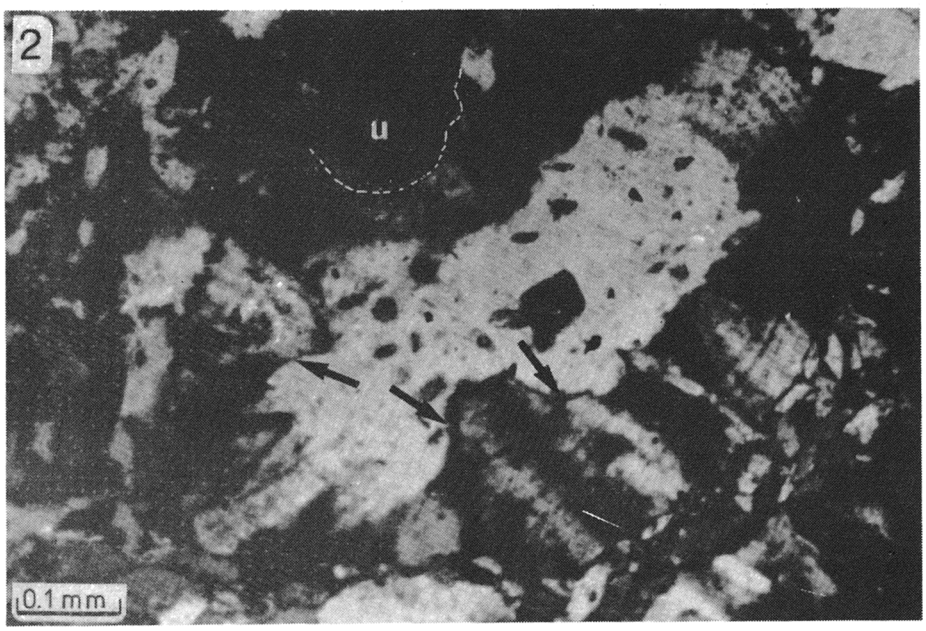

1 — Thin section from Pl. 8, Fig. 3 seen under crossed nicols; gypsum ooid with radial and chaotic boundaries of cortical crystals and small grain with quasi-radial arrangement of crystals; crystals with chaotic boundaries extinct light nearly synchronically (light areas in upper right and lower left part of ooid)

2 — Gypsum ooid (detail of Pl. 16, Fig. 1, *top left*, seen under crossed nicols) showing: aggregates of cortical crystals with fan-like sweeping light extinction and obliterated (in places sharp) boundaries; unclear boundary nucleus/cortex; cortical crystals syntaxial to nucleus in opposite sides of it; sharp boundaries (*arrowed*) between aggregates with sweeping extinction and areas of uniform extinction syntaxial to nucleus; cortical crystal uniformly extincting light (*u*); calcite crystals and concentric dark laminae corresponding to Becke lines (*see* Pl. 16, Fig. 1)

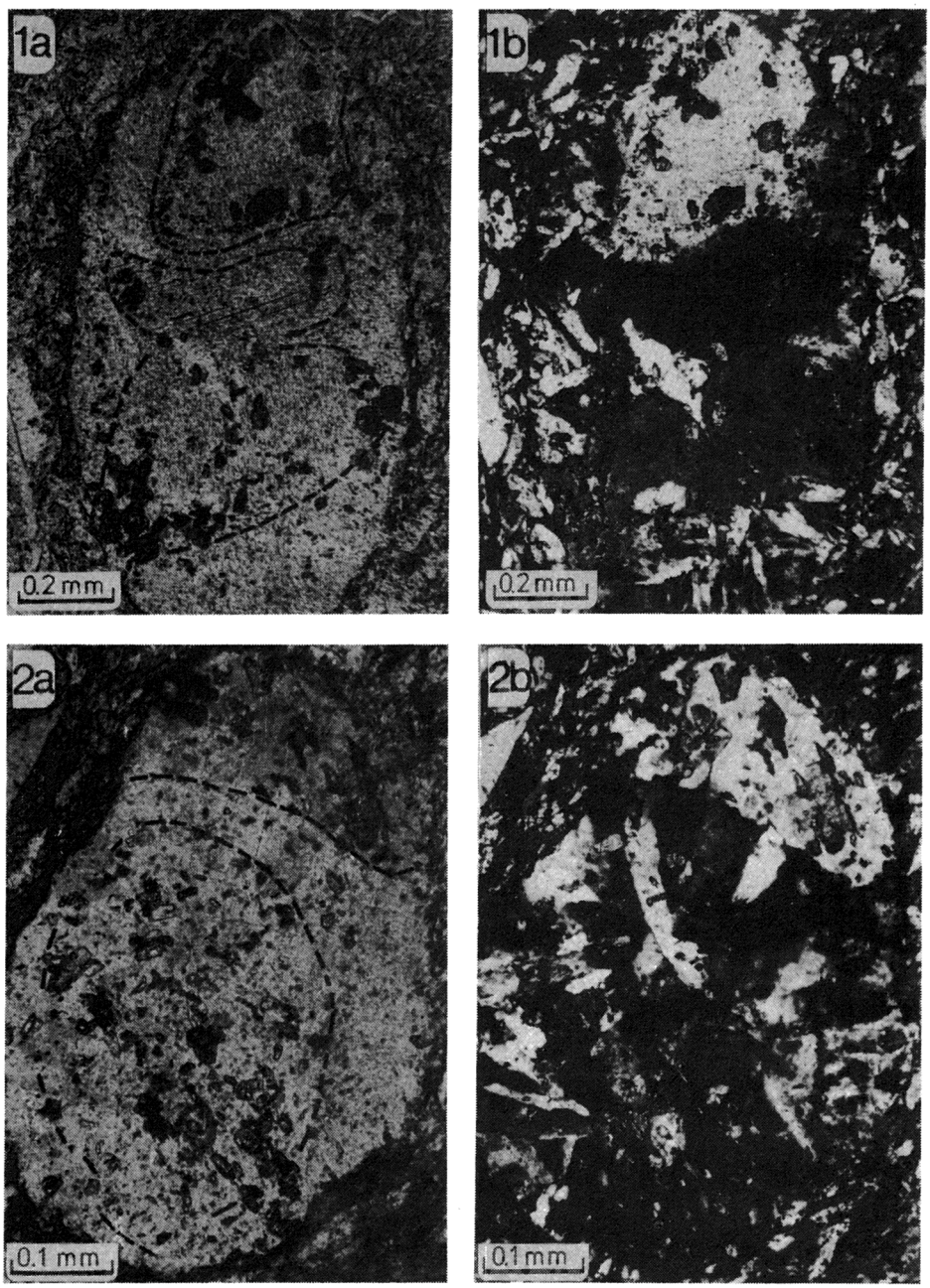

1a-1b — Gypsum ooid, probably abraded or dissolved, interpreted as complex; sweeping light extinction allow to distinguish cortices (Fig. 1a, *outlined areas*) of two cemented grains; note dark calcite crystals (Fig. 1a)

2a-2b — Abraded or dissolved gypsum ooid with nearly radial cortical crystals showing sweeping (Fig. 2a, *outlined area*) and uniform light extinction (within external rim; Fig. 2b; *light area, top*); note dark calcite crystals (Fig. 2a)

Polarized light, parallel (Figs 1a, 2a) and crossed nicols (Figs 1b, 2b)

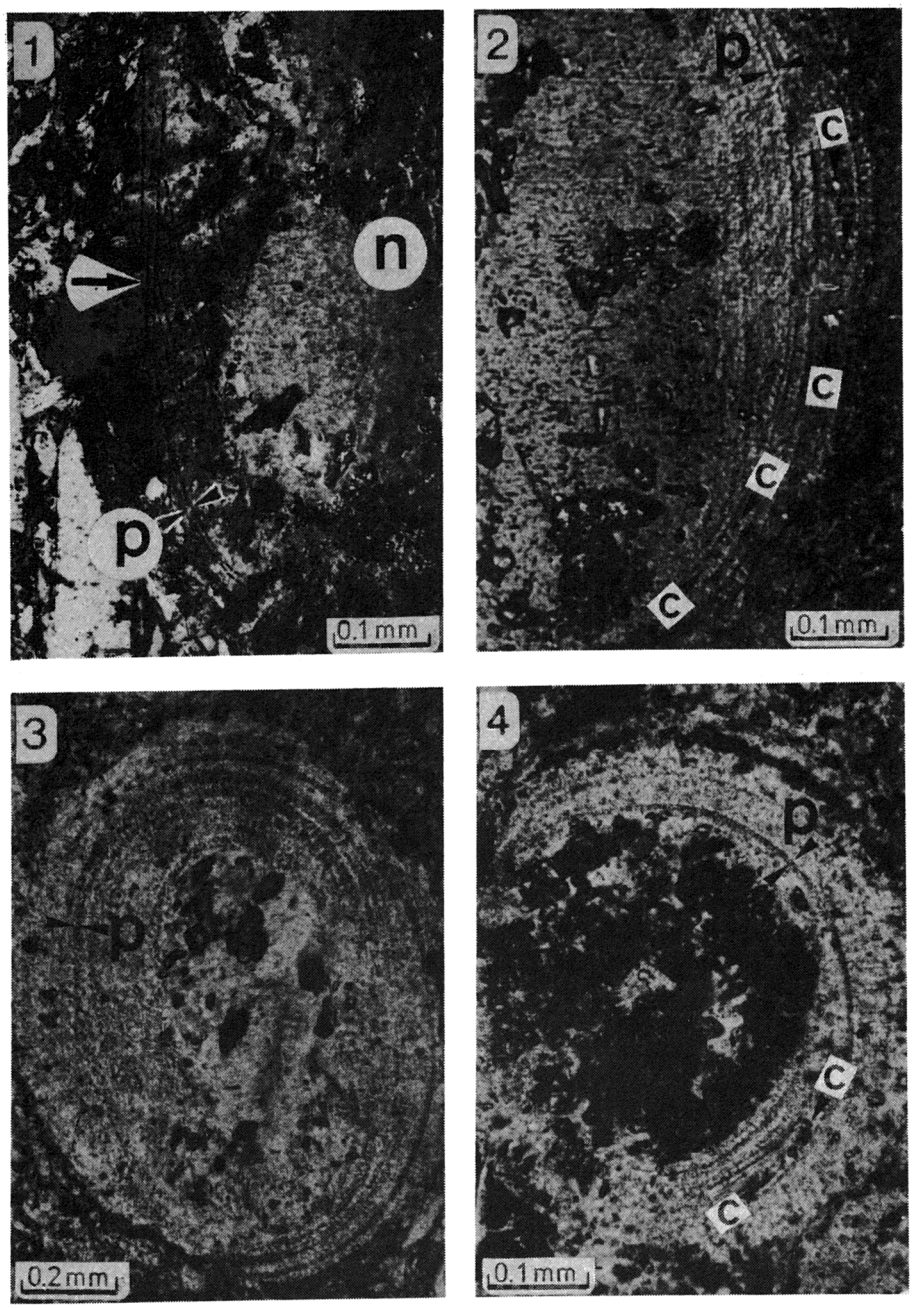

1-4 — Gypsum ooids showing concentric bands formed by: i) concentric Becke lines between zones of low referactive indices (*p in* Figs 1—2), ii) dense radial Becke lines (*p in* Figs 3—4); bands laterally disappear, coalesce (Figs 2—4) and cut each other (Fig. 1; *arrowed*), in the latter case indicating regeneration of ooid (*n* marks its nucleus); calcite crystals (*dark*) are placed within nuclei (numerously *in* Fig. 4), form envelopes (Fig. 4, *top*) and are scattered (*c in* Figs 2, 4) between bands formed by Becke lines; ooid in Fig. 3 is abraded or dissolved; in Figs 2, 4 — eccentric; polarized light; parallel (Figs 2—4) and partly crossed nicols (Fig. 1); oblique illumination (Fig. 2)

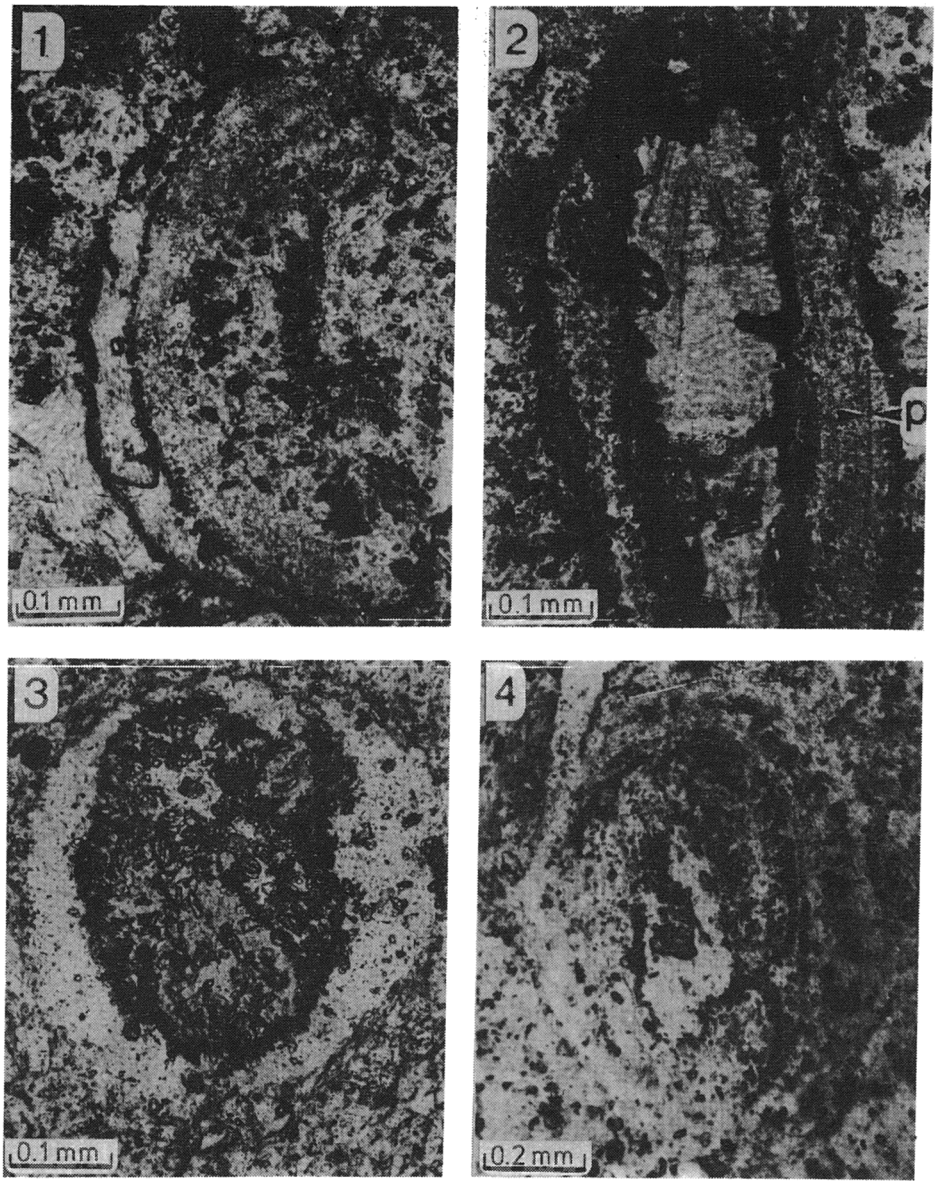

1-4 — Gypsum ooids with calcite crystals (*dark*) creating discontinuous envelopes (Figs 1—2, 4, note outer envelope formed by large crystals *in* Fig. 4) and included within nucleus (Fig. 3); wavy black envelope within external rim in Fig. 1 (*left*) is formed by opaque patches of presumably organic matter; gray lamina (*marked* p *in* Fig. 2) — by dense Becke lines; nucleus in Fig. 2 is built of a crystal previously lenticular in habit as indicated by its growth zones (*upper part*); ooid in Fig. 1 is eccentric; note prismatic calcite crystals in Figs 2—3; polarized light, parallel nicols

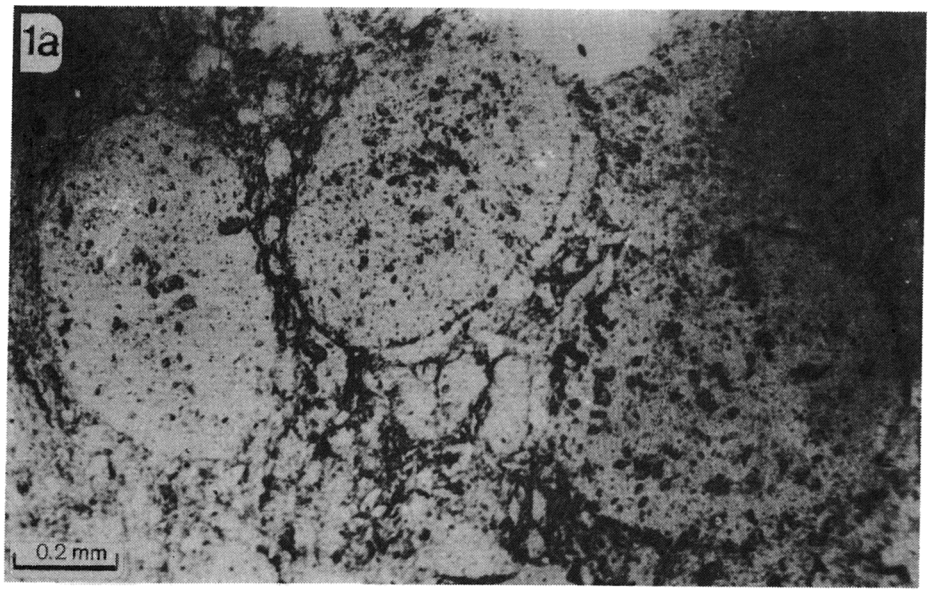

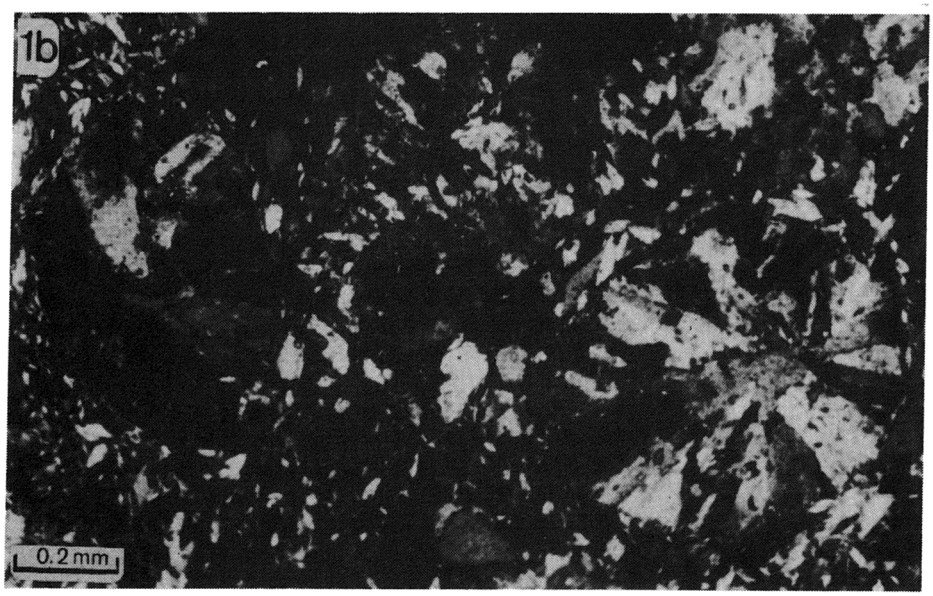

1a-1b — Gypsum grains (or ooids) containing calcite crystals (*dark*); right and left grain show quasi-radial arrangement of crystals (Fig. 1b); central grain is an abraded or dissolved ooid with concentric envelope of calcite crystals (Fig. 1a) and with nearly chaotic arrangement of gypsum crystals (Fig. 1b); polarized light; parallel (Fig 1a) and crossed nicols (Fig. 1b)

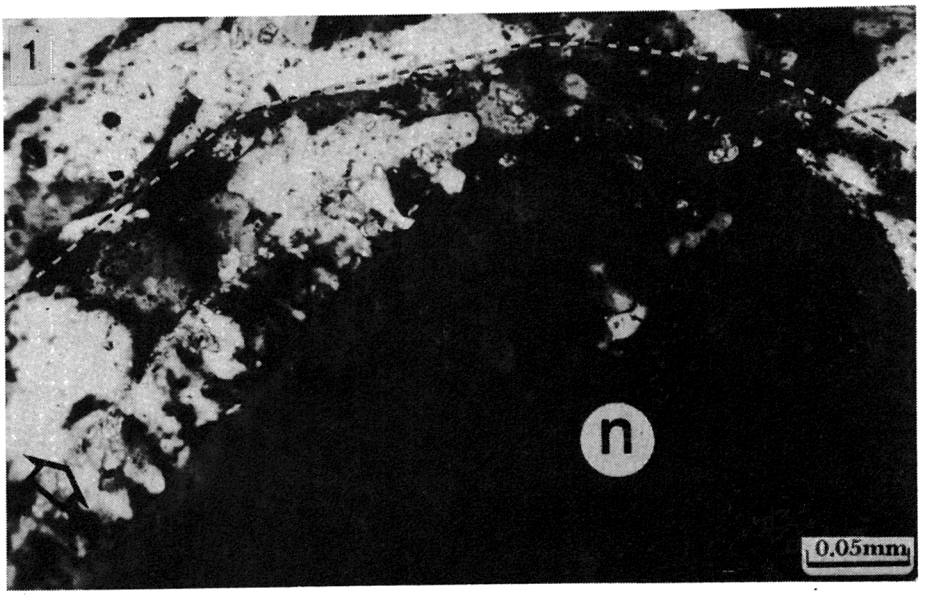

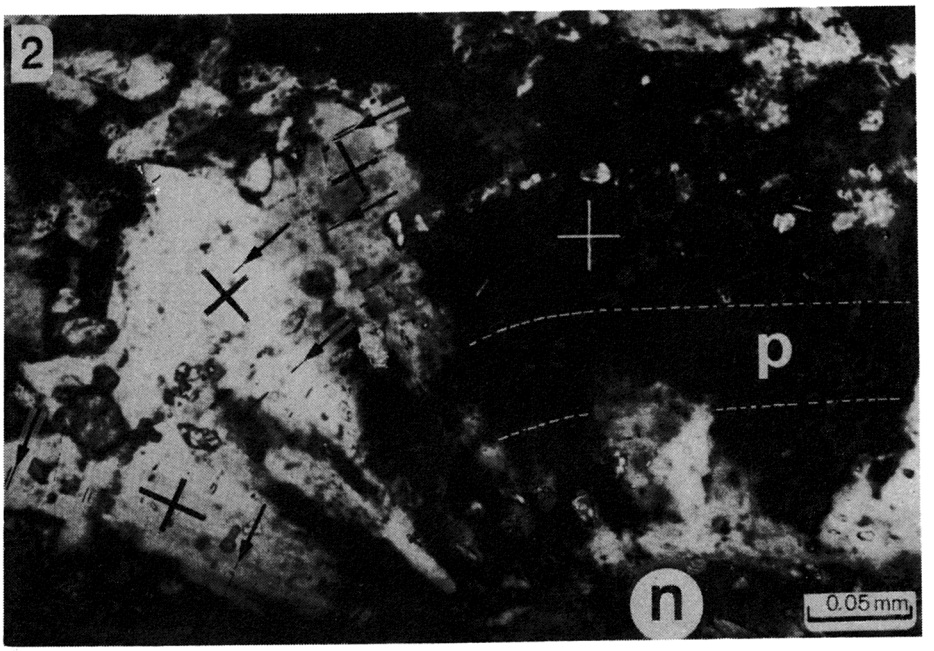

1 — Gypsum cortex coating single crystal (*n*); cortical crystals show unordered arrangement, irregular light extinction, obliterated and in places sharp boundaries; envelope of calcite crystals is arrowed, boundary of ooid — outlined; polarized light, crossed nicols

2 — Gypsum cortex (detail of Pl. 8, Fig. 1b) showing syntaxial relations with nucleus (*n*); concentric lamina of radial Becke lines (*p: outlined*); envelope of calcite crystals (*see* Pl. 8, Fig 1a); traces of 010 cleavage (*arrowed*) running along cortical layering; tooth-saw crystal apices of external rim (*left top*); radial arrangement of cortical subcrystals (= fields relatively uniformly extincting light); sweeping light extinction (crosses mark extinction positions of subcrystals)

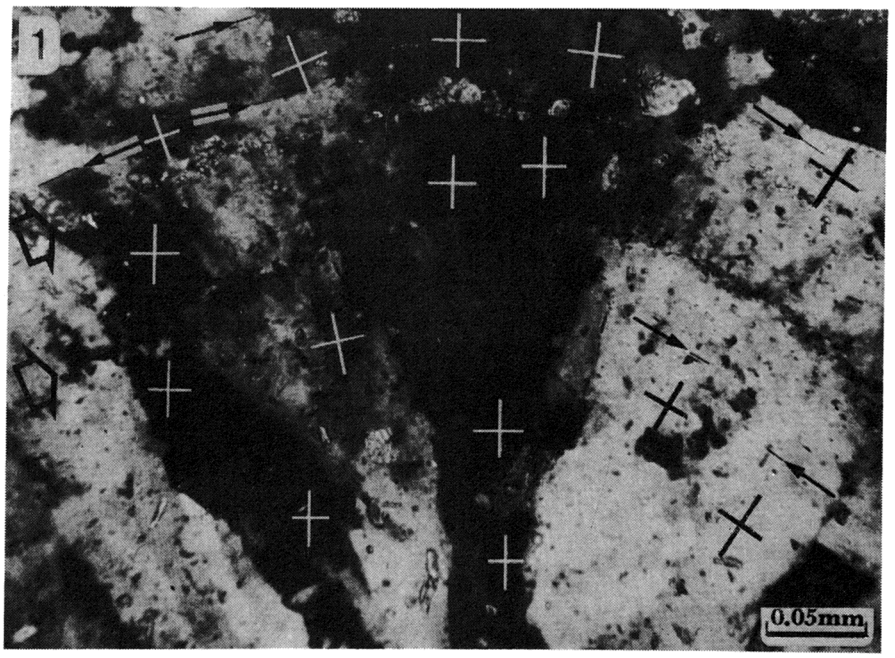

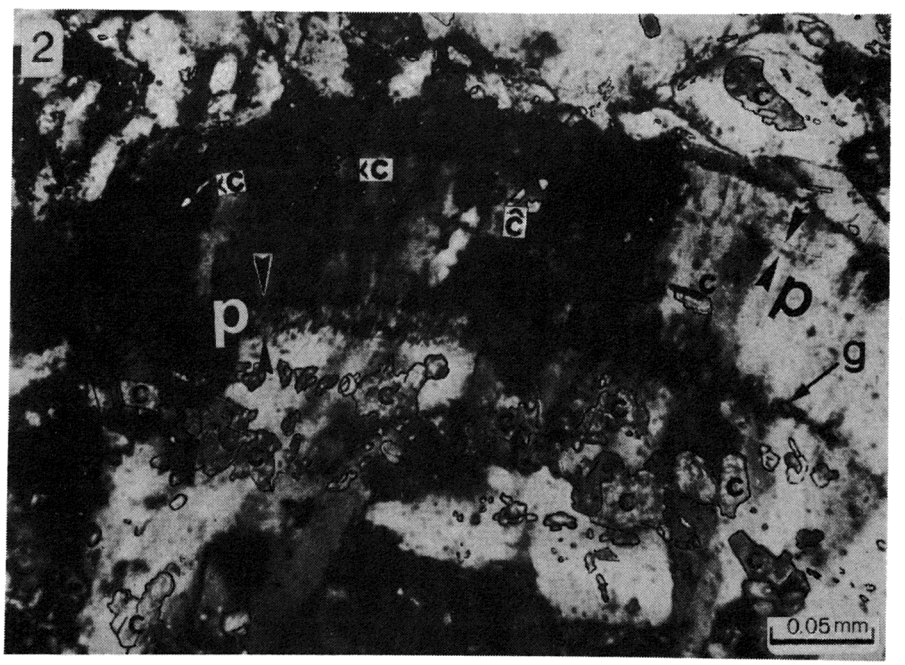

1 — Gypsum cortex showing: radial subcrystals (crosses mark extinction positions of some of them); envelopes of calcite crystals (*large, empty arrows*); traces of 010 cleavage (*solid arrows*) running along cortical layering; sharp radial crystal boundaries (*bottom*) upwardly grading into obliterated; polarized light, crossed nicols

2 — Gypsum cortex showing: concentric bands corresponding to dense radial Becke lines (*p*); tiny radial subcrystals within bands; calcite crystals (*c*) placed between bands; sharp crystal boundaries (*bottom*) grading into obliterated; single gypsum crystals (*g*); polarized light, crossed nicols

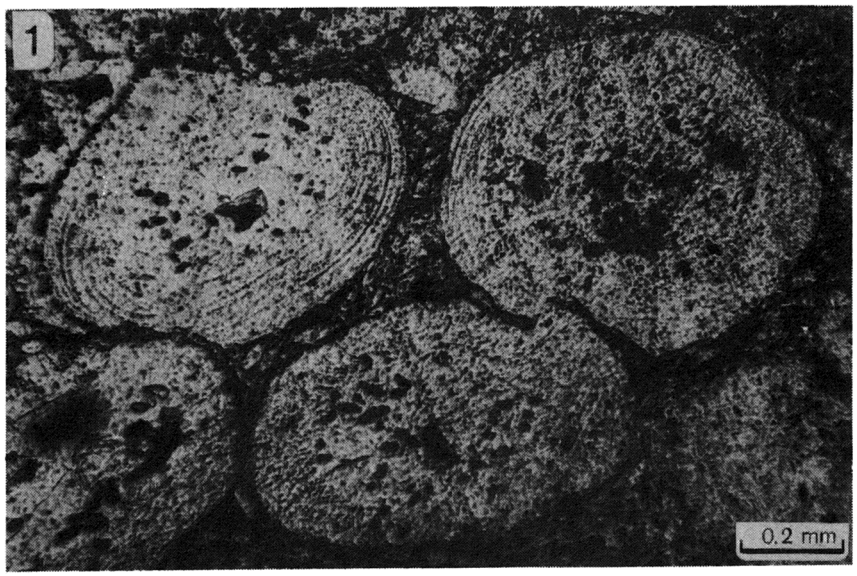

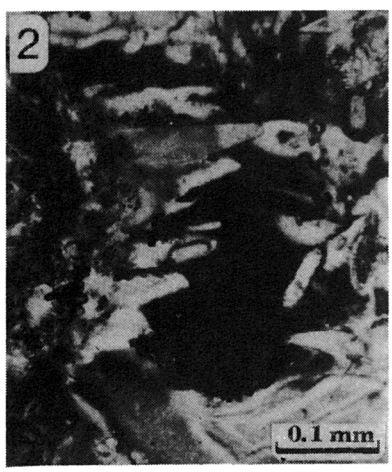

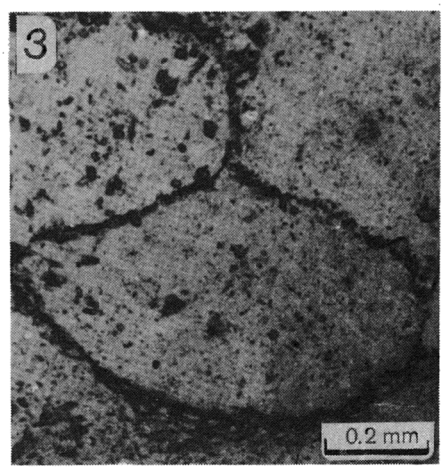

1 — Pitted gypsum ooids with smooth, dish-like (*left*) and dentate contact (*right*); nuclei and matrix contain dark calcite crystals; abraded ooid (*top left*) shows concentric lamina of calcite crystals at its upper left side, at the base of external rim; other dark concentric laminae are formed by dense radial Becke lines

2 — Pore space (*black*) in gypsum oolitic grainstone and lenticular crystals of syntaxial gypsum cement on surface of grain containing many dark calcite crystals (*left*)

3 — Pitted gypsum grains containing scarce calcite crystals

Polarized light, parallel (Figs 1, 3) and partly crossed nicols (Fig. 2)

GYPSUM GRAPESTONES

Formerly, the present authors (KASPRZYK & BĄBEL 1986) introduced the term *grapestone,* first used for clusters of calcareous ooids (*see* ILLING 1954; FABRICIUS 1977, p. 16), to describe the aggregates of gypsum ooids and grains. The aggregates comprise several grains, sometimes only 2—3 grains joined together. The largest aggregates reach the size of 1 cm. They are distinguishable in the polished sections due to the light color of the grains contrasting with the gray matrix (Pl. 5, Figs 1—2). The aggregates look as fragments of tightly packed oolitic grainstone of the upper part of the discussed layer. There is no any apparent traces of abrasion of the periphery of the aggregates. This excludes the possibility that the aggregates derived from the erosion and reworking of the older gypsum rocks. It seems that the aggregates originated from redeposition of the poorly consolidated grainy gypsum sediment. A periphery of the aggregates looks like that described from the carbonate grapestones; "the component rounded grains commonly protrude from the lumps giving an appearance resembling that of a bunch of grapes" (ILLING 1954, p. 30). The interior of some larger gypsum aggregates preserves its original porosity (Pl. 5, Fig. 1) which is also typical of the carbonate grapestones (PURDY 1963, p. 344).

The component ooids show evident pitted contacts. Such contacts in carbonate ooids are recognized as a result of pressure solution acting in unconsolidated and/or uncemented sediments (*see* RADWAŃSKI 1965, RADWAŃSKI & BIRKENMAJER 1977). BATHURST (1971, Figs 322—323) illustrated also the pitted surface between the early generation of cement and the ooid.

If the grapestones were consolidated by gypsum cement the pitted surfaces represent the pitting between the ooids and the cement. However, another possibility seems to be more probable, such as the grapestones could be consolidated by organic mucilage matter. Carbonate grapestones originate by gluing of the grains by algal mucilage and the following biochemical cementation (BATHURST 1971, p. 317; FABRICIUS 1977). Such biochemical cementation is, however, not recognized and documented in the case of gypsum. Thus the discussed gypsum grapestones, so far not described from natural environments, could be created in the same way as the most initial forms of carbonate grapestones.

MODEL OF OOID GROWTH

The fabric of cortices can reflect the environmental conditions of their accretion allowing to interpret the history of growth of the individual ooid. Taking into account the fabric of cortical gypsum layers it is thought that the ooids were formed under three basic environmental conditions. Two of these

conditions correspond to the porous and massive cortical layers, the third one was mainly destructive for the cortices. The repetition of these conditions is reflected in the most fully developed cortices by successive massive and porous layers as well as by their spatial relations. The original cortical fabric was subsequently diagenetically modified.

MODERATE AGITATION IN SUPERSATURATED BRINE

The porous cortical layers originated in moderately, presumably wave agitated brine supersaturated in respect of gypsum (Text-fig. 5; growth stage *1*). It is experimentally proved that the agitation occurring in supersaturated solution promotes the spontaneous nucleation and it largely increases the growth rate of crystals (*see* discussion of literature *in* HALLEY 1977, p. 1108). In such environment the new crystals could nucleate on the ooid surface or, when nucleating within the brine, could be collected on the ooid surface according to the *snow-ball mechanism* (*see* BATHURST 1971, HALLEY 1977, FABRICIUS 1977). The crystals rooted to the ooid surface could grow rapidly. Quick radial growth of crystals dominated over their tangential spreading and large intercrystalline voids oriented radially could be formed. Continuous formation of new cortical crystals and their rapid growth produced porous fabric of the originated layer.

The mechanical abrasion of ooids occurring in such environment acted against radial (syntaxial) growth of cortical crystals by mechanical destruction of their apices (*see* DAVIES, BUBELA & FERGUSON 1978). In such a way, in supersaturated solution, a large amount of microcrystalline debris was produced, which, when suspended in the brine, was a potential source of nuclei for the new cortical crystals originating according to the snow-ball mechanism. It was abrasion which controlling round shape of ooids and even growth of cortical layers, finally produced perfect concentric structure of gypsum cortical layers (*see* HELLER, KOMAR & PEVEAR 1980). It is to note that similar porous fabric occurs in the all marine aragonitic ooids which originate in highly agitated environments (RICHTER 1983).

WEAK AGITATION AND LACK OF AGITATION IN SUPERSATURATED BRINE

The massive cortical layers originated in supersaturated but relatively less agitated brine (Text-fig. 5; growth stage *2*). In such conditions relatively less new cortical crystals were produced. The pre-existing crystals could grow both radially and laterally and could create larger forms coalescing with each other and displaying competitive growth fabric (*see* BATHURST 1971). Such fabric was reported from radial aragonite ooids of the Great Salt Lake (SANDBERG 1975) originated in relatively low energetic environment, as well as from the ancient radial calcitic ooids (SIMONE 1983, p. 342) which are believed to be low

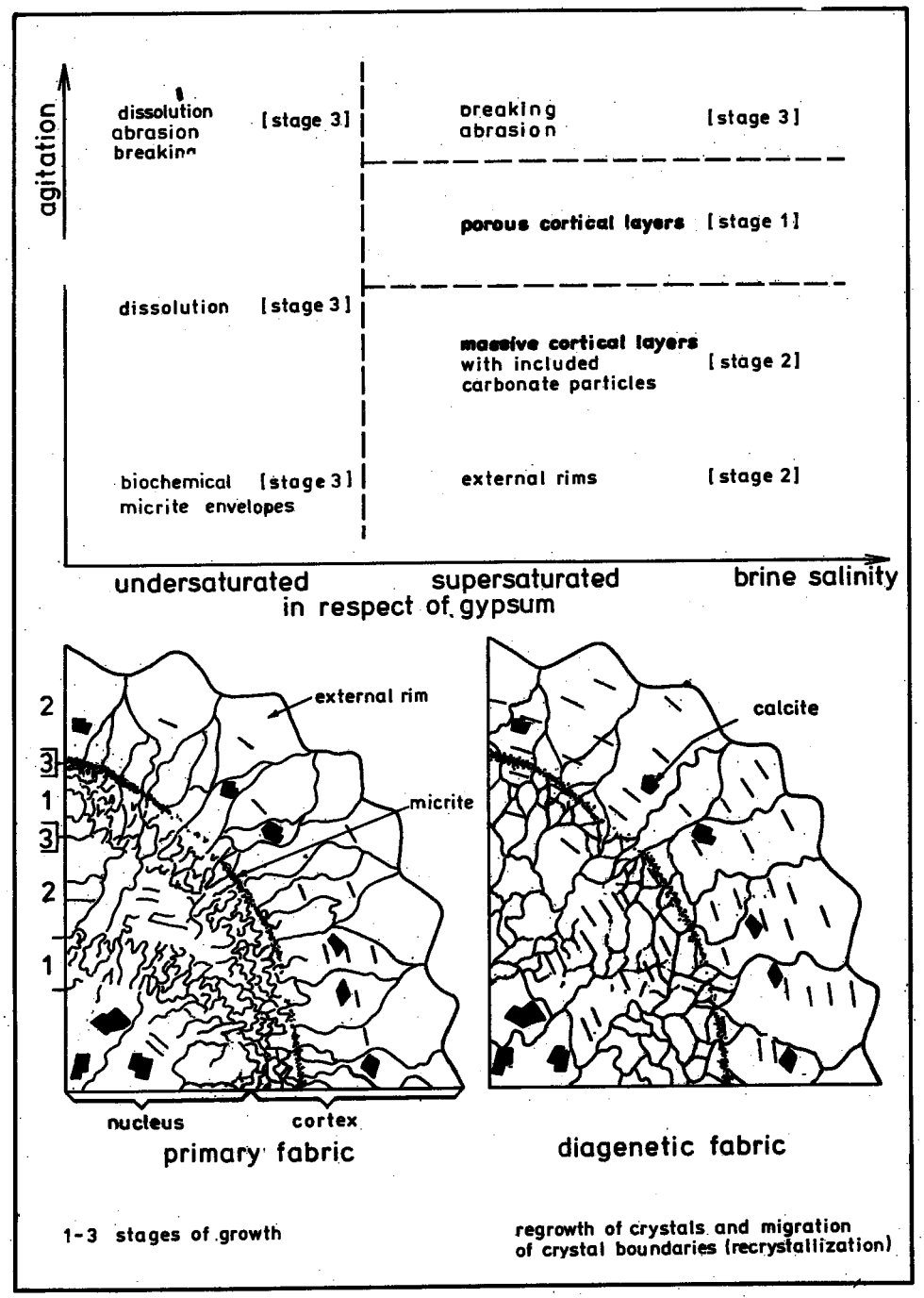

Fig. 5. Scheme and diagram illustrating model growth conditions of the investigated gypsum ooids; detailed explanation in the text

energetic. Such a fabric is typical of any crystal druses originating in the closed, extremely calm environment.

When this stage of cortical growth followed the first one, the pre-existing lens-like cortical crystals growing syntaxially in the radial direction, thicken, enlarge laterally and gradually coalesce, often merging into larger polycrystalline units. The intercrystalline spaces gradually disappear and typical compromise boundaries are developed (*see* Pl. 27, Figs 1—2 *and* Pl. 25, Fig. 2).

The massive cortical layers accreted relatively quicker on upper parts of the ooids resting on the bottom. Because of that the ooids grew eccentric, sometimes developing the asymmetric massive cortex or external rim only on one flattened side of a nucleus (the ooid in Pl. 5, Fig. 3 is shown in its growth position). Recent quiet-water calcareous ooids described by FREEMAN (1962) tend to grow asymmetrically in the same manner because a rounding effect of abrasion is lacking.

The external rim of the ooids can be considered as forming in extremely calm environment directly on the bottom or within the loose unconsolidated gypsum sediments, in the latter case similarly as syntaxial cement. The tooth-like crystal terminations observed on the outer surface of the rims prove the lack of abrasion in time of their formation.

The calm environment enabled in some periods the carbonate particles to settle and adhere to the ooid surface and to be incorporated by the growing cortical crystals, strictly according to the snow-ball mechanism of oolitic accretion. The particles usually settled on the upper sides of the resting grains and hence they usually do not envelope the whole ooid.

SCHREIBER (1978, p. 66) interpreted the carbonate envelopes in gypsum ooids from the Apennines as representing "periods of refreshment perhaps with associated algal growth causing the formation of carbonate". Some of the micritic envelopes in the investigated ooids (Pl. 6, Fig. 1; Pl. 12, Fig. 4) can have similar origin and can result from colonization of the ooid surface by algae in time of refreshment. Laminae of opaque matter of presumed organic origin are included within some external rims (Pl. 12, Fig. 1). Lens-shaped habit of cortical crystals can indicate the existence of organic compounds in the brine (*see* CODY 1979; KIROV 1982; *and references in* BĄBEL 1990), additionally supporting the above opinion.

However, in most cases the cortical carbonate particles represent not micrite but grains of larger dimensions, up to 0.05 mm, which are randomly scattered and do not form continuous envelopes. The carbonate crystals do not exhibit fabric or orientation typical of precipitation on a substrate. The cases, in which single minute prismatic crystals of carbonate are oriented radially, are very scarce. The simplest explanation of the derivation of the discussed carbonate grains is their accretion according to the snow-ball mechanism. It is to note that, according to the authors' opinion, such grains are the indicator of calm environment of growth.

The above interpretation concerns calcite particles included within cortices; derivation of carbonate crystals placed within the nuclei and matrix will not be discussed.

AGITATION AND LACK OF AGITATION IN UNDERSATURATED BRINE; HIGH AGITATION IN SUPERSATURATED BRINE

The ooids were subjected to destruction in time of fall of saturation (refreshment periods) and/or of extremely high agitation (Text-fig. 5; growth stage *3*). These episodes are reflected by broken, abraded or dissolved, and regenerated ooids as well as by numerous coalescing and pinching out of cortical layers. As dissolution of gypsum in time of refreshment is obvious, the abrasion of gypsum grains in supersaturated agitated brine needs a discussion.

In the case of aragonitic ooids agitation can increase the abrasion but can also increase the growth rate of cortical layers (*see* BATHURST 1971, pp. 314—316; HALLEY 1977). Many authors show that high agitation is necessary for growth of aragonitic ooids (*see* ŁABĘCKI & RADWAŃSKI 1967; BATHURST 1968, 1971, pp. 301—302; FABRICIUS 1977, pp. 47—48; SIMONE 1981), however problem of balance between abrasion and precipitation in growing aragonitic cortices is still unsolved. In the case of uncalcareous ooids influence of high agitation on their growth is weakly known. The present authors believe that the discussed ooids grew in shallow, rather moderately agitated brine, similarly as halite and mirabilite ooids (WEILER, SASS & ZAK 1974; LAST 1984, 1989). On the other hand, it is unquestionable that only high agitation can produce large amount of broken ooids as well as can rework them into abraded (ŁABĘCKI & RADWAŃSKI 1967).

Taking this into account the authors distinguished the destruction stage in the area of supersaturated brine in Text-fig. 5.

As it was suggested above, in time of refreshment on some less mobile grains micritic envelopes could be formed, biochemically precipitated by algae in the manner described by SCHREIBER (1978).

HISTORY OF GROWTH OF SOME OOIDS

The history of growth of those ooids which show unclear boundary nucleus/cortex, well developed concentric porous bands and external rim can be reconstructed as follows. The initial growth on a small nucleus took place mainly in suspension and was very weakly affected by abrasion. Thus syntaxial radial growth dominated and concentric structure was not produced (*see* HELLER, KOMAR & PEVEAR 1980). When the ooid grew larger it was more affected by abrasion. The ooid, due to increasing weight, was agitated and grew mainly in the bottom among other larger grains, so in place where both frequency and energy of grain collisions were greater (*see* BATHURST 1968). Thus, the even concentric cortical layers could be formed (*see* HELLER, KOMAR

& PEVEAR 1980). Finally, when the ooid attains considerable size and weight, it could rest for a longer period as unmoving grain on the bottom or within loose grainy sediments. Then, the external rim could grow, in the manner resembling syntaxial cements.

ORIENTED GROWTH OF CORTICAL CRYSTALS

The cortical crystals grew having their axes *b* oriented normally to the substrate. To the knowledge of the present authors such orientation is exceptional among gypsum crystals, especially in those forming druses.

As a rule a gypsum crystal grows having the axis *b* oriented tangentially to the growth surface, *i. e.* with the 010 planes less or more perpendicular to the substrate (*see* CATALANO, RUGGIERI & SPROVIERI 1978; SCHREIBER 1978; WARREN 1982). Single crystals with the 010 plane parallel to the surface of growth are observed in druses of a lenticular gypsum. The exceptional case in which the whole crystals were oriented in such a way was recognized by KREUTZ (1916) in the vein of the fibrous gypsum from Swoszowice, in the Fore-Carpathian Depression in southern Poland (*see* Text-fig. 1*A*). However, in other fibrous gypsum veins the 010 plane is typically oriented perpendicularly to the growth substrate (*see* KREUTZ 1916, MACHEL 1985). In the gypsum ooids from Italy, SCHREIBER (1978, Fig. 3.43) recognized the growth zones of the 120 prism faces within the external overgrowth rims so it seems that the cortical crystals have their 010 planes oriented radially.

Parallel orientation of crystals growing together on the surface can result from their competition for space in which the crystals with the direction of the quickest growth, corresponding to the longest dimension of their habit, oriented normally to the substrate survive (BATHURST 1971, p. 422; KENDALL & BROUGHTON 1978). If the radial orientation of axis *b* resulted from such competition the individual crystals should have their habit apparently elongated parallel to the axis *b*. Such habit is scarcely recorded among gypsum crystals (*see* review of gypsum morphology *in* GOLDSCHMIDT 1918). The elongation parallel to the axis *b* occurs in some lenticular crystals but it is never strong (*see* MASSON 1955, KIROV 1982). Probably due to the rarity of such habit gypsum druses with the 010 planes tangential to the substrate are not recorded. The competition for space in the gypsum druses leads as a rule to the growth with the 010 planes perpendicular to the substrate since for gypsum typical is tabular or prismatic habit (SIMON & BIENFAIT 1965, CODY 1979) always being elongated perpendicular to the axis *b*.

The lens-shaped habit of investigated cortical crystals allows to interpret their orientation as resulted from the competitive growth. However, this does not seem to be a satisfactory explanation. In case of the lens-shaped habit every axis lying in the plane of flatness of the lenticular crystal (*b* is only one of them) is in the same degree favored in radial orientation in time of the competitive growth. The competitive growth structures were recognized mainly in the massive parts corresponding to the external rim. In the porous cortical layers continuous creation of new crystals should lead to apparent deviations in tangential orientation of the 010 planes but it was not observed. It seems that a lot of cortical crystals started to grow with the 010 plane oriented tangentially to the substrate. From these reasons, it is believed that the orientation of cortical crystals results not only from their competition for space but also from the fact that they were initially created on the surface of the ooid with their axes *b* oriented radially.

Cortical crystals generally could be created in two ways: *i*) by nucleation on the ooid surface, (*ii*) by attachement of a pre-existing nucleus or microcrystal to the ooid surface.

The first way of a creation is typical of the crystals growing in natural environments (BATHURST 1968). The second one, known as the snow ball mechanism (in the broad meaning), was first postulated by SORBY (1879, *fide* BATHURST 1971) and now it has several modifications (*see* HALLEY 1977).

The orientation with 010 tangential can be realized by surface nucleation when the original cluster of atoms is deposited on the ooid surface preferentially with a symmetry plane, corresponding to the 010, parallel to the substrate. Such type of nucleation for calcium carbonate ooids was discussed by LIPPMANN (1973). DAVIES, BUBELA & FERGUSON (1978) showed experimentally that some organic compounds, present in the water, are necessary for creation of the new cortical crystals. The organic compounds form membranes coating the ooid surface and provide substrate required for nucleation of new crystals.

The second way of the creation of cortical crystals involve deposition of small microcrystals on the surface of the ooid. It means that the microcrystals are formed outside of the ooid, theoretically as both nuclei and detrital debris. The microcrystals can be welded to the ooid surface, according to SORBY (1879, *fide* BATHURST 1971) by forces of mechanical adhesion, according to SHEARMAN, TWYMAN & ZAND KARIMI (1970) and HALLEY (1979) by organic mucilage covering the ooid, and according to BATHURST (1971; pp. 308, 310), when microcrystals are of colloidal size, not larger than hundreds of Ångstroms, by forces of adsorption.

A striking coincidence of the tangential 010 plane with a plane of the perfect cleavage of cortical crystals suggests the following origin of the orientation of cortical crystals.

Presumably the gypsum ooids grew in the areas of wave agitation (KASPRZYK & BĄBEL 1986), similarly as recent halite and mirabilite ooids (WEILER, SASS & ZAK 1974; LAST 1984, 1989). In such an environment, gypsum crystalline debris were continuously produced by abrasion of gypsum crystals and grains. Such debris, suspended in dense brine, probably were mainly composed of cleaved fragments flattened along the 010 because gypsum crystals break preferentially along this direction of perfect cleavage. This crystalline debris were the source of nuclei for the new cortical crystals.

The gypsum cortical crystals could originate strictly according to the hypothesis proposed by BATHURST (1968; 1971, p. 310) for the tangential aragonitic ooids. He assumed that pieces of microcrystalline aragonitic debris, produced by abrasion and suspended in brine, will be flatted in a plane containing the crystallographic axis *c*, because of the strong 010 and 110 cleavages of aragonite. These microcrystalline pieces of colloidal sizes may become adsorbed to the ooid surface preferentially with the axis *c* tangential, since the area of contact will thus be greatest. Such oriented adsorption of crystal nuclei explains the tangential position of the axis *c* observed in the cortices of the marine aragonitic ooids originated in agitated brine. The same argumentation can be shown for the studied gypsum ooids.

The above interpretation explains the orientation of newly created cortical crystals. It is to emphasize that within the cortices the radial syntaxial growth evidently dominated, having been associated with splitting and coalescing of

the crystals. This growth produced radial polycrystalline rays or bundles of crystals nearly parallelly oriented. Such rays or bundles, observed under a scanning microscope, are probably represented by fan-like aggregates of subcrystals in polarized light. Their growth in many aspects was similar to the growth of calcite crystals described by KENDALL & BROUGHTON (1978) from speleothems. Similarly, the fabric ot the gypsum cortices can be explained as a result of competitive growth of the radial polycrystalline rays or bundles combined with their splitting and coalescing, as well as with creation of new cortical crystals

DIAGENETIC MODIFICATIONS

The numerous pitted structures observed in the oolitic layer (Pl. 2, Fig. 3; Pl. 3, Fig. 6; Pl. 4, Figs 1—6; Pl. 5, Fig. 1; Pl. 16, Figs 1 and 3) record the pressure-solution processes probably of the compactional nature (*see* RADWAŃSKI 1965). The pitted structures are the most pronounced within the oolitic grainstone (Pl. 1, Figs 1—2). It seems that together with the pressure dissolution the growth of gypsum crystals occurred in the pores within the grainstone. The crystals grew syntaxially on the ooid surfaces in the drusy manner now being undistinguishable from the cortical crystals of the external rims. These cement crystals have lens-shaped morphology visible in preserved open pores (Pl. 16, Fig. 2).

The ooids of the grainstone, which was evidently affected by the pressure solution and cementation, show under a scanning microscope a massive fabric, interpreted herein as diagenetic (Pl. 30, Fig. 2; Pl. 31, Figs 1—2; Pl. 32, Figs 1—2). In that fabric the cortical crystals exhibit migrating boundaries unlike the straight radial boundaries in the porous cortices.

The present authors believe that together with the pressure solution the regrowth of the cortical crystals took place eliminating the original micropores and finally producing diagenetic massive fabric. The regrowth was probably followed by slight boundary migration, which created larger crystals or polycrystals as in the classic model of recrystallization (*see* BATHURST 1971). The new diagenetic fabric differs from the original one by lacking of porosity, relatively larger crystal sizes and migrating character of crystal boundaries, which are not radial and straight.

All of these diagenetic features are practically undistinguishable in polarized light from the primary ones. The cortical crystals modified by recrystallization still preserve their original orientation (radial position of the axis *b*) and they look similarly under a polarizing microscope as the unmodified. Only the lack of cortical bands formed by Becke lines, indicating existence of pores, and coarse-crystalline structure can suggest recrystallization. Such bands, in fact, are relatively scarce within the dissussed grainstone.

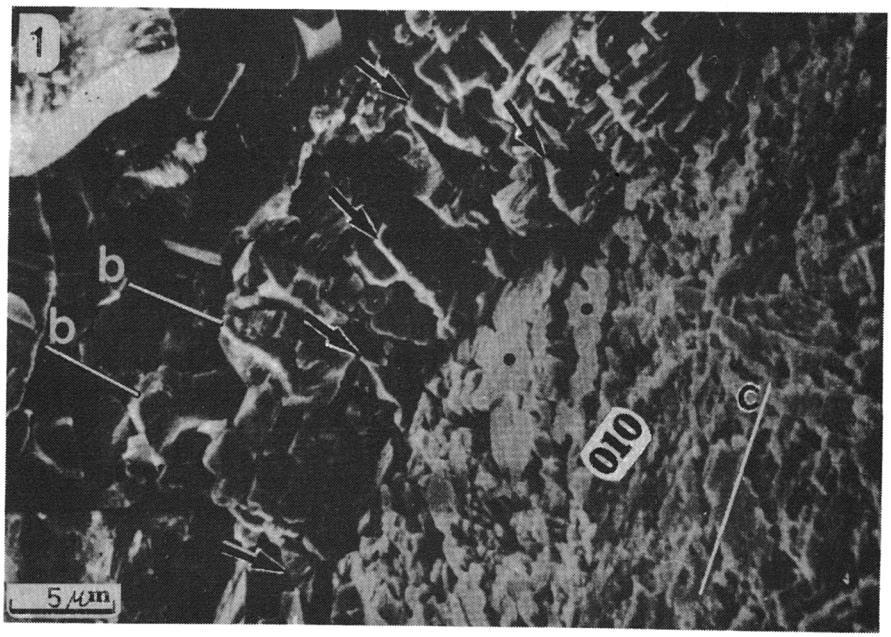

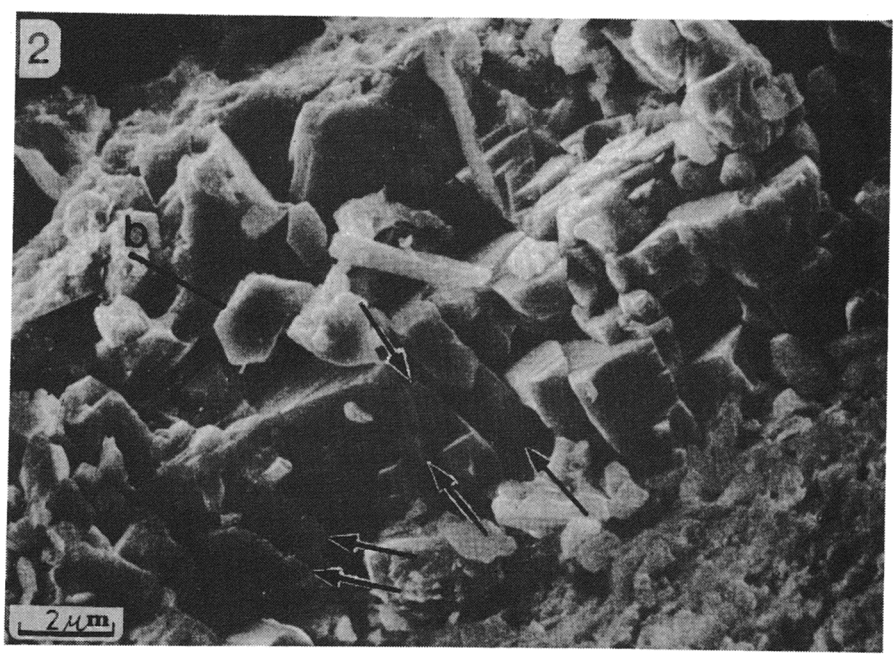

1-2 — Fracture surfaces of gypsum porous cortices (Fig. 1 — detail of Pl. 21, Fig. 1, *top left*); 010 cleavage planes are parallel (crystals — perpendicular) to cortical layering; lenticular crystals flattened perpendicularly to plane of photo are arrowed, flattened along plane of photo have their crystallographic axis *b* marked; crystals are arranged parallelly in groups and aggregates, some of them massive (*marked by points;* Fig. 1); tooth-saw boundary of aggregates with shown axes *b* is seen in Fig. 1; the axis *c* is marked in Fig. 1, interpreted from traces of cleavage, morphology of crystals and pores resembling negative gypsum crystals; scanning electron micrographs

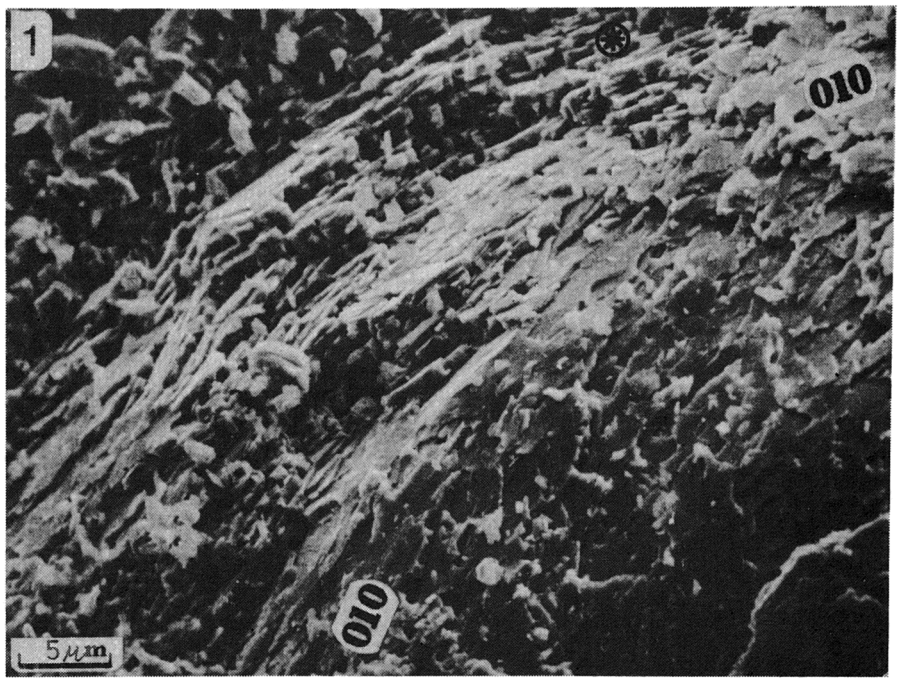

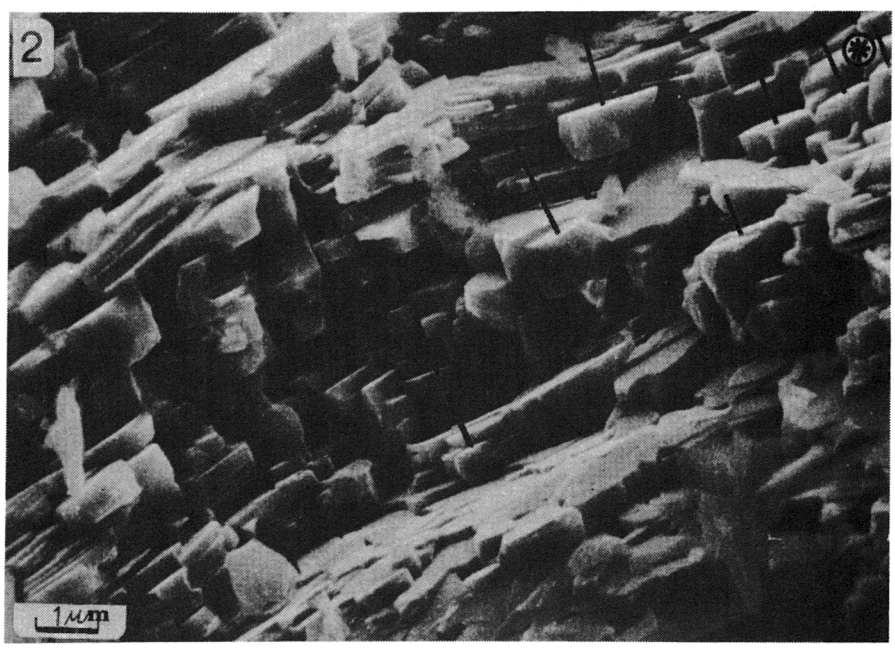

1 — Surface of gypsum ooid, exposed by splitting off outer envelope along 010 cleavage; scanning electron micrograph

2 — Detail of Fig. 1 (*asterisked*) showing: radial crystals with nearly parallel 010 cleavage planes running along cortical layering; lenticular habit of some crystals (those flattened along plane of photo have their axis *b* marked by lines)

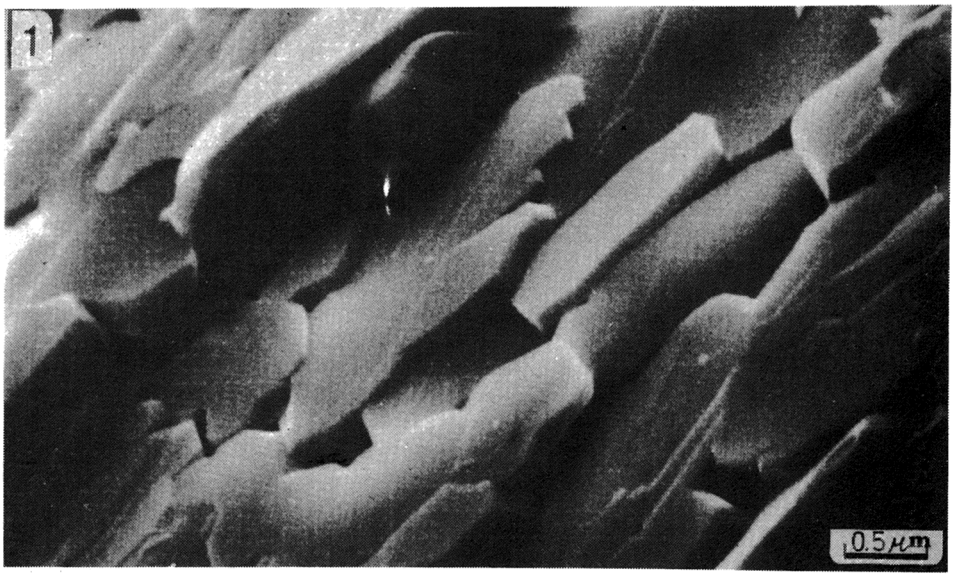

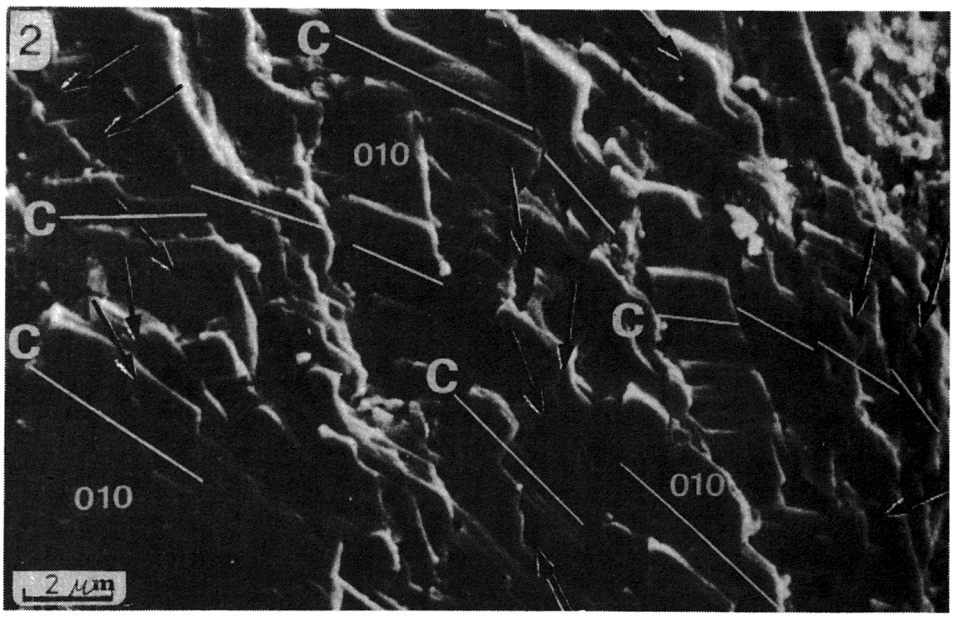

1 — Surface of gypsum cortex (the same sample as in Pl. 18); upper surface of crystals is probably 010 cleavage plane, which is not exactly flat within separate crystals presumably due to their polycrystalline structure; note crystal (*top centre*) differently oriented than the others; scanning electron micrograph

2 — Surface of gypsum cortex built of elongated crystals forming fan-like aggregates; positions of crystallographic axis *c* are shown as parallel to traces of 100 cleavage on 010 planes; pores (or etch pits) resembling negative gypsum crystals are arrowed; scanning electron micrograph

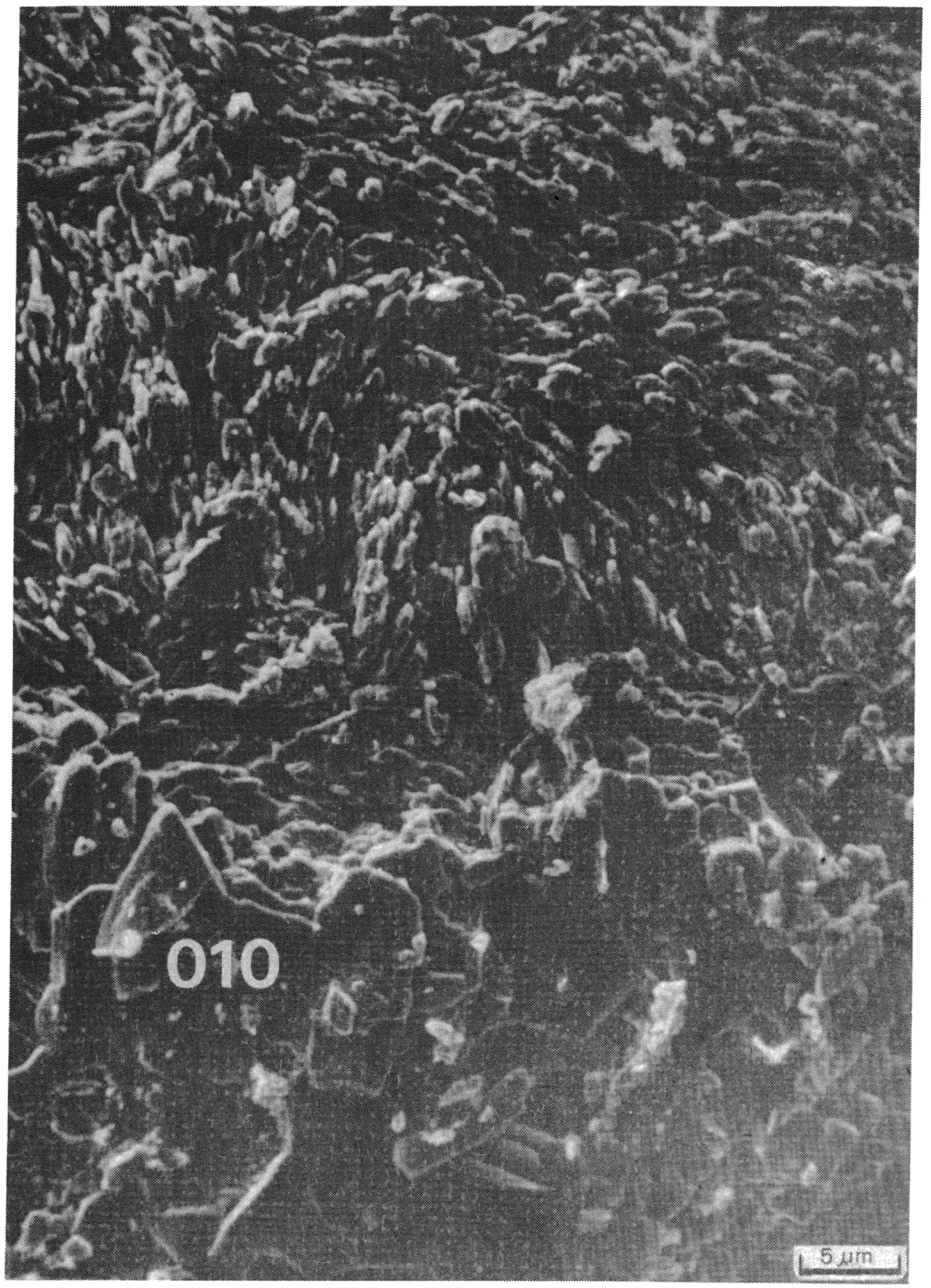

Surface of gypsum porous fine-crystalline cortical layer (*top*) covered by massive and coarse-crystalline layer (*bottom*); crystal surfaces parallel to plane of photo represent mainly 010 cleavage plane; elongated, lens-shaped crystals form groups and aggregates of sub-parallel crystals, which penetrate each other and create wavy patterns; scanning electron micrograph

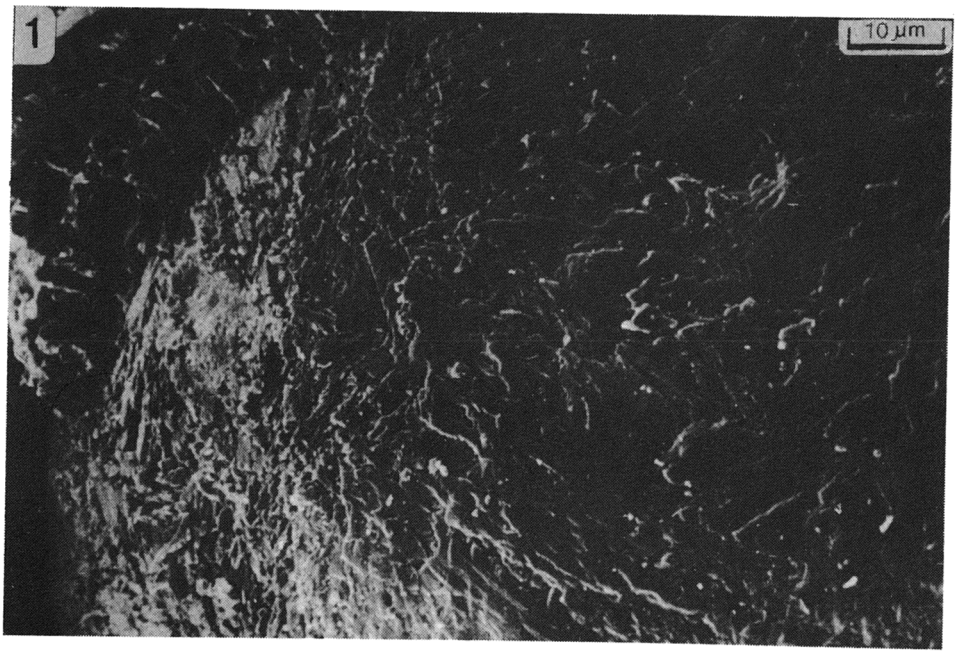

1 — Surface of gypsum ooid exposed by splitting off outer cortical layer, mainly along 010 cleavage planes of cortical crystals; porous areas are built of fine crystals, massive — of aggregates of sub-parallel crystals or polycrystals; scanning electron micrograph

2 — Surface of gypsum cortex; crystal surfaces represent mainly 010 cleavage planes; 010 is not exactly flat within polycrystal at centre (due to its block structure); note overlapping crystals and pores; scanning electron micrograph

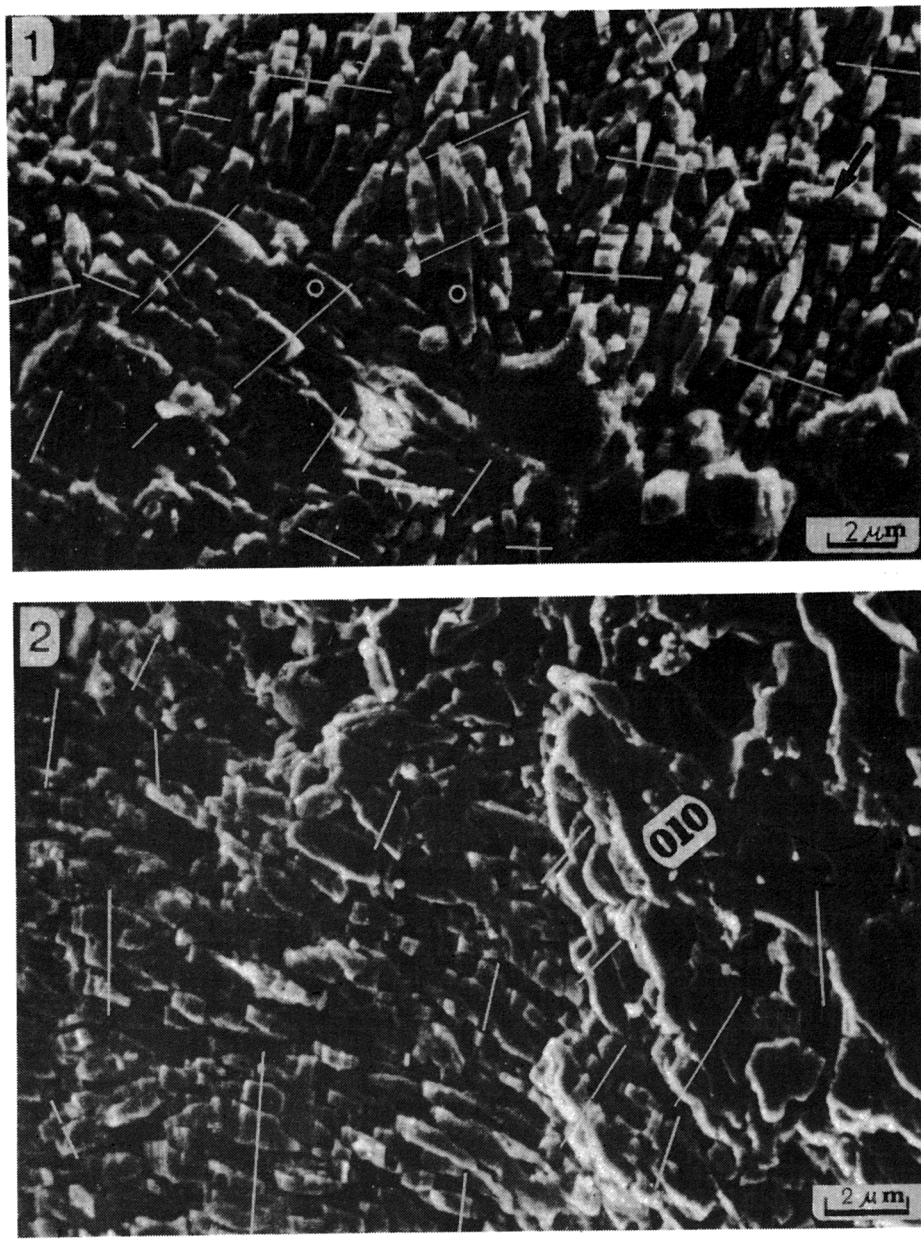

1-2 — Surface of porous gypsum cortical layer (in Fig. 2 *at right* covered by coarser crystalline massive layer); elongated, lens-shaped crystals, rooted in the interior of ooid (one not rooted is *arrowed* in Fig. 1), form groups and aggregates (*marked by circles*; Fig. 1) of sub-parallel crystals; surfaces parallel to plane of photo represent mainly 010 cleavage plane; positions of crystallographic axis *c* (*white lines*) are shown as normal to convex faces of lenticular crystals and parallel to traces of additional cleavage interpreted as 100; scanning electron micrographs

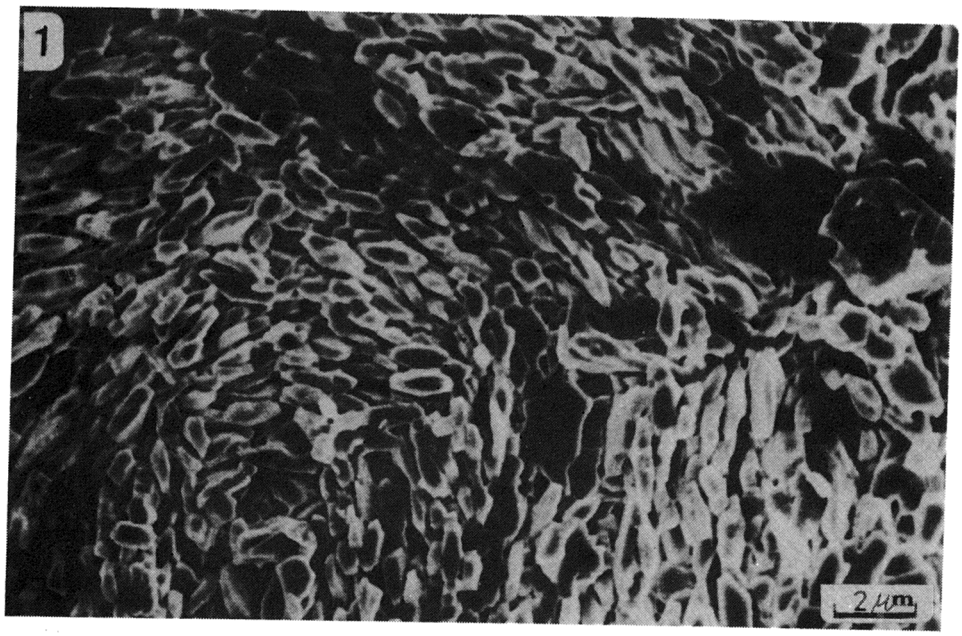

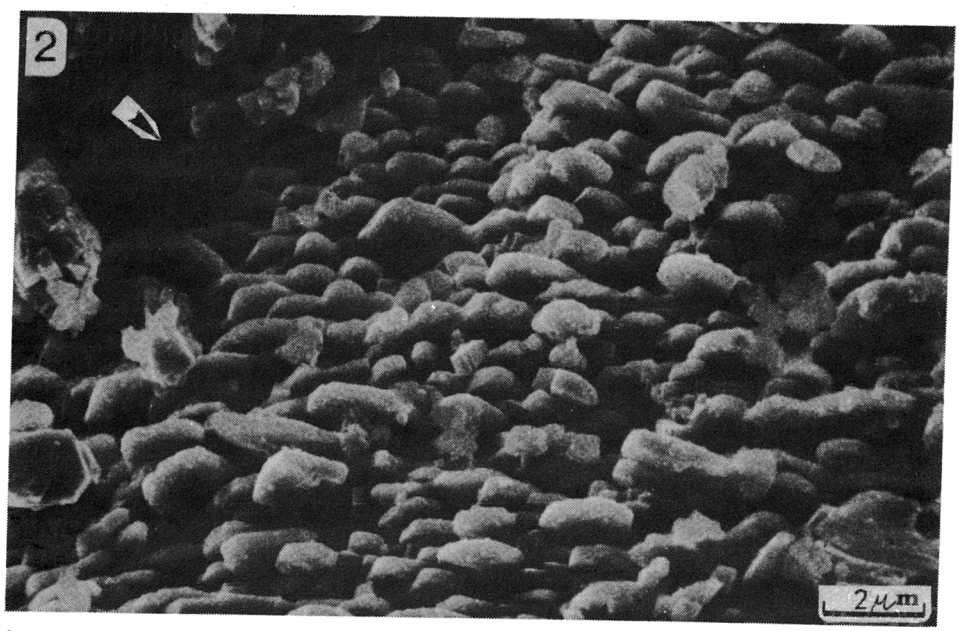

1 — Porous surface of gypsum ooid; elongated, lens-shaped cortical crystals arranged sub-parallelly form swirl pattern; scanning electron micrograph

2 — Porous surface of gypsum cortex showing rounded crystals; lenticular crystal elongated parallelly to cortical layering is arrowed; scanning electron micrograph

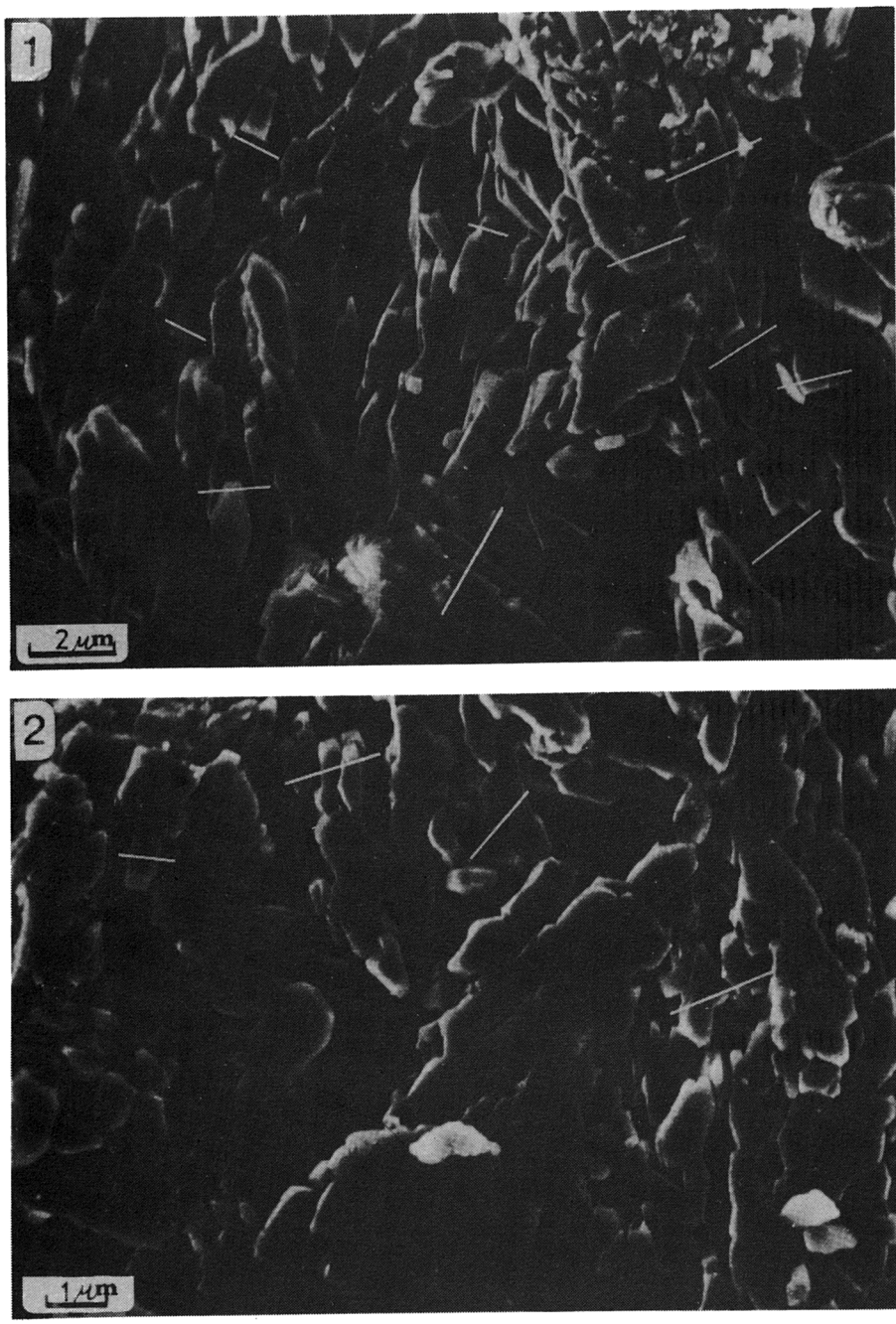

1-2 — Porous surfaces of gypsum ooids; elongated, lens-like crystals form groups and aggregates of sub-parallel crystals; most crystals are rooted in interior of ooid; surfaces parallel to plane of photos represent mainly 010 plane; positions of crystallographic axis *c* (*white lines*) are interpreted as being perpendicular to elongation of lenticular crystals and parallel to traces of additional 100 cleavage; note lens-shaped pores, re-entrant angles on edges of crystal aggregates, and overlapping crystals (Fig. 2); scanning electron micrographs

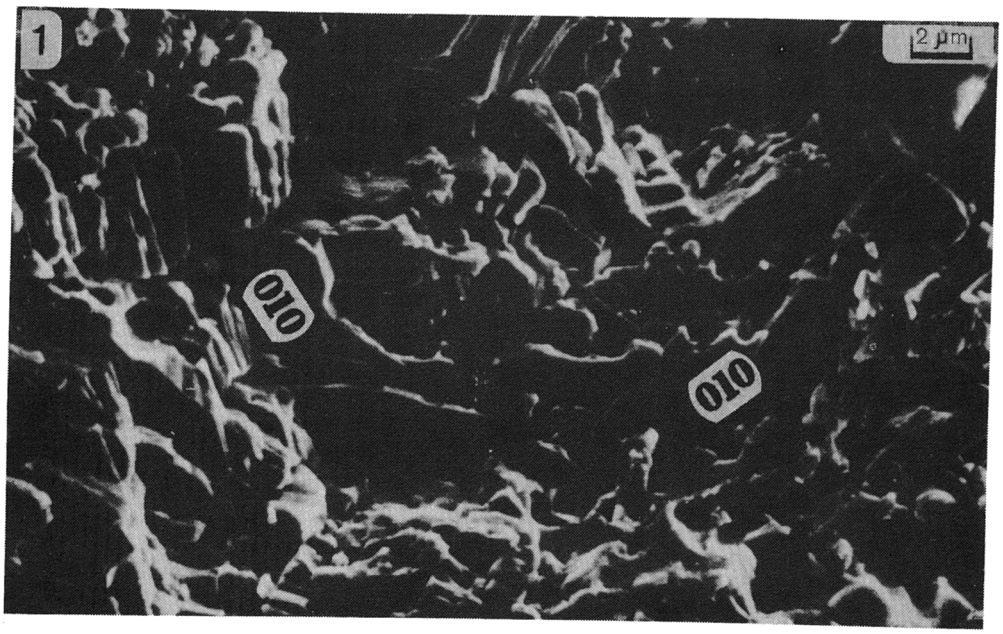

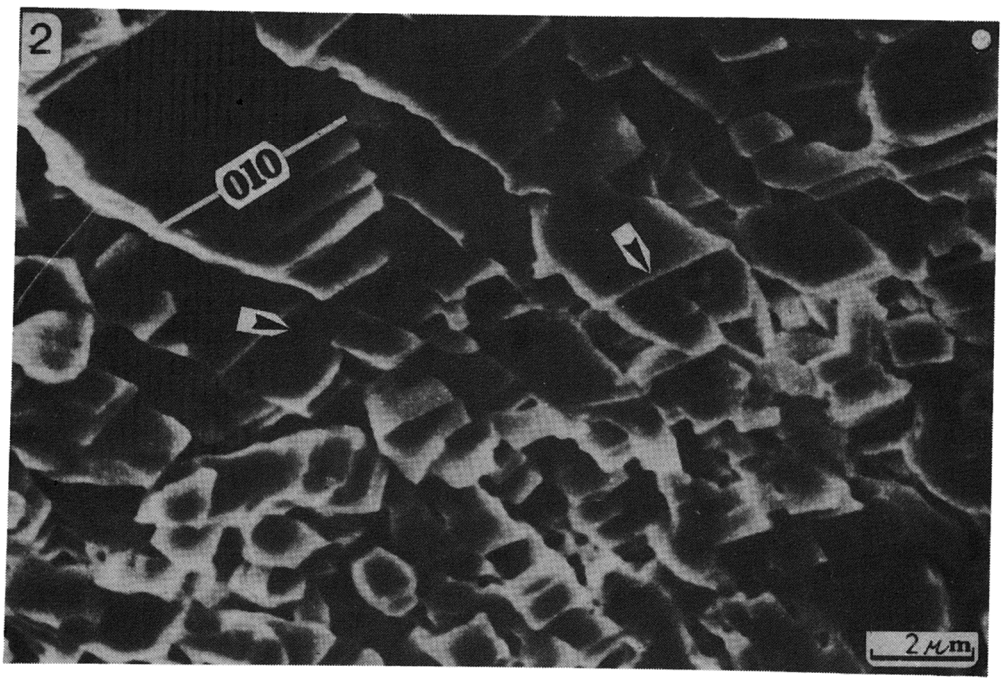

1 — Onion-like structure of fracture surface of gypsum ooid resulted from tangential 010 cleavage of cortical crystals; scanning electron micrograph

2 — Section of cortex (detail of Pl. 27, Fig. 1; *marked by a point*) showing transition from porous, fine- to massive coarse-crystalline layer; radial crystal boundaries (*arrowed*) disappear within polycrystals with boundaries of component crystals not etched; etched traces of 010 planes are marked by lines

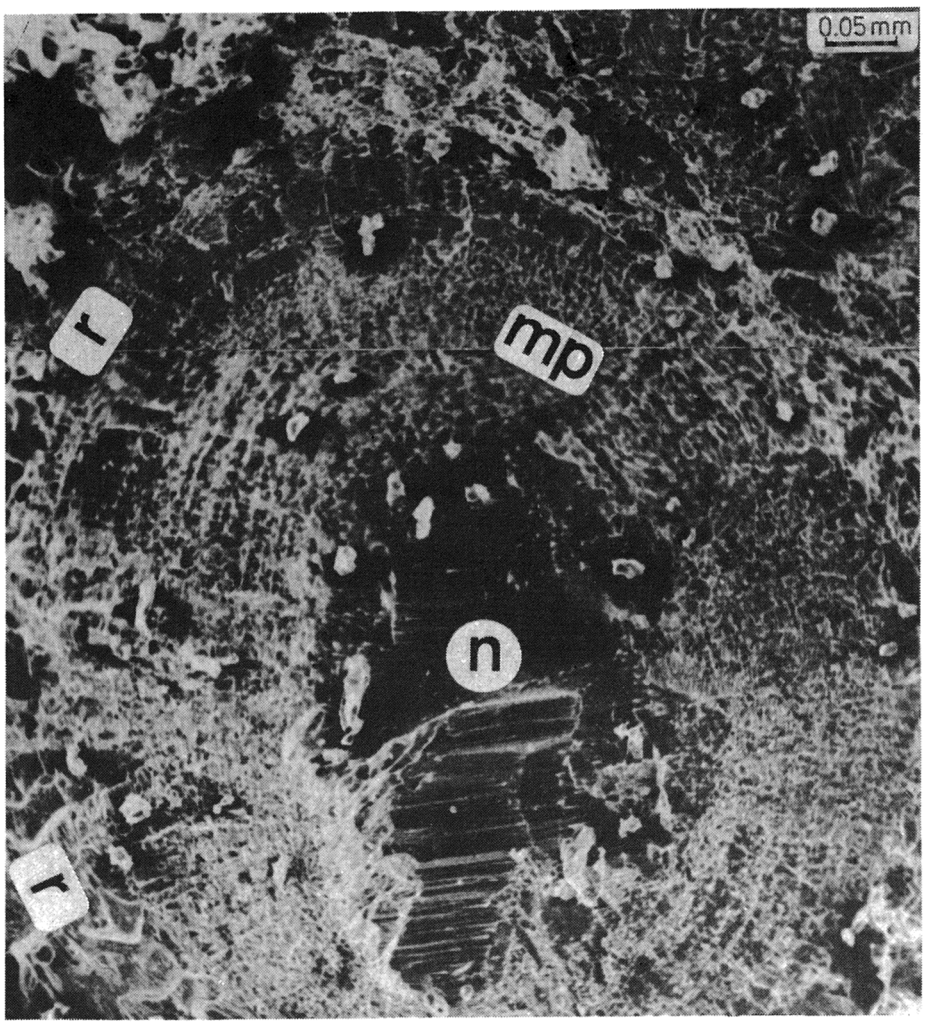

Water etched section of gypsum ooid showing nucleus (*n*), composed of large crystals, massive and porous cortical layers (*mp*, porous layers are lighter, built of smaller crystals), and asymmetric external rim (*r*), composed of large crystals; etched striations parallel to 010 planes, visible as light lines, run concentrically around nucleus; calcite crystals, exhibited by etching, are seen as protruding, light particles in dark halo; scanning electron micrograph

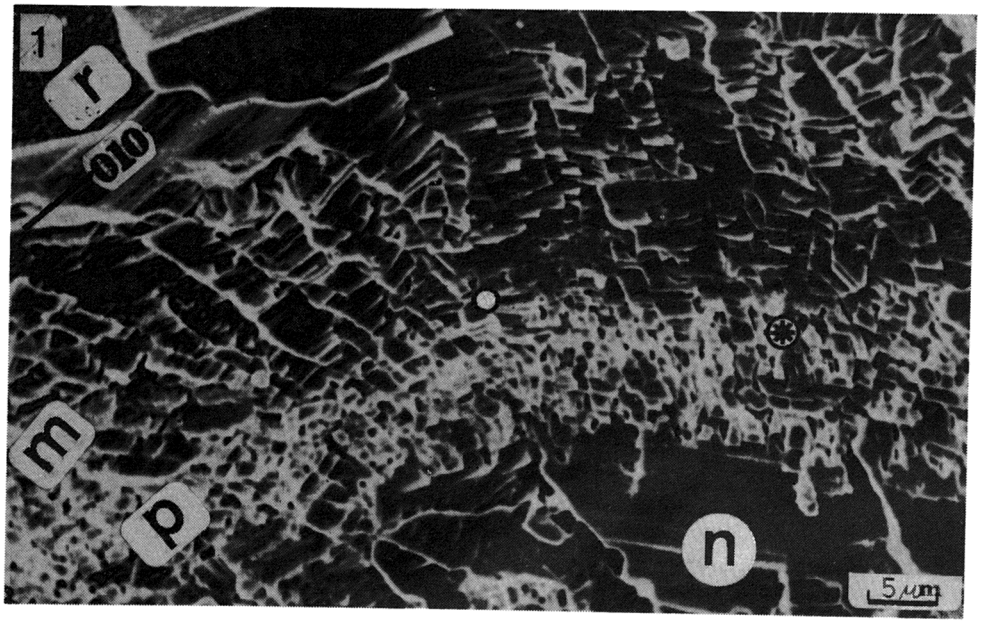

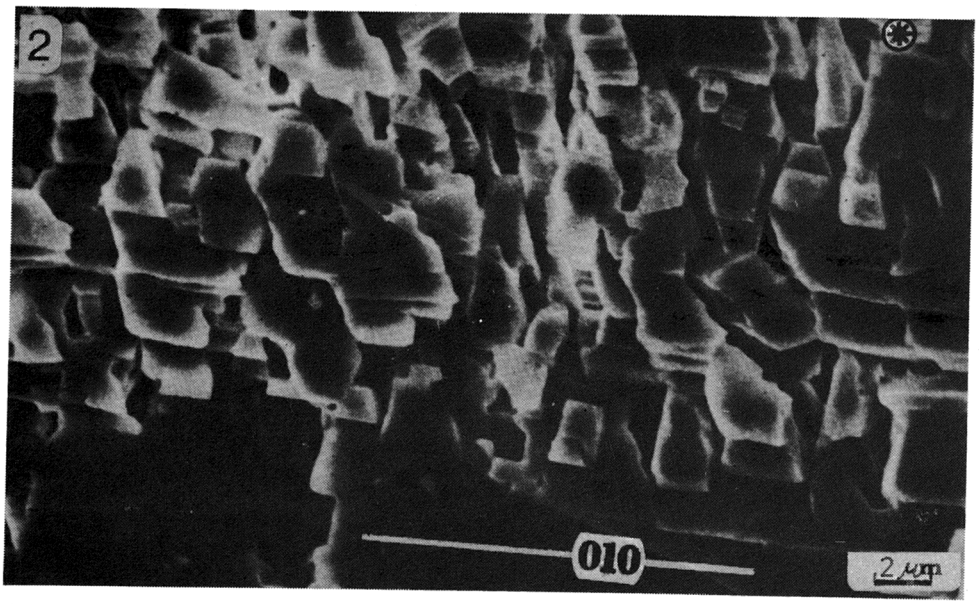

1 — Section of gypsum ooid showing nucleus (*n*), porous (*p*) and massive (*m*) cortical layers, and external rim (*r*); etched traces of 010 planes are marked by lines; cortical crystals are radially arranged; transition from porous to massive layer is gradual due to syntaxial growth of crystals, which coalesce into polycrystals with crystal boundaries not etched (within *m*), or developed compromise boundaries (visible in external rim); details shown in Fig. 2 and Pl. 25, Fig. 2 are marked by *asterisk* and *point;* scanning electron micrograph

2 — Detail of Fig. 1 (*asterisked*) showing lens-shaped cortical crystals created by splitting of the gypsum nucleus in time of syntaxial growth perpendicular to traces of 010 plane

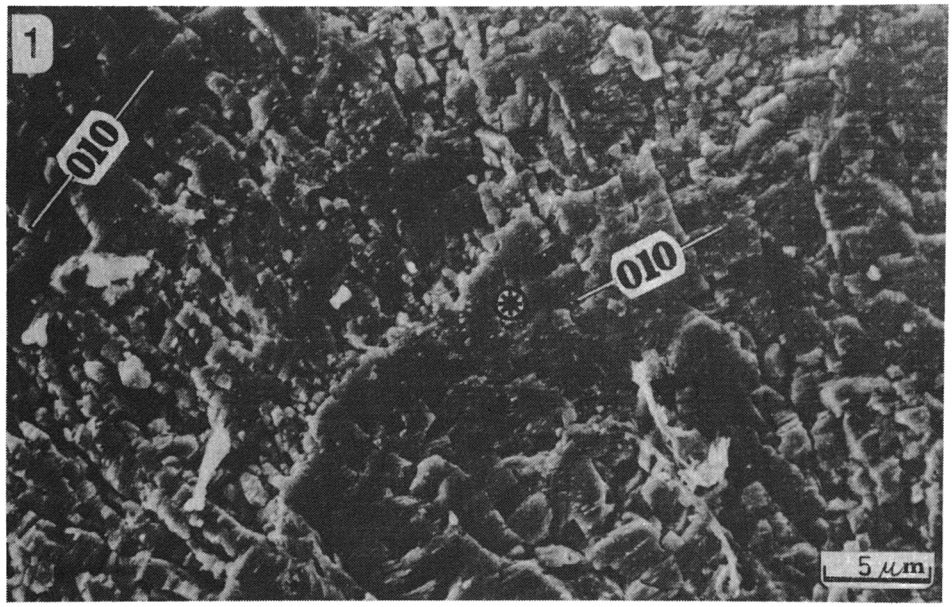

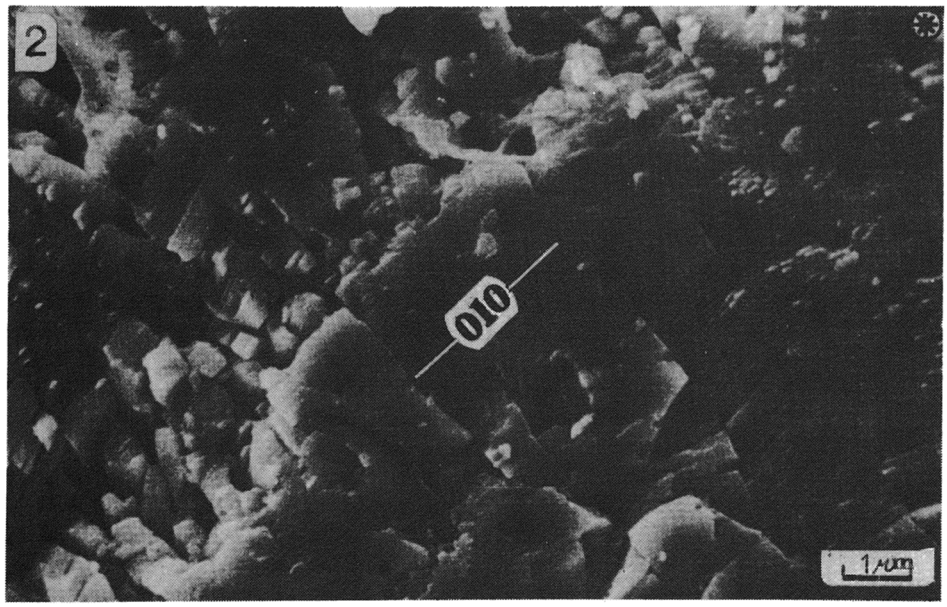

1-2 — Section of gypsum cortex showing porous and massive layers and radial straight crystal boundaries (detail shown in Fig. 2 is *asterisked*); etched traces of 010 planes (*marked by lines*) run along cortical layering; transitions from massive to porous and to massive layers are due to splitting (crystal boundaries grade into pore spaces between lenticular crystals) and coalescence of crystals into massive units with crystal boundaries not etched; note porous and massive fabric within one cortical layer; scanning electron micrographs

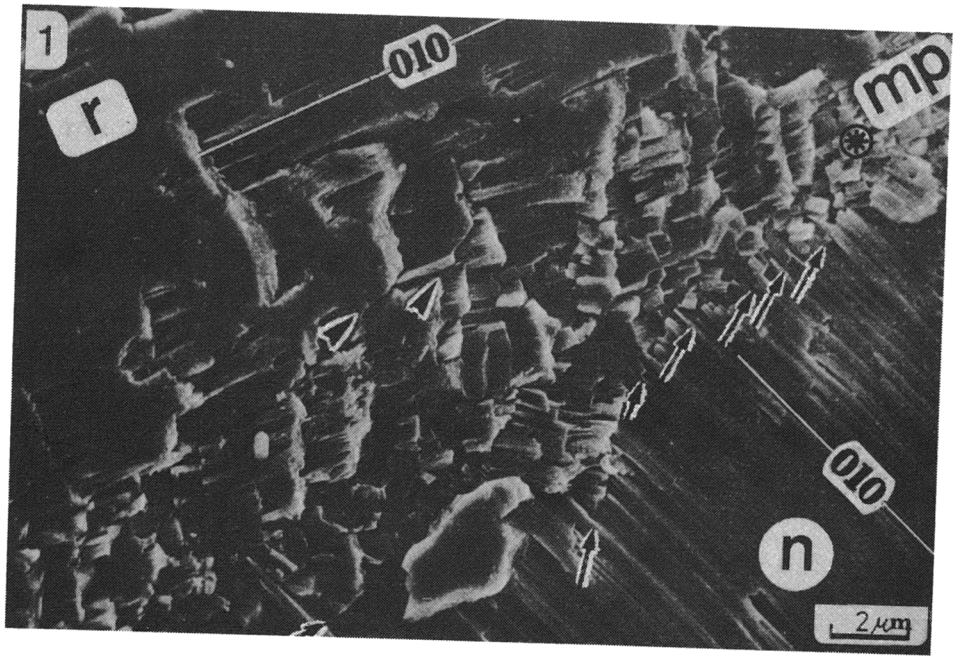

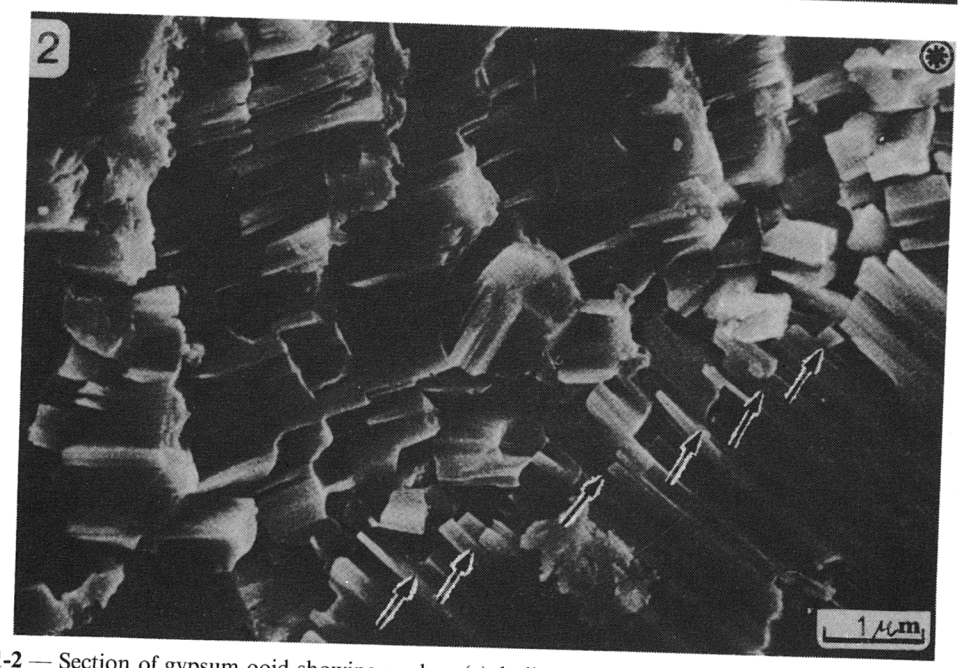

1-2 — Section of gypsum ooid showing nucleus (*n*), built of single crystal, alternating massive and porous cortical layers (*mp*), and external rim (*r*); detail shown in Fig. 2 is asterisked; etched traces of 010 planes are marked by lines; some cortical crystals are syntaxially rooted in nucleus; parallel crystal boundaries oblique to cortical layering are arrowed; radial crystals coalesce into polycrystalline units with crystal boundaries not etched; scanning electron micrographs

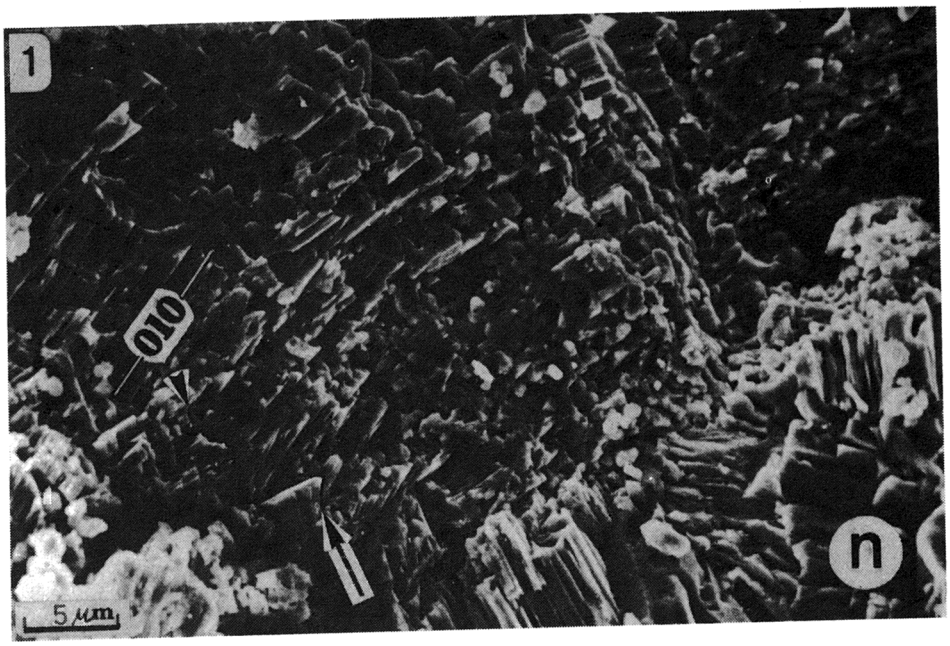

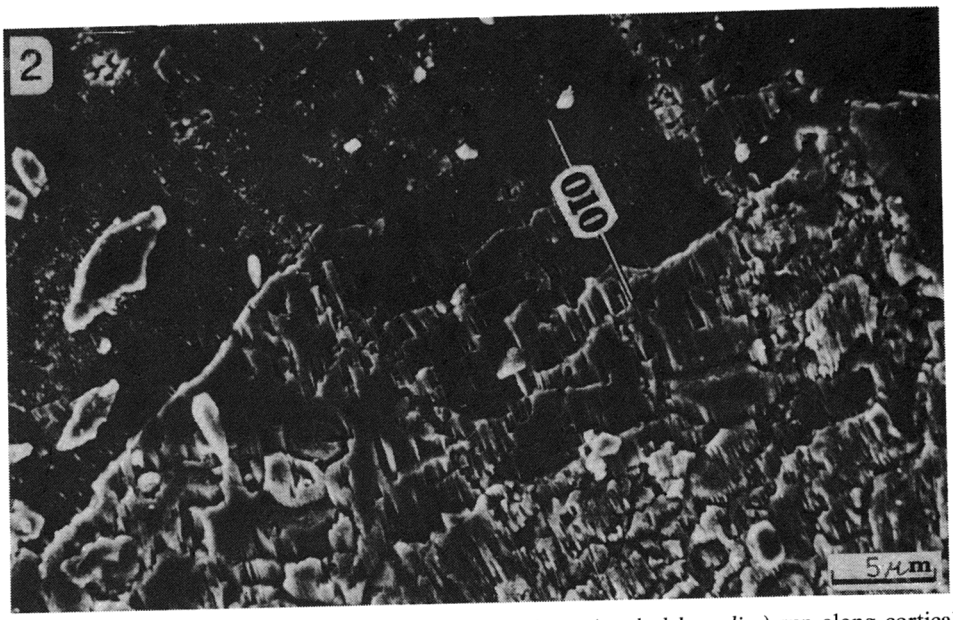

1 — Section of gypsum ooid; etched traces of 010 planes (*marked by a line*) run along cortical layering; nucleus (*n*) is built of differently oriented crystals; porous cortex shows radial straight (*top right*) and zig-zag crystal boundaries (*arrowed*); scanning electron micrograph

2 — Section of gypsum cortex, probably slightly recrystallized; etched 010 traces (*marked by a line*) run along cortical layering; relic(?) concentric porous layers and radial straight and tooth-saw crystal boundaries are visible; upper part is weaker etched; scanning electron micrograph

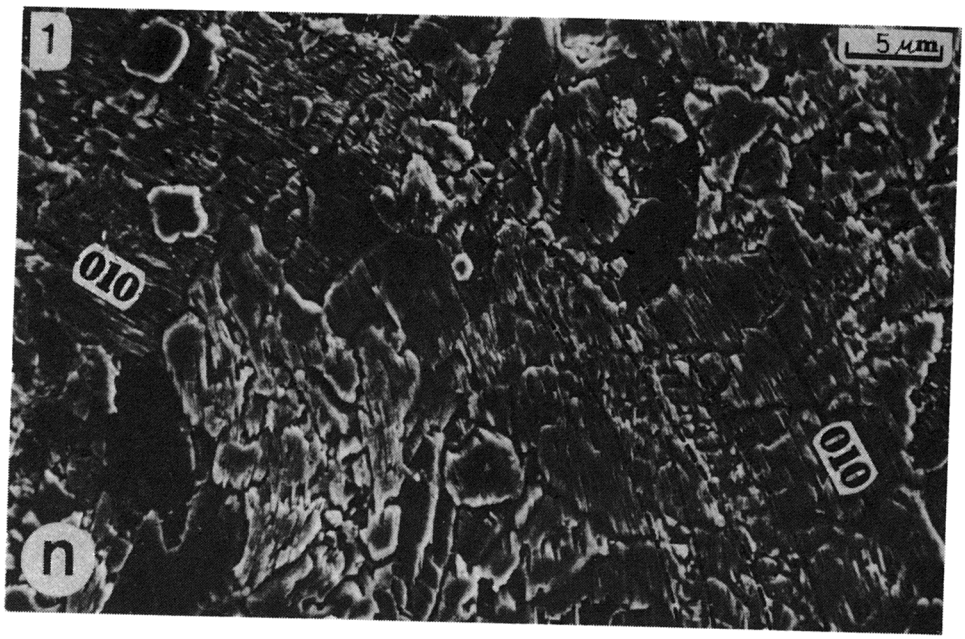

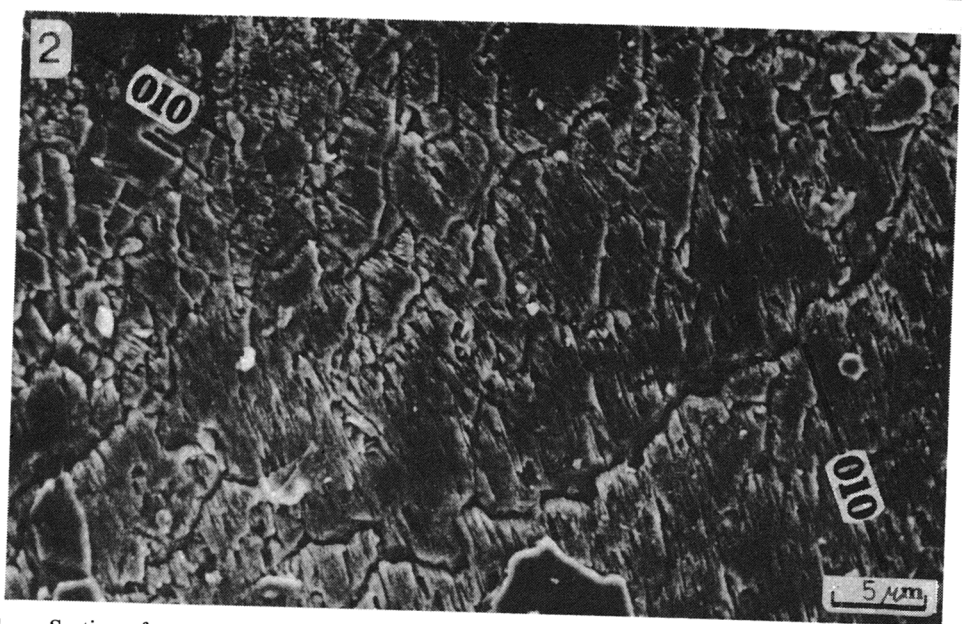

1 — Section of gypsum ooid interpreted as recrystallized; etched traces of 010 planes (*marked by lines*) run along cortical layering; nucleus (*n*) pass into massive cortex built of crystals with migrating boundaries, forming coarse- and fine-crystalline layers, the latter being relic porous cortical layers; outlined layers are shown as cutting each other; scanning electron micrograph

2 — Section of gypsum cortex interpreted as recrystallized; etched 010 traces (*marked by lines*) run along cortical layering; large crystals and polycrystals show massive fabric and migrating boundaries; scanning electron micrograph

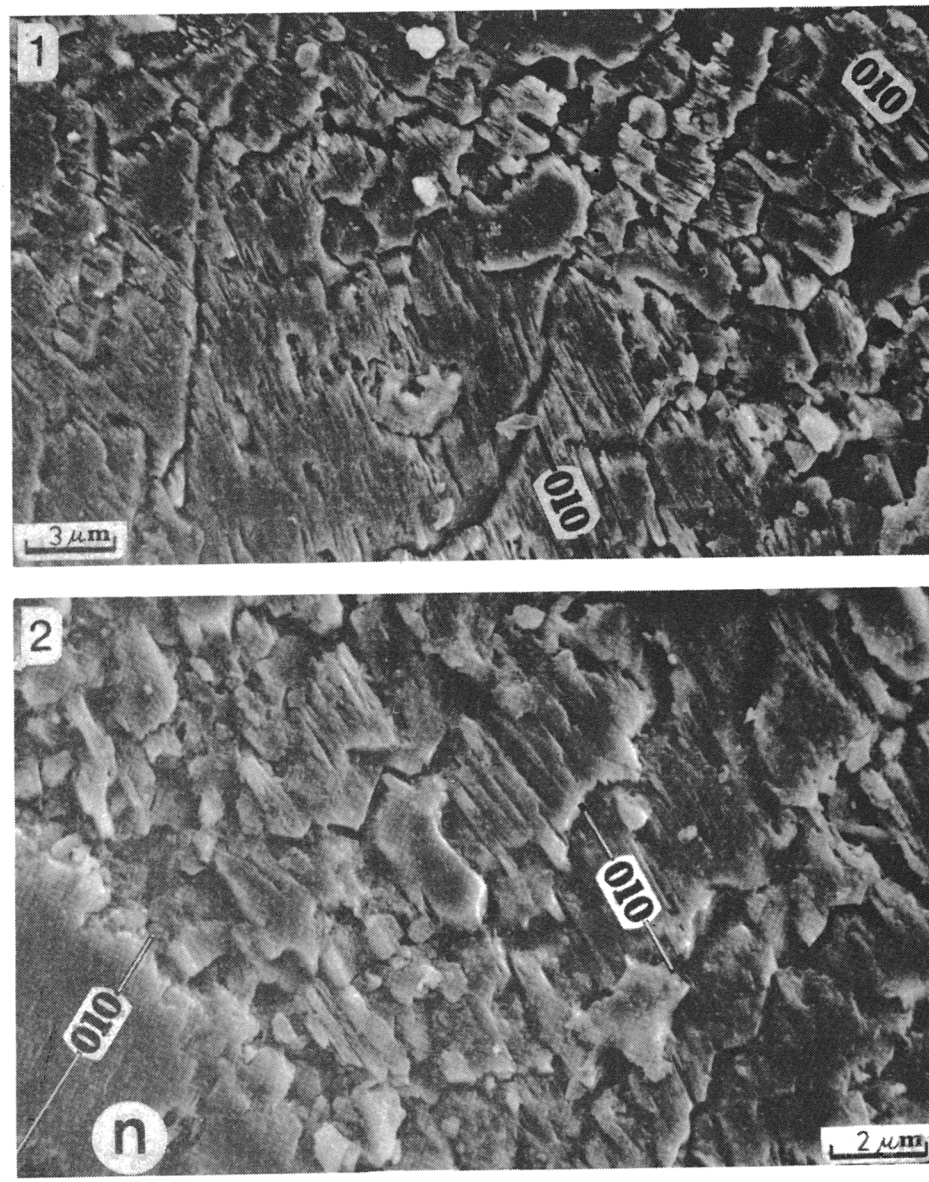

1 — Detail of cortex from Pl. 31, Fig. 2; nucleus is beyond the lower left corner of photo; large crystals with migrating boundaries display massive fabric; fine crystals (*top right*), within partly porous area (probably relict of porous layer), show tooth-saw boundaries with edges of teeth directed along traces of 010 planes (*marked by lines*)

2 — Section of gypsum ooid probably slightly recrystallized; etched 010 traces (*marked by lines*) run along cortical layering; nucleus (*n*) is coated by porous layer passing into more massive coarser crystalline layer; note migrating and tooth-saw crystal boundaries, the latter with edges of teeth directed along 010 traces; faces of teeth correspond with 120 form; scanning electron micrograph

The above interpretation is based on the position of the ooids within the area evidently affected by pressure solution and cementation, and not on the shape of the crystal boundaries itself, which is not sure indicator of recrystallization (*see* discussion *in* KENDALL & BROUGHTON 1978, pp. 533, 535). It is to note that either zig-zag or tooth-saw crystal boundaries were also observed in the ooids showing the primary fabric (Pl. 17, Fig. 1; Pl. 30, Fig. 1).

PRIMARY ACCRETION *VERSUS* RECRYSTALLIZATION

In a view of the above interpretation it is possible to discuss some controversial features of grains of the oolitic layer. The first problem is the origin of the lateral disappearing of the porous cortical layers (= white cortical layers in polished sections; Pl. 2, Figs 1—12; Pl. 3, Figs 1—12; *and* bands formed by Becke lines in thin sections; Pl. 8, Fig. 1a; Pl. 11, Figs 1—4; Pl. 12, Fig. 2; Pl. 16, Fig. 1), which are replaced by the massive unporous gypsum. The first impression is that this massive parts represent an effect of the diagenetic recrystallization and they are younger because they cut the concentric cortical layers.

It is to believe that such massive parts can have double origin, one not excluding the other, *i. e.* they can be both the result of local secondary regrowth of cortical crystals and of the primary growth. It seems that the ooids could grow in one part of the cortex with the porous and in another one with the massive fabric. In polished sections of ooids, massive coarse-crystalline rays often protrude from nucleus into layered cortex and some of them are blunted and covered by successive white porous cortical layers (Pl. 3, Figs 6, 9—10; Pl. 4, Fig. 2). It is doubtful that such blunting can be produced by recrystallization; the massive crystal rays were abraded or dissolved before the accretion of covering cortical layer and thus they are primary.

In the recent Great Salt Lake ooids, especially in the cerebroid ones (CAROZZI 1962), similar radial massive aragonite polycrystals grow simultaneously with the porous masses of smaller crystals placed between them (SANDBERG 1975, HALLEY 1977). Similar primary radial crystals are recorded from many calcite ooids. HALLEY (1977, p. 1112) noted that growth of massive polycrystals and porous fine-crystalline aragonite in the Great Salt Lake ooids was controlled by substrate. The large polycrystals continue growth from the surfaces of older exposed massive crystals. Such massive crystals in the cerebroid ooids protrude over the surface. Similar substrate controlled growth could take place in the gypsum ooids. The substrate controlled growth is also recognized in calcite cements (*see* BATHURST 1971, pp. 430—431).

It is worth to note that direction of syntaxial growth of cortical gypsum crystals depended on crystallographic orientation of the substrate and on environmental factors controlling crystal morphology, strictly on the factors which promote lenticular habit (*see* BĄBEL 1990). The radial

syntaxial growth (as illustrated in Pl. 27, Fig. 2), took place on such substrate or cortical surface along which crystallographic axis *c* was placed, because lenticular crystals growth is most rapid in direction normal to the axis *c* (CODY 1979). In the cross-sections of gypsum ooids the axis *c* often coincides with the traces of the 010 plane, because the 010 plane is tangential, and the axis *c* is situated in this plane. Where the axis *c* was inclined or normal to the ooid surface the growth was not syntaxial or it was syntaxial in oblique direction and at a short distance (Pl. 29, Figs 1—2; Pl. 30, Fig. 1; Pl. 32, Fig. 2) or, sometimes, it could probably continue forming a large scale, imbricating pattern of crystals (*see* Text-fig. 2 *and* Pl. 3, Fig. 10).

The ooid was found, built of a large gypsum crystal with one part exhibiting cortical layering (*see* g *in* Text-fig. 2; *and also* Pl. 2, Fig. 4; Pl. 3, Figs 1—2, 5; Pl. 4, Figs 3—4). Layering is exactly parallel to the round outline of the crystal and sharply disappears within massive transparent area. The pronounced round shape of the grain exclude the possibility of its recrystallizational origin. Such a shape is typically the product of primary growth of ooids, not of recrystallization. Thus the gypsum crystal grew like any ooid with its round shape controlled by abrasion, simultaneously with accreting fine-crystalline cortical layers within its one side. An occurrence of recent halite ooids built of single crystals (WEILER, SASS & ZAK 1974) fully supports this interpretation.

Calcite inclusions within nuclei built of large gypsum crystals are sometimes arranged nearly concentrically, presumably indicating an oolitic growth of such crystals; both single ones (Pl. 7, Fig. 2; Pl. 12, Fig. 2) and aggregates (Pl. 5, Fig. 3; Pl. 8, Figs 1—3; Pl. 9, Fig. 1; Pl. 12, Fig. 2; Pl. 10, Fig. 1; Pl. 26). In cross polarized light, especially within transitional areas between nucleus and cortex, large massive crystals with uniform light extinction occur in lateral contact with crystals exhibiting sweeping extinction and cortical bands formed by Becke lines (Pl. 8, Fig. 1; Pl. 9, Fig. 2). This can also be explained as simultaneous primary growth of large single crystal together with adjacent fine-crystalline porous masses.

On the other hand, the massive cortical parts can be formed by local diagenetic regrowth of cortical crystals, taking place, for example, near the pressure solution contact with the neighboring ooid, or in any other favourable area.

The second controversial problem is the origin of some gypsum grains which do not exhibit pronounced concentric structure in the polished sections and in the cross-polarized light show neither concentric nor radial structure being undistinguishable from the matrix (Pl. 1, Figs 2—3; Pl. 2, Figs 1, 5; Pl. 4, Figs 1—3, 7—8; Pl. 5, Fig. 2; Pl. 7, Fig. 1; Pl. 9, Fig. 1; Pl. 10, Figs 1—2; Pl. 13, Fig. 1). Transparency and lack of Becke lines indicate that some of such grains are massive. Many grains are difficult to be classified as ooids because it is impossible to distinguish a cortex and nucleus or center of crystallization in them. Since their structure does not reflect clearly the centrifugal growth, as in associated ooids, it is also the first impression that such grains represent the ooids with the primary fabric obliterated by recrystallization.

To supply an evidence for recrystallization in considered grains is, however, not easy. Unordered arrangement of crystal boundaries, chaotic structure, lack of competitive growth fabric, seen under cross nicols, only seemingly neglect centrifugal primary growth of the discussed grains. KENDALL & BROUGHTON (1978) showed very similar fabric from speleothems, resulted from primary competitive growth of polycrystalline rays or bundles, which split and penetrate each other.

From several reasons many of these grains seem to be primary. Firstly, highly unordered arrangement of crystals, observed in some grains, can not be

explained as originated from recrystallization of the porous ooids. Such ooids exhibit, as a rule, relatively perfect radial orientation of the crystallographic axes *b* of cortical crystals, and recrystallization should preserve this orientation (*see* SANDBERG 1975, p. 510). It is difficult to explain why, or how, the cortical crystals being recrystallized could change their initial orientation and form an unordered structure. Paradoxically, the more unordered structure is observed, the more unchanged it should be.

Primary nature of many discussed grains is supported by their rounded shape and relatively sharp and pronounced boundary with surrounding gypsum matrix (Pl. 8, Fig. 3; Pl. 10, Figs 1—2; Pl. 13, Fig. 1). Recrystallization should rather obliterate this boundary if acted after deposition of the grain. It is more probable that the grain and its unordered cortical part represent primary form created before deposition of the oolitic layer.

The chaotic structure can be explained as a result of unordered primary accretion. Taking into account the proposed model of ooid growth, such unordered accretion is possible in low agitated brine when abrasion and oriented nucleation with the 010 tangential is less frequent (*see* Text-fig. 5; growth stage *2*). As it was shown these two factors are responsible for creation of perfect concentric and radial structure.

The accretional nature of many of the discussed grains is visible by envelopes of calcite crystals, quasi-radial arrangement of crystals, and their sweeping light extinction observed in places in their external parts (Pl. 10, Figs 1—2). The numerous transitional forms exist between such grains and the perfect ooids.

It is highly possible that the most of the considered grains represent primary accretionary forms which grew in the manner similar to the clusters of halite crystals and mirabilite accretionary grains found in agitated environments by KARCZ & ZAK (1987) and LAST (1984, 1989). The grains with massive fabric could originate generally in relatively less agitated brine than the associated porous gypsum ooids; especially in such conditions in which porous cortical layers were not created (lack of the growth stage 1; *see* Text-fig. 5).

Summarizing, the grains of the oolitic layer represent forms originating in different environmental conditions and their structure can be used as indicator of these conditions in the manner similar as in calcareous ooids. The main factors controlling the structure of the grains were a degree of agitation and supersaturation.

Acknowledgments

The authors would like to thank Professor A. RADWAŃSKI (Institute of Geology, University of Warsaw), and Ass.-Professor T. M. PERYT (State Geological Institute, Warsaw) for their critical comments and helpful suggestions on the earlier drafts of that paper; Ass.-Professor A. NOWAKOWSKI (Institute of Geochemistry, Mineralogy and Crystallography; University of Warsaw)

for valuable help in interpretation of optical data, Dr. A. GĄSIEWICZ, and G. CZAPOWSKI, M. Sc., for discussions. B. MALINOWSKA, A. SZYMAŃSKI, L. ŁUSZCZEWSKA, M. Sc., B. DROZD, M. Sc.; and S. ULATOWSKI are acknowledged for taking the photos of the polished slabs; and H. STEC and T. MOSZCZYŃSKA for their help in drafting works. Thanks are also offered for the staffs of the SEM-laboratories of the Institute of Geochemistry, Mineralogy and Crystallography of the University of Warsaw (Dr. P. DZIERŻANOWSKI, E. KLICHOWICZ, M. Sc., I. BAŁAZY, M. Sc.) and of the State Geological Institute in Kielce (A. SKRZYPCZYK).

Institute of Geology
of the University of Warsaw,
Al. Żwirki i Wigury 93,
02-089 Warszawa, Poland
(M. Bąbel)

Holy Cross Division
of the State Geological Institute,
ul. Zgoda 21,
25-593 Kielce, Poland
(A. Kasprzyk)

REFERENCES

ARAKEL, A. V. 1988. Modern halite sedimentation processes and depositional environments, Hutt Lagoon, Western Australia. *Geodinamica Acta; Rev. Géol. Dyn. Géogr. Phys.*, **2** (4), 169—184. Paris.

BATHURST, R. G. C. 1968. Precipitation of ooids and other aragonite fabrics in warm seas. *In:* C. MÜLLER & G. M. FRIEDMAN (*Eds*), Recent developments in carbonate sedimentology in Central Europe, pp. 1—10. *Springer-Verlag;* Berlin—Heidelberg—New York.

— 1971. Carbonate sediments and their diagenesis. Developments in Sedimentology, **12**, pp. 1—620. *Elsevier Publ. Comp.;* Amsterdam—London—New York.

BĄBEL, M. 1986. Growth of crystals and sedimentary structures in the sabre-like gypsum (Miocene, southern Poland). *Przegl. Geol.*, **34** (4), 204—208. Warszawa.

— 1987. Giant gypsum intergrowths from the Miocene evaporites of southern Poland. *Acta Geol. Polon.*, **37** (1/2), 1—20. Warszawa.

— 1990. Crystallography and genesis of the giant intergrowths of gypsum from the Miocene evaporites of Poland. *Archiwum Miner.*, **44** (2), 103—135. Warszawa.

CAROZZI, A. V. 1962. Cerebroid oolites. *Trans. Illinois State Acad. Sci.*, **55** (3/4), 239—249. Springfield, Illinois.

— 1963. Half-moon oolites. *J. Sedim. Petrology*, **33** (3), 633—645. Menasha, Wisconsin.

CATALANO, R., RUGGIERI G. & SPROVIERI, R. (*Eds*) 1978. Messinian evaporites in the Mediterranean. *Mem. Soc. Geol. Italiana*, **16**, 1—385. Palermo.

CIARANFI, N., DAZZARO, L., PIERI, P. & RAPISARDI, L. 1980. I depositi del Miocene superiore al confine Molisano-Abruzzese. *Boll. Soc. Geol. Italiana*, **99**, 103—118. Roma.

—, —, —, —, & SARDELLA, A. 1978. Preliminary description of some Messinian evaporitic facies along the Abruzzi-Molise boundary. *Mem. Soc. Geol. Italiana*, **16**, 251—260. Palermo.

CODY, R. D. 1979. Lenticular gypsum: occurrences in nature and experimental determinations of effects of soluble plant material on its formation. *J. Sedim. Petrology*, **49** (3), 1015—1028. Menasha, Wisconsin.

DAVIES, P. J., BUBELA, B. & FERGUSON, J. 1978. The formation of ooids. *Sedimentology*, **25** (5), 703—730. Abigdon, Oxfordshire.

FABRICIUS, F. H. 1977. Origin of marine ooids and grapestones. *In:* H. FÜCHTBAUER, A. P. LISITZYN, J. D. MILLIMAN & E. SEIBOLD (*Eds*), Contributions to Sedimentology, **7**, pp. 1—113. *E. Schweizebart'sche Verlagsbuchhandlung (Nägele u. Obermiller);* Stuttgart.

FREEMAN, T. 1962. Quiet water oolites from Laguna Madre, Texas. *J. Sedim. Petrology*, **32** (3), 475—483. Menasha, Wisconsin.

GARLICKI, A. 1979. Sedimentation of Miocene salts in Poland. *Prace Geol. PAN Oddz. w Krakowie (Geol. Transactions)*, **119**, 1—67. Wrocław.

GOLDSCHMIDT, V. 1918. Atlas der Krystallformen; Bd. 4. Gips, pp. 93—102 *and* Taf. 63—73. *Carl Winters Universitätsbuchhandlung;* Heidelberg.

HALLEY, R. B. 1977. Ooid fabric and fracture in the Great Salt Lake and the geologic record. *J. Sedim. Petrology*, **47** (3), 1099—1120. Menasha, Wisconsin.

HARDIE, L. A. & EUGSTER, H. P. 1971. The depositional environment of marine evaporites: a case for shallow clastic accumulation. *Sedimentology*, **16** (3/4), 187—220. Abigdon, Oxfordshire.

HELLER, P. L., KOMAR, P. D. & PEVEAR, D. R. 1980. Transport processes in ooid genesis. *J. Sedim. Petrology*, **50** (3), 943—952. Menasha, Wisconsin.

ILLING, L. V. 1954. Bahaman calcareous sands. *Bull. Amer. Ass. Petrol. Geol.*, **38** (1), 1—95. Tulsa, Oklahoma.

KARCZ, I. & ZAK, I. 1987. Bedforms in salt deposits of the Dead Sea brines. *J. Sedim. Petrology*, **57** (4), 723—735. Menasha, Wisconsin.

KASPRZYK, A. 1988. Korelacja litostratygraficzna osadów siarczanowych w profilach otworów wiertniczych w rejonie Chmielnika — Staszowa. *Kwart. Geol.*, **32** (2), 511—512. Warszawa.

— 1989. Content of strontium in Miocene gypsum rocks of the Staszów area. *Przegl. Geol.*, **37** (4), 201—207. Warszawa.

— 1990. Lithology of the Miocene sulphate deposits in the Staszów area. *Kwart. Geol.*, **33** (2), 241—267. Warszawa.

— & BĄBEL, M. 1986. Gypsum ooids from the Miocene deposits of the vicinity of Staszów. *Przegl. Geol.*, **34** (4), 208—210. Warszawa.

KENDALL, A. C. & BROUGHTON, P. L. 1978. Origin of fabrics in speleothems composed of columnar calcite crystals. *J. Sedim. Petrology*, **48** (2), 519—538. Menasha, Wisconsin.

KERR, P. F. 1959. Optical mineralogy, pp. 1—442. *McGraw-Hill Book Company;* New York—Toronto—London.

KIROV, G. K. 1982. The peculiarities of the gypsum crystallization by counter-diffusion in agar gels. *Geochim. Miner. and Petrol.*, **15**, 3—32. Sofia.

KREUTZ, S. 1916. Gipsy polskie; *I.* Podkarpacie. *Rozprawy Wydz. Mat. Przyrodn. Akad. Umiejętności, Ser. 3, Nauki Mat.-Fiz.*, 15A, 169—235. Kraków.

KUBICA, B. 1983. Rozwój litofacjalny mioceńskich osadów chemicznych między Chmielnikiem a Tarnobrzegiem, pp. 1—124. *Ph. D. thesis;* State Geological Institute, Warszawa.

KWIATKOWSKI, S. 1970. Origin of alabasters, intraformational breccias, folds and stromatolites in Miocene gypsum of Southern Poland. *Bull. Acad. Polon. Sci., Sér Sci. Géol. Géogr.*, **18** (1), 37—42. Warszawa.

— 1972. Sedimentation of gypsum in the Miocene of southern Poland. *Prace Muzeum Ziemi*, **19**, 1—94. Warszawa.

LAST, W. M. 1984. Sedimentology of playa lakes of the northern Great Plains. *Can. J. Earth Sci.*, **21** (1), 107—125. Ottawa.

— 1989. Sedimentology of a saline playa in the northern Great Plains, Canada. *Sedimentology*, **36** (1), 109—123. Abigdon, Oxfordshire.

LIPPMANN, F. 1973. Sedimentary carbonate minerals, pp. 1—228. *Springer-Verlag;* Berlin—Heidelberg—New York.

LOREAU, J.-P. & PURSER, B. H. 1973. Distribution and ultrastructure of Holocene ooids in the Persian Gulf. *In:* B. H. PURSER (*Ed.*), The Persian Gulf, pp. 279—328. *Springer-Varlag;* New York—Heidelberg—Berlin.

ŁABĘCKI, J. & RADWAŃSKI, A. 1967. Broken ooids in lagoonal Keuper deposits of the western margin of the Holy Cross Mts. *Bull. Acad. Polon. Sci., Sér. Sci. Géol. Géogr.*, **15** (2), 93—99. Warszawa.

MACHEL, H.-G. 1985. Fibrous gypsum and fibrous anhydrite in veins. *Sedimentology*, **32** (3), 443-454. Abigdon, Oxfordshire.

MASSON, P. H. 1955. An occurrence of gypsum in Southwest Texas. *J. Sedim. Petrology*, **25** (1), 72—77. Menasha, Wisconsin.

PALACHE, C., BERMAN, H. & FRONDEL, K. 1951. The system of mineralogy of J. D. Dana and E. S. Dana (Yale University, 1837—1892), Vol. **2**, pp. 1—1124. *John Wiley & Sons Inc.;* New York, and *Chapman & Hall Ltd.;* London.

PAWŁOWSKI, S., PAWŁOWSKA, K. & KUBICA, B. 1985. Geology of the Tarnobrzeg native sulphur deposit. *Prace IG*, **144**, 1—109. Warszawa.

PURDY, E. G. 1963. Recent calcium carbonate facies of the Great Bahama Bank; *1.* Petrography and reaction groups. *J. Geology*, **71** (3), 334—355. Chicago.

RADWAŃSKI, A. 1965. Pitting processes in clastic and oolitic sediments. *Ann. Soc. Géol. Pologne*, **35** (2), 179—210. Kraków.

— 1968. Lower Tortonian transgression onto the Miechów and Cracow Uplands. *Acta Geol. Polon.*, **18** (2), 387—445. Warszawa.

— 1969. Lower Tortonian transgression onto the southern slopes of the Holy Cross Mts. *Acta Geol. Polon.*, **19** (1), 1—164. Warszawa.

— & BIRKENMAJER, K. 1977. Oolitic/pisolitic dolostones from the Late Precambrian of south Spitsbergen: their sedimentary environment and diagenesis. *Acta Geol. Polon.*, **27** (1), 1—40. Warszawa.

RICHTER, D. K. 1983. Calcareous ooids: a synopsis. *In:* T. M. PERYT (*Ed.*), Coated grains, pp. 61—99. *Springer-Verlag*, Berlin—Heidelberg—New York—Tokyo.

SANDBERG, P. A. 1975. New interpretation of Great Salt Lake ooids and of ancient non-skeletal carbonate mineralogy. *Sedimentology*, **22** (4), 497—537. Abigdon, Oxfordshire.

SCHREIBER, B. C. 1978. Environments of subaqueous gypsum deposition. *In:* E. DEAN & B. C. SCHREIBER (*Eds*), Marine evaporites. SEPM Short Course No. **4**, pp. 43—73. Oklahoma City.

— TUCKER, M. E. & TILL, T. 1986. Arid shorelines and evaporites. *In:* H. G. READING (*Ed.*), Sedimentary environments and facies (*2nd ed.*), pp. 189—228. *Blackwell Scientific Publ.*; Oxford.

SHEARMAN D. J., TWYMAN J. & ZAND KARIMI M. 1970. The genesis and diagenesis of oolites. *Proc. RGeol. Assoc.*, **81** (3), 561—575. Colchester.

SIESSER, W. G. & ROGERS, J. 1976. Authigenic pyrite and gypsum in south West African continental slope sediments. *Sedimentology*, **23** (4), 567—577. Abigdon, Oxfordshire.

SIMON, B. & BIENFAIT, M. 1965. Structure et méchanisme de croissance du gypse. *Acta Cryst.*, **19**, 750—756. Copenhagen.

SIMONE, L. 1981. Ooids: a review. *Earth Sci. Reviews*, **16** (4), 319—355. Amsterdam.

VOORTHUYSEN, J. H. van 1951. Anhydrite formation in the saline facies of the Münder Mergel (Upper Malm). *Geol. Mijnbouw*, **13** (8), 279—282. Gravenhage.

WALA, A. 1961. Litologia mioceńskiej serii ewaporatów w okolicy Pińczowa. *Sprawozd. z Pos. Komisji Nauk. Oddz. PAN Kraków*, 1—6, 275—280. Kraków.

— 1962. Charakterystyka petrograficzna profili serii gipsowej w okolicy Buska, Wiślicy i Gartatowic oraz próba korelacji ich z profilem w Gackach koło Pińczowa. *Sprowozd. z Pos. Komisji Nauk. Oddz. PAN Kraków*, 1—6, 269—271. Kraków.

— 1963. Korelacja litostratygraficzna serii gipsowej obszaru nadnidziańskiego. *Sprawozd. z Pos. Komisji Nauk. Oddz. PAN Kraków* (1962), 7—12, 530—532. Kraków.

— 1979. Badania litologiczne mioceńskich warstw gipsowych i ilastych z wierceń na obszarze Niecki Nidy. *W:* Sprawozdanie z prac badawczych na obszarze Niecki Nidy. *Unpubl.*, Archiwum PG, Kraków.

WARREN, J. K. 1982. The hydrological setting, occurrence and significance of gypsum in late Quaternary salt lakes in South Australia. *Sedimentology*, **29** (5), 609—637. Abigdon, Oxfordshire.

WEILER, Y., SASS, E. & ZAK, I. 1974. Halite oolites and ripples in the Dead Sea, Israel. *Sedimentology*, **21** (4), 623—632. Abigdon, Oxfordshire.

WINCHELL, A. N. 1949. Elements of optical mineralogy. An introduction to microscopic petrography; Part *1*, Principles and methods (*5th ed.*), pp. 1—263. *John Wiley & Sons, Inc.*; New York, and *Chapman & Hall, Ltd.*; London.

M. BĄBEL i A. KASPRZYK

GIPSOWE OOIDY Z BADEŃSKICH EWAPORATÓW OKOLIC STASZOWA

(Streszczenie)

Przedmiotem pracy jest analiza budowy oraz rekonstrukcja procesów tworzenia się gipsowych ooidów znalezionych w badeńskich gipsach okolic Staszowa (fig. 1; KASPRZYK & BĄBEL 1986). Obserwacje zgładów, płytek cienkich i preparatów skaningowych (fig. 2—4 *oraz* pl. ¶—32) wykazały, iż ooidy posiadają radialną i koncentryczną budowę. Powłoki ooidów zbudowane są

z warstw porowatych, zawierających drobne kryształy (widocznych na zgładach jako białe pasy zaś w płytkach cienkich jako strefy o zagęszczonych radialnych bądź koncentrycznych liniach Beckego), oraz warstw masywnych, bardziej grubokrystalicznych, w obrębie których występują kryształy i agregaty kryształów kalcytu, często tworzące nieciągłe powłoki o mikrytowym wykształceniu. Zaproponowany model warunków wzrostu ooidów (fig. 5) wyjaśnia budowę powłok jako zależną od stopnia wzburzenia i zasolenia wody. Powłoki porowate tworzyły się w przesyconej względem gipsu i wzburzonej wodzie, masywne — w przesyconej lecz stosunkowo spokojniejszej wodzie. Powłoki mikrytowe były wytrącane biochemicznie przez glony zasiedlające powierzchnie spoczywających ooidów w czasie spadku zasolenia. Pojedyncze większe kryształy kalcytu mogły być przechwytywane przez rosnące ooidy zgodnie z tzw. mechanizmem kuli śniegowej (*zob.* HALLEY 1977) w warunkach zmniejszonego wzburzenia wody.

Kryształy gipsu w najlepiej wykształconych ooidach układają się płaszczyznami 010 tangencjalnie do powierzchni powłok. Orientacja taka jest nietypowa dla kryształów gipsu rosnących na podłożu. Wśród rozmaitych przyczyn mogących ją wytłumaczyć na uwagę zasługuje jedna (*zob.* BATHURST 1968), zakładająca, iż zalążki powłokowych kryształów tworzyły się w wyniku adsorpcji lub osiadania na powierzchni ooidu mikrokrystalicznych odłupków gipsu, spłaszczonych wzdłuż kierunku doskonałej łupliwości 010. Odłupki te mogły być wytwarzane przez abrazję oolitowych ziarn we wzburzonej wodzie.